

REPORT DOCUMENTATION PAGE	1. REPORT NO. FHWA/TX-85/08+240-4F	2.	3. Recipient's Accession No.
4. Title and Subtitle Evaluation of Flyash Test Sites Using a Simplified Elastic Theory Model and Field Measurements		5. Report Date March, 1984	
7. Author(s) S.M. Alam, D.N. Little, W.B. Ledbetter		8. Performing Organization Rept. No. Research Report 240-4F	
9. Performing Organization Name and Address Texas Transportation Institute Texas A&M University College Station, Texas 77843		10. Project/Task/Work Unit No.	
		11. Contract(C) or Grant(G) No. (C) 2-9-79-240 (G)	
12. Sponsoring Organization Name and Address Texas State Department of Highways and Public Transportation Transportation Planning Division P.O. Box 5051 Austin, Texas 78763		13. Type of Report & Period Covered Final - September 1978 March 1984	
		14.	
15. Supplementary Notes Study conducted in cooperation with the U.S. Department of Transportation, Federal Highway Administration, Study titled "Flyash Experimental Projects".			
16. Abstract (Limit: 200 words) <p>This report summarizes the evaluation of 8 experimental flyash test sites located on selected Texas Highways. The analysis utilized Dynaflect measured field deflections and a new method for characterizing lime-flyash stabilized pavement structures. The method was developed utilizing a "simplified elastic theory" model and is most cost effective for analyzing a large number of field measured data. Each test site in the study consisted of several test sections of differing designs.</p> <p>For low PI clayey soils (6 sites), it was found that lime is essential, with the flyash, for development of effective structural support in the stabilized layers. The optimum lime-flyash ratios found, for low PI clayey soils, were 0.08 to 0.5 using a minimum of 2% lime.</p> <p>Substantial gains in the stiffness of the stabilized layers were noted when 20% to 40% flyash, with no lime, was used with very low PI coarse sandy soils (1 site).</p>			
17. Document Analysis a. Descriptors Fly ash, Lime, Dynaflect, Layered Elastic Theory, Bessel Functions			
b. Identifiers/Open-Ended Terms			
c. COSATI Field/Group			
18. Availability Statement No restrictions. This document is available to the public through the National Technical Information Service Springfield, Virginia 22161		19. Security Class (This Report) Unclassified	21. No. of Pages 192
		20. Security Class (This Page) Unclassified	22. Price

EVALUATION OF FLY ASH TEST SITES
USING A SIMPLIFIED ELASTIC THEORY MODEL
AND FIELD MEASUREMENTS

by

Shah M. Alam

Dallas N. Little, P.E.

W. B. Ledbetter, P.E.

Research Report 240-4F
Research Study 2-9-79-240

Sponsored by

The Texas Department of Highways and Public Transportation
In cooperation with
The U.S. Department of Transportation
Federal Highway Administration

March 1984

Texas Transportation Institute
Texas A&M University
College Station, Texas 77843

FOREWORD

The information contained herein was developed on Research Study 2-9-79-240 titled "Fly Ash Experimental Projects" in a cooperative research program with the Texas State Department of Highways and Public Transportation and the U.S. Department of Transportation, Federal Highway Administration.

This report was taken from a Master of Science thesis by Shah M. Alam titled "Equations for Predicting the Layer Stiffness Moduli in Pavement Systems Containing Lime-Flyash Stabilized Materials" (May 1984, Texas A&M University).

This is the fourth report on this study. The first three reports are:

- 204-1 "Analysis of Fly Ashes Produced in Texas" January 1981
- 204-2 "Construction of Fly Ash Test Sites and Guidelines for Construction" October 1981
- 204-3 "Preliminary Evaluation of Fly Ash Test Sites Using Static and Dynamic Deflection Systems" April 1983

ABSTRACT

In this study, a new approach for characterizing the stress-strain behavior of n-layer lime-flyash stabilized pavement structures from the Dynaflect measured field deflections was developed. This method employed a simplified form of elastic theory and utilized the J_0 Bessel functions. With this approach, the need for the mathematical integration of complex expressions involving Bessel functions, typically used in the multi-layered elastic theory, is eliminated. This in turn results in very significant savings in the computational costs and, therefore, makes it practicable to analyze a large number of field measurements and to infer the stiffness modulus of the layers with reasonable accuracy.

The method was used to evaluate the structural strengths of 43 pavement sections located at eight test sites on the state highways of Texas.

The results have shown that flyash, by itself, was generally ineffective in promoting stiffness gains in low PI clayey soils, but provided effective structural support when used with lime. The optimum lime-flyash ratios found, for low PI clayey soils, were 0.08 to 0.5 (by weight) using a minimum of 2% lime.

For very low PI coarse sandy soil, stabilization with 'flyash only' (20 to 40% by weight) was very effective and resulted in substantial stiffness gains in the base layers of all the sections.

The effect of time on the stabilized layers of the test sections was also studied in this thesis. The time study has indicated that the testing temperature and the pavement moisture have a significant effect on the computed stiffness of the layers. The results have shown a progressive stiffening of some of the test sections. For low PI clayey soils, the optimum

lime-flyash ratios for long term stiffness gains were found to be 0.08 to 0.5 using a minimum of 2% lime. For very low PI coarse sandy soils, 20 to 40% flyash with no lime, was found effective.

IMPLEMENTATION STATEMENT

The simplified method of approximating the Dynaflect loading scheme discussed in this report affords a reliable, inexpensive method for determining in situ stiffness moduli. Constants for the "Russian model" used to predict the basin shape were developed in this report for lime-flyash stabilized pavement layers.

The researchers recommend incorporation of this "Russian" deflection model in the Texas FPS design and evaluation approach when pavements with lime-flyash layers are encountered in flexible pavements.

Based on the results of this study, or a general rule, lime should be used in combination with flyash in lieu of flyash (even Type C) alone in the stabilization of fine grained soils.

ACKNOWLEDGEMENTS

The authors wish to acknowledge the valuable assistance and support given by various people within the Texas Department of Highways Transportation Planning Division. In particular, Mr. Kenneth Hankins of the Planning and Research Division who was responsible for obtaining all the Dynaflect deflection measurements at the various test sites, and Mr. Jim Brown. Mssrs. Robert Long, Harold Albers and Billy Banister of the Materials and Tests Divisions provided valuable guidance and direction to the research effort. Personnel in Districts 15, 19, 4, 5, 18, and 21, and the Houston Urban Office assisted in obtaining pertinent data on test sites in their District. Their help and support really made this study possible.

The cooperation and assistance of many individuals in the Texas Transportation Institute given during the preparation of this report is appreciated. Dr. R. L. Lytton's guidance and interest in this research was especially helpful.

Acknowledgement is also extended to Koninklijke/Shell-Laboratorium, Amsterdam (Shell Research, N.V.) for the use of the BISTRO computer program.

While the field deflections data were gathered by the Highway Department, the contents of this report reflect the views of the authors who are responsible for the facts and accuracy of the data. The contents do not necessarily reflect the official views or policies of the Federal Highway Administration. This report does not constitute a standard, specification or regulation.

SUMMARY

In this study, a new approach for characterizing the stress-strain behavior of n-layer lime-flyash stabilized pavement structures from the Dynaflect measured field deflections was developed. This method employed a simplified form of elastic theory and utilized the J_0 Bessel functions. With this approach, the need for the mathematical integration of complex expressions involving Bessel functions, typically used in the multi-layered elastic theory, is eliminated. This in turn results in very significant savings in the computational costs and, therefore, makes it practicable to analyze a large number of field measurements and to infer the stiffness modulus of the layers with reasonable accuracy.

The method was used to evaluate the structural strengths of 43 pavement sections located at eight test sites on the state highways of Texas.

The results have shown that flyash, by itself, was generally ineffective in promoting stiffness gains in low PI clayey soils, but provided effective structural support when used with lime. The optimum lime-flyash ratios found, for low PI clayey soils, were 0.08 to 0.5 (by weight) using a minimum of 2% lime.

For very low PI coarse sandy soil, stabilization with 'flyash only' (20 to 40% by weight) was very effective and resulted in substantial stiffness gains in the base layers of all the sections.

The effect of time on the stabilized layers of the test sections was also studied in this thesis. The time study has indicated that the testing temperature and the pavement moisture have a significant effect on the computed stiffnesses of the layers. The results have shown a progressive stiffening of some of the test sections. For low PI clayey soils, the optimum lime-flyash ratios for long term stiffness gains were found to be 0.08 to 0.5 using a minimum of 2% lime. For very low PI coarse sandy soils, 20 to 40% flyash with no lime, was found effective.

TABLE OF CONTENTS

	<u>PAGE</u>
List of Tables	x
List of Figures	xi
1. INTRODUCTION	1
1.1 Background	1
1.2 Objectives	3
1.3 Scope	3
1.4 Test Sites	3
1.4.1 Test Site 1 located on FM 3378 in Bowie County	7
1.4.2 Test Site 2 located on US 59 in Panola County	7
1.4.3 Test site 3 located on FM 1604 in Bexar County	8
1.4.4 Test Site 4 located on FM 1604 in Bexar County	8
1.4.5 Test Site 5 located on FM 1604 in Bexar County	8
1.4.6 Test Site 8 located on SH 335 in Potter County	9
1.4.7 Test Site 12 located on FM 2697 in Wheeler County	9
1.4.8 Test Site 13 located on US 87 in Wilson County	9
1.5 Research Approach	10
2. METHODS FOR DEFLECTION ANALYSIS	14
2.1 Deflection Measurement with Dynaflect	14
2.2 Significance and Interpretation of Bessel Functions .	18
2.2.1 Bessel Function of the First Kind and Order Zero $J_0(x)$	18
2.3 Methods for Computing In-Situ Elastic Moduli	23
2.3.1 Multi-Layered Elastic Theory Approach	23
2.3.2 "Empi" Method	24
2.3.3 "Elastic Modulus I" Method	27
2.3.4 "Russian Equations" Method	28
3. THEORETICAL BACKGROUND AND STATISTICAL PROCEDURE	30
3.1 Deflection Equation for Single Elastic Layer	30
3.2 Odemark's Assumption	33
3.3 Derivation of Deflection Equation for Multi-Layered Pavements	35
3.4 Statistical Analysis Procedure	38
3.4.1 Pattern Search Technique	39
3.4.2 Regression Analysis Number 1, for the Determination of Constant m	42
3.4.3 Regression Analysis Number 2, for the Determination of constants n, C, B and H ...	44
3.4.4 Regression Analysis Number 3, for the Prediction of Deflections and Elastic Moduli	46

	<u>Page</u>
4. ANALYSIS AND RESULTS	49
4.1 Deflection Basin Fitting Analysis	49
4.1.1 "Average Percentage Variation" Criterion	51
4.1.2 Fitted Elastic Moduli Results	52
4.2 Regression Analysis Number 1	52
4.2.1 Effect of Physical Properties of Pavements on Constant m	54
4.3 Regression Analysis Number 2	63
4.3.1 Effect of Physical Properties of Pavements on Constants n, C, B and H	71
4.4 Investigations Using K_0 Bessel Function	71
4.5 Regression Analysis Number 3	74
4.5.1 Predicted Elastic Moduli Results	75
4.6 Effect of Time on Lime-Flyash Stabilized Layers	86
5. CONCLUSIONS AND RECOMMENDATIONS	100
5.1 Conclusions	100
5.2 Recommendations	102
References	104
Appendix A. Typical Layouts and Sections of Test Sites	107
Appendix B. Elastic Modulus of Pavement Layers Determined by Basin Fitting Technique	116
Appendix C. Vertical Deflections at Selected Pavement Depths, Computed at Dynaflect Sensor-1 Location	133
Appendix D. Values of Constants n, C, B and H Determined by Regression Analysis Number 2	144
Appendix E. Predicted Elastic Modulus of Pavement Layers, Computed by Regression Analysis Number 3	146
Appendix F. Dynaflect Deflection Measurements of the Test Sites, Used in This Study	166

LIST OF TABLES

<u>TABLE</u>		<u>PAGE</u>
1	Test Site Summary	5
2	Summary of test sites and dyanflect deflection data selected for development of deflection equation for lime-flyash stabilized sections	12
3	Values of constants m , n and H' determined by Regression Analysis Number 1 - Site 1	55
4	Values of constants m , n and H' determined by Regression Analysis Number 1 - Site 2	56
5	Values of constants m , n and H' determined by Regression Analysis Number 1 - Site 3	57
6	Values of constants m , n and H' determined by Regression Analysis Number 1 - Site 4	58
7	Values of constants m , n and H' determined by Regression Analysis Number 1 - Site 5	59
8	Values of constants m , n and H' determined by Regression Analysis Number 1 - Site 8	60
9	Values of constants m , n and H' determined by Regression Analysis Number 1 - Site 12	61
10	List of regression coefficients of linear and log-linear relationships between the constant m versus modular ratios K_1 , K_2 and K_3 and layer thickness ratio D	64
11	List of regression coefficients of log-linear relationship between constants n , C , B and H with modular ratios K_1 , K_2 and K_3 and layer thickness ratio D	72

LIST OF FIGURES

<u>FIGURE</u>		<u>PAGE</u>
1	Location of Flyash Test Sites in Texas (6)	4
2	Typical deflection basin reconstructed from Dynaflect readings. Only half of the basin is measured (15) ...	15
3	Radial location of Dynaflect sensors from loading points (10)	16
4	Actual imprint of Dynaflect loading wheels taken during testing at Texas Transportation Institute on July 14, 1969	17
5	Graphical representation of Bessel functions of the first kind - $J_0(x)$ and $J_1(x)$	19
6	Graphical representation of modified Bessel functions of the first kind - $I_0(x)$ and $I_1(x)$	20
7	Graphical representation of modified Bessel functions of the second kind - $K_0(x)$ and $K_1(x)$	20
8	Schematic of multilayered elastic system (18)	21
9	Stresses on a typical element r-inches from axis of the load and z-inches below the surface (18)	22
10	Schematic of a 2-layer elastic system (19)	26
11	Load distribution system of a single elastic layer over a rigid layer	31
12	Transformed thicknesses of k-layers for multilayered pavements	34
13	Pattern search technique (22)	41
14	Flow Chart for Regression Analysis Number 1	43
15	Flow Chart for Regression Analysis Number 2	45
16	Flow Chart for Regression Analysis Number 3	47
17	Subgrade modulus as a function of sensor-5 reading of the Dynaflect, in log-log form	53

<u>Figure</u>	<u>Page</u>
18 Trends in variation of exponential constant m for lime-flyash stabilized test sections	62
19 Plot of the constants m , n , C , B and H computed for lime-flyash stabilized test sections - Site 1	66
20 Plot of the constants m , n , C , B and H computed for lime-flyash stabilized test sections - Site 2	67
21 Plot of the constants m , n , C , B and H computed for lime-flyash stabilized test sections - Site 3, 4, 5 and 8	68
22 Plot of the constants m , n , C , B and H computed for lime-flyash stabilized test sections - Site 12	69
23 Predicted elastic modulus values of pavement layers - Site 1	76
24 Predicted elastic modulus values of pavement layers - Site 2	77
25 Predicted elastic modulus values of pavement layers - Site 3	78
26 Predicted elastic modulus values of pavement layers - Site 4	79
27 Predicted elastic modulus values of pavement layers - Site 5	80
28 Predicted elastic modulus values of pavement layers - Site 8	81
29 Predicted elastic modulus values of pavement layers - Site 12	82
30 Variation in the base modulus E_1 , subbase modulus E_2 and subgrade modulus E_{sg} with time - Site 1	87
31 Variation in the subbase modulus E_3 and subgrade modulus E_{sg} with time - Site 2	88
32 Variation in the subbase modulus E_2 and subgrade modulus E_{sg} with time - Site 3	89
33 Variation in the subbase modulus E_2 and subgrade modulus E_{sg} with time - Site 4	90

<u>Figure</u>	<u>Page</u>
34 Variation in the subbase modulus E_2 and subgrade modulus Esg with time - Site 5	91
35 Variation in the subbase modulus E_2 and subgrade modulus Esg with time - Site 8	92
36 Variation in the base modulus E_1 and subgrade modulus Esg with time - Site 12	93
37 Mean pavement temperature versus Deflection adjustment factor (26)	95

1. INTRODUCTION

1.1 Background

The performance of a pavement structure is dependent on a large number of physical variables that include materials, construction, traffic and environment. For evaluating the performance of a pavement structural system, mechanistic design procedures are commonly employed. Typically in this analysis, multilayered elastic and finite element theories are utilized to compute stresses in the pavement structure, and the computed stresses are input into a fatigue equation to predict performance life of the structural layer. Use of these theories requires that the constitutive behavior of the pavement materials be identified and the materials characterized in terms of a stiffness modulus and Poisson's ratio.

The deflection of the pavement structure in response to an induced load has been shown to represent performance (23). Non-destructive testing devices such as the Dynaflect operate on the principle of a vibratory force applied on the surface of the pavement and measure the induced deflections.

The use of field deflection measurements for the estimation of in-situ values of elastic moduli of pavement layers is gaining in popularity and usage. To accomplish this, multi-layered elastic theory has been used to predict actual Dynaflect measurements (7), and several computer-based methods have evolved (16).

Lytton and Michalak (2) formulated equations which may be effectively used to predict load induced deflections and thus elastic

a need exists to extend the application of this method to lime-flyash stabilized pavement layers. The available equations are not currently applicable to lime-flyash stabilized layers as there were no lime-flyash stabilized layers in the Texas Transportation Institute test sections (14) used in Lytton's study.

1.2 Objectives

The objective of this study is to utilize the field measured Dynaflect deflections, of the flyash experimental test sites, to develop new equations based on the simplified elastic theory model. Then apply the newly formed equations to compute the in-situ layer stiffnesses of the lime-flyash test sections and, also, examine the effect of time on these test sections.

1.3 Scope

This research was a continuation of previous investigations by McKerrall, Ledbetter and Teague (5) on "Analysis of Flyashes Produced in Texas" and Ledbetter et al., (6) on "Construction of Flyash Test Sites and Guidelines for Construction". In this study, the structural support capability of lime-flyash stabilized layers was evaluated by analyzing field measured Dynaflect deflection data of 51 lime-flyash stabilized test sections (6) constructed by Texas State Department of Highway and Public Transportation at 8 test sites in Texas.

1.4 Test Sites

The test site locations are indicated in Figure 1 and a test site summary is provided in Table 1. While detailed description of the

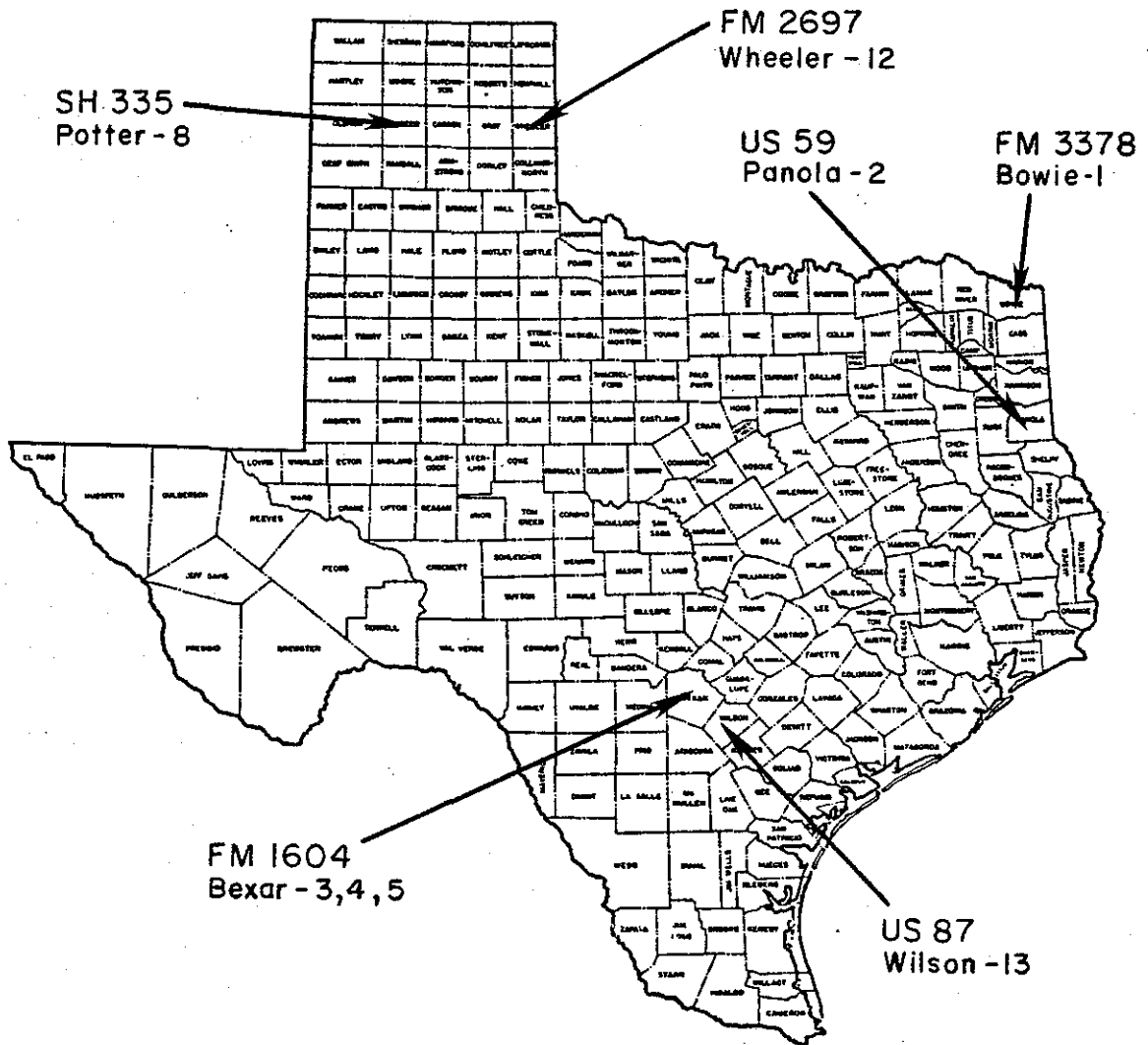


Figure 1. Location of Flyash Test sites in Texas (6).

Table 1. Test Site Summary

Test site No	County	Highway	Date Completed	Flyash source	No. of sections	Length of sections	Test site data ^a	
							Section construction	Subgrade Soil type
1	Bowie	FM 3378	Oct, 1979	M	10	800 ft	1 course surf. treat, 8 in. L-FA base 8 in. L or FA subbase	Low/Medium plasticity silty clay
2 ^b	Panola	US 59	Sept, 1979	W	9	1000 ft	1 course surf. treat, 2 in. HMAC 12 in. flexible base 8 in. L-FA subbase	Low PI, silty clay (with sand)
3	Bexar	FM 1604	Dec, 1979	D	6	800 ft	2 course surf. treat, 10 in. flexible base 6 in. L-FA subbase	Low PI clayey silt
4	Bexar	FM 1604	Oct, 1979	D	6	800 ft	2 course surf. treat, 14 in. flexible base 6 in. L-FA subbase	Low PI clayey silt
5	Bexar	FM 1604	Mar, 1980	D	8	800 ft	2 course surf. treat, 12 in. flexible base 6 in. L-FA subbase	Low PI clayey silt
8	Potter	SH 335	Mar, 1979	H	6	800 ft	2 course surf. treat, 1 in. HMAC 12 in. flexible base 6 in. L-FA subbase	Medium/low PI clay
12	Wheeler	FM 2697	Nov, 1979	H	5	900 to 5400 ft	2 course surf. treat, 6 in. FA base	Very low PI (3) Sandy soil

Table 1. Test Site Summary continued

Test Site data ^a								
Test site no	County	Highway	Date Completed	flyash source	No. of sections	Length of sections	Section construction	Subgrade Soil type
13	Wilson	US 87	Apr, 1980	D	1	1½ miles	1 in. Asph. concrete, 6 in. L-FA base 12 in. River gravel subbase	River gravel low PI (7)

^aRefer to Appendix B for lime-flyash ratios and to reference (5) for flyash compositions.

^bDynaflect data not available for section 10 in site 2. Site 2 resurfaced with 2 in. HMAC in October 1980.

construction procedures employed for the test sites is available in reference (6), the typical layout and cross section of the sites are given in Appendix A and field measurements, that were used in the study, are given in Appendix F.

1.4.1 Test Site 1 located on FM 3378 in Bowie County This project consisted of 10 sections which used lime-flyash stabilization in the base layer. Each section consisted of an 8 inch subbase stabilized with either four percent lime or six percent flyash. The base for each section consisted of 8 inches of lime-flyash stabilized layer. The wearing surface was one course bituminous surface treatment approximately 1/4 inch thick. The base course used varying amounts of lime and flyash to stabilize a low to medium PI silty clay soil. The typical layout and cross section is given in Figure A-1, Appendix A and Dynaflect deflection measurements in Tables F-1 to F-4 in Appendix F.

1.4.2 Test Site 2 located on US 59 in Panola County This project was constructed of 8 inch lime-flyash stabilized subbase covered by a 12 inch flexible base. The wearing surface was originally constructed of one course bituminous surface treatment. All ten sections of the test site were re-surfaced in October 1980 with a 2 inch hot mix concrete overlay. Varying amounts of lime and flyash were used in the subbase to stabilize a low PI silty clay (with sand) soil. Figure A-2 Appendix A shows the typical cross section and layout. Dynaflect deflection measurements are in Tables F-5 and F-6

in Appendix F.

1.4.3 Test Site 3 located on FM 1604 in Bexar County This test site consisted of six test sections constructed of 10 inch flexible base over a 6 inch lime-flyash stabilized subbase. The sections were surfaced with a two course bituminous surface treatment. Varying amounts of lime and flyash were used in the subbase to stabilize a low PI clay silt. Test sections were approximately 800 feet long with a transition between each test section. The typical layout and cross section are given in Figure A-3 Appendix A, and Dynaflect deflection measurement in Tables F-7 to F-11 in Appendix F.

1.4.4 Test Site 4 located on FM 1604 in Bexar County This project has six test sections constructed of 14 inch flexible base over 6 inch lime-flyash stabilized subbase. Varying amounts of lime and flyash were used in the subbase to stabilize a low PI clay silt. Two course bituminous surface treatment approximately 1/2 inch in thickness provides the wearing surface. Typical layout and cross sections are given in Figure A-4 Appendix A, and Dynaflect deflection measurements in Tables F-12 to F-15 in Appendix F.

1.4.5 Test Site 5 located on FM 1604 in Bexar County This test site has eight test sections, approximately 800 feet long, constructed on the west-bound lane of FM 1604 between the San Antonio river and Elmendorf. The sections consisted of a 12 inch flexible base over 6 inch lime-flyash stabilized subbase. Varying amounts of lime and flyash were used in the subbase to stabilize a low PI clay silt soil.

The wearing surface is a two course bituminous treatment. The layout and cross section of the test site are given in Figure A-5 Appendix A, and Dynaflect deflection measurements are in Tables F-16 to F-20 Appendix F.

1.4.6 Test Site 8 located on SH 335 in Potter County This project has six test sections constructed of 12 inch flexible base over 6 inch lime-flyash stabilized subbase. Varying amounts of lime and flyash were used in the subbase to stabilize a medium to low PI clay. The wearing surface was a two course bituminous surface treatment covered by a one inch HMAC layer. The layout and cross section of the test site are given in Figure A-6 Appendix A, and Dynaflect deflection measurements in Tables F-21 to F-23 Appendix F.

1.4.7 Test Site 12 located on FM 2697 in Wheeler County The project was three miles long and consisted of 5 test sections of varying lengths. Each section is constructed of a 6 inch Flyash stabilized base on natural subgrade. Varying amounts of flyash were used in the base course to stabilize a coarse sandy soil of very low PI. The wearing surface is a two course bituminous surface treatment. The layout and cross section of the test site are given in Figure A-7 Appendix A, and Dynaflect deflection measurements in Tables F-24 to F-26 Appendix F.

1.4.8 Test Site 13 located on US 87 in Wilson County The project consisted of only one section constructed as a 6 inch lime-flyash stabilized base over a 12 inch river gravel flexible subbase.

The wearing surface was a 1 inch asphalt concrete surface. The layout and cross section are given in Figure A-8 Appendix A, and Dynaflect deflection measurements in Table F-27 Appendix F. This site was not included in the portion of study dealing with development of predictive equations and is evaluated for current stiffness in Chapter 4.

1.5 Research Approach

Stiffness coefficients and elastic moduli are properties used in the Texas flexible pavement system to characterize the structural support capability of pavement layers. Stiffness coefficients, derived from Dynaflect data by a trial-and-error procedure (15, 16) appear to be dependent on the thickness and location of pavement layers (2) and are not fully indicative of the stiffness characteristics of the layer material. The elastic modulus provides a more rational method for characterization and is a property measurable in laboratory for comparison and control.

Using elastic moduli as a measure of stress-strain behavior of pavement material layers, the approach taken in this research was to study and develop relationships between physical properties of constructed pavements and the assumed constants of the simplified deflection equation by Vlasov and Leont'ev (3). From these relationships, new equations, which would predict deflections and elastic moduli of lime-flyash stabilized layers with reasonable accuracy, were derived. The basic equation and the significance of the constants will be discussed in more detail in Chapter 3. The

Dynalect deflection measurements selected for the portion of study dealing with development of the new equations are identified in Table 2 and referenced to appropriate appendices. In Table 2, the "lime only" control sections are not included.

The pavement sections containing lime-flyash stabilized layers were classified into four categories by types of construction:

1. Lime-flyash stabilized base over lime or flyash stabilized subbase.
2. Hot mix asphalt concrete layer over flexible base and lime-flyash stabilized subbase.
3. Flexible base over lime-flyash stabilized subbase.
4. Flyash stabilized layer over natural subgrade.

To meet the defined objectives, the analyses were performed in the following steps, and the results are presented in Chapter 4:

- Step 1. Estimation of the elastic modulus of each pavement layer by a basin fitting technique for all test sections including "lime only" control sections, using multi-layered elastic theory.
- Step 2. Determination of vertical deflections in the pavement at selected depths below the surface at geophone location W_1 (see Figure 2) of the Dynalect, using multi-layered elastic theory.
- Step 3. Application of regression analysis number 1, described in Chapter 3, to vertical deflections computed in Step 2. Curve fitting constants were obtained for the

Table 2. Summary of test sites and Dynaflect deflection data selected for development of the deflection equation for lime-flyash stabilized sections.

Construction Type	Test site No	Selected sections		Deflection data age (months) ^a	Deflection data reference
		Section No	Number of Sections in Construction Type		
1	1	2,3,4,6 7,8,9,10	8	36	Table F-4 Appendix F
2	2	2,3,4,5, 6,7,8,9	8	37	Table F-6 Appendix F
3	3	1,2,3, 5,6	22	33	Table F-10 Appendix F
	4	2,3,4,5, 6		37	Table F-15 Appendix F
	5	1,2,3,4, 6,7,8		33	Table F-19 Appendix F
	8 ^b	2,3,4,5, 6		26	Table F-23 Appendix F
4	12	1,2,3,4, 5	5	22	Table F-25 Appendix F

^aConstruction types are defined on page 10. Deflection data is in reference to the construction date.

^bSite 8 is included in construction type 3 assuming no structural strength in the 1 in. HMAC layer.

sections and relationships were derived between the constant m (see page 54) and the physical properties of pavements for each type of construction.

Step 4. Application of regression analysis number 2, described in Chapter 3, utilizing relationships for constant m determined in Step 3 and field measured Dynaflect deflections at geophones location W_1 through W_5 (see Figure 2). Curve fitting constants were obtained for the sections and relationships were derived between the constants n , C , B and H (see page 71) and the physical properties for each type of construction.

Step 5. Application of regression analysis number 3, described in Chapter 3, utilizing relationships for constants m , n , C , B and H determined in Steps 3 and 4, and field measured Dynaflect deflections at geophone locations W_1 through W_5 . Predicted deflections and elastic moduli were computed for all lime-flyash stabilized sections.

Step 6. Determination of change in the stiffness of lime-flyash stabilized layers with time, by application of regression analysis number 3 to field measured data of different survey periods.

For practical considerations, it was necessary in this study to utilize average deflection measurements of sections instead of individual basin readings. The average basin was computed from the average of each deflection sensor.

2. METHODS FOR DEFLECTION ANALYSIS

The past decade has witnessed a trend towards increased use of non-destructive methods of testing to evaluate structural support capability of flexible pavements. A wide variety of computer based methods, available as analytical tools, have been developed to utilize field measured deflection data to determine elastic moduli of pavement layers and permit overall evaluation of the pavement system with reasonable accuracy. In this chapter a brief description of the state-of-the-art analytical techniques for determination of material properties from field measured deflections is given. The Dynaflect, as a field deflection measurement device, is emphasized and special attention is devoted to the significance and interpretation of J_0 Bessel functions used in some of these techniques.

2.1 Deflection Measurement with Dynaflect

The Dynaflect operates on the principle of a vibratory force applied to the pavement surface by two masses rotating in opposite directions. This induces a cyclic peak-to-peak live load of 1000 pounds with a frequency of 8 Hz applied on two steel load wheels in contact with the pavement. The load induced deflections are measured by five geophones at 12 inch intervals (10, 15, 17). The measured deflections are indicative of the displacement and shapes of deflected surface, as shown in Figure 2, at distances of 10, 15.62, 26, 37.36 and 49.03 inches from load points. Figure 3 indicates the location of loading points, and Figure 4 documents the contact radius of each load

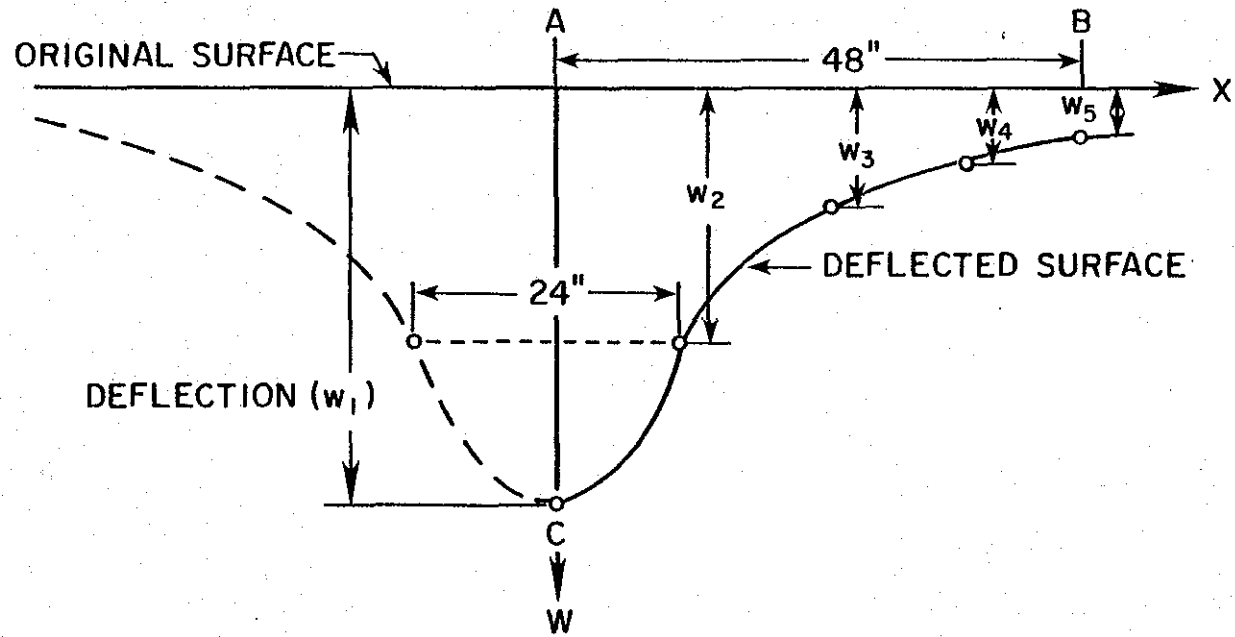


Figure 2. Typical deflection basin reconstructed from Dynaflect readings. Only half of the basin is measured (15).

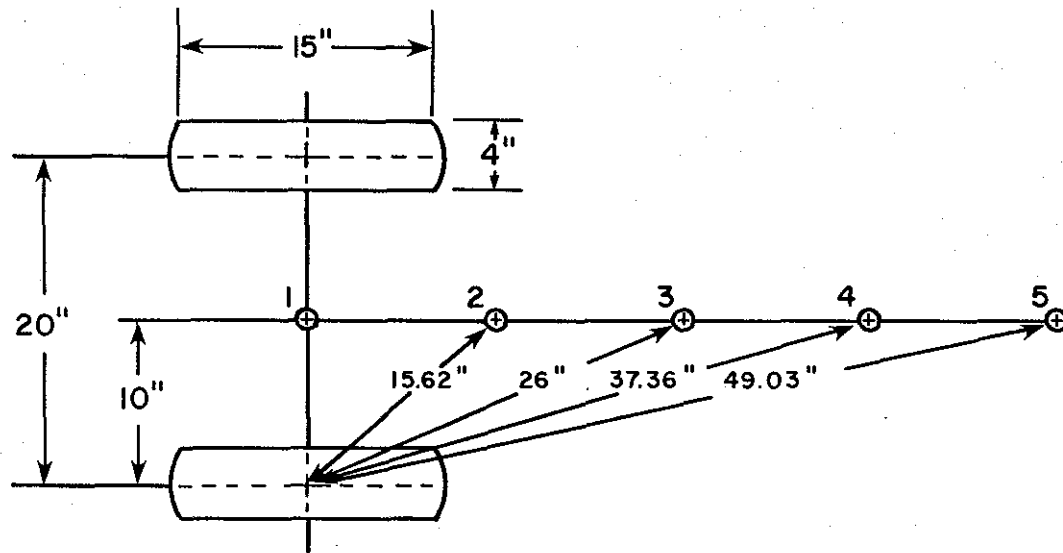
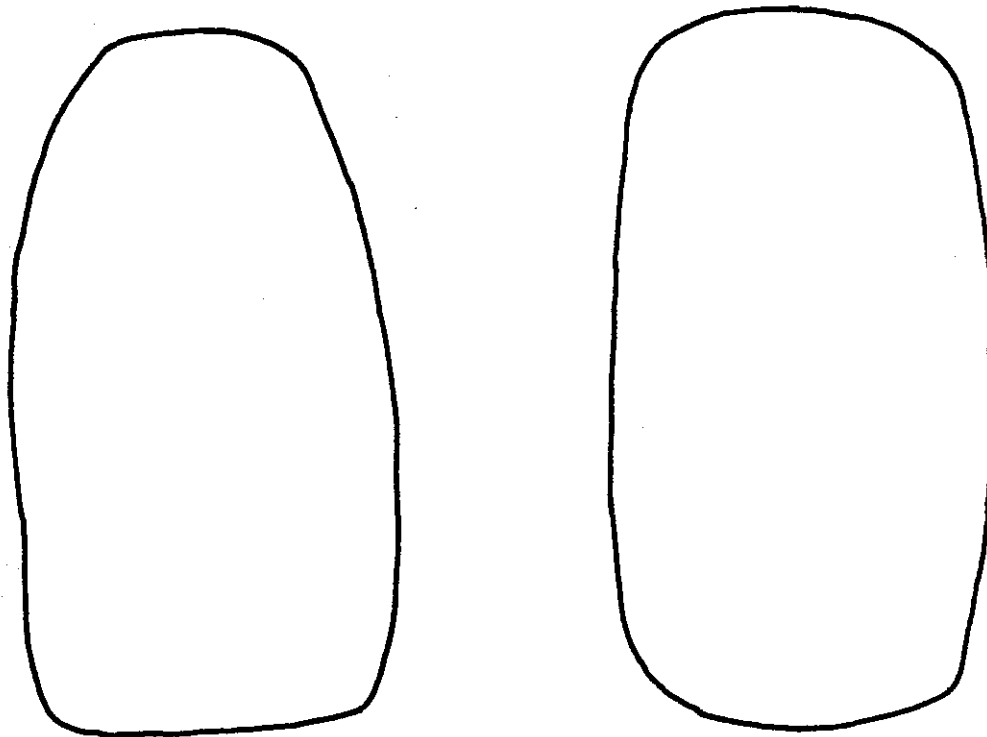


Figure 3. Radial location of Dynaflect sensors from loading points. (10)



Average contact radius of each load approximately 1.41 inches.

Figure 4. Actual imprint of Dynaflect loading wheels taken during field testing at Texas Transportation Institute on July 14, 1969. (Note: The distance between these imprints is not shown to scale. The actual distance is 20 inches.)

estimated to be 1.41 inches.

2.2 Significance and Interpretation of Bessel Functions

Bessel mathematical functions, named after the German astronomer F. W. Bessel, present solutions in the form of infinite series that are useful in interpreting the effect of a vibratory load applied on the pavement surface. Multi-layered elastic theory makes wide use of Bessel functions in the computations of stresses, strains and deflections (9). The generalized Bessel differential equation is of the form:

$$x^2 y'' + xy' + (x^2 - n^2)y = 0 \quad (2-1)$$

where: $n \geq 0$, y'' is the second derivative and y' is the first derivative with respect to x .

Solutions of the differential equation are called Bessel functions of the order n .

2.2.1 Bessel Function of the First Kind and Order Zero $J_0(x)$

By the theory of differential equations, the equation (2-1) has two distinct and linearly independent solutions. The first solution, $J_n(x)$, of the differential equation is called the Bessel function of the 'first kind and order n ' and is of the form:

$$J_n(x) = \frac{x^n}{2^n \Gamma(n+1)} \left\{ 1 - \frac{x^2}{2(2n+2)} + \frac{2x^4}{2 \cdot 4(2n+2)(2n+4)} \dots \right\} \quad (2-2)$$

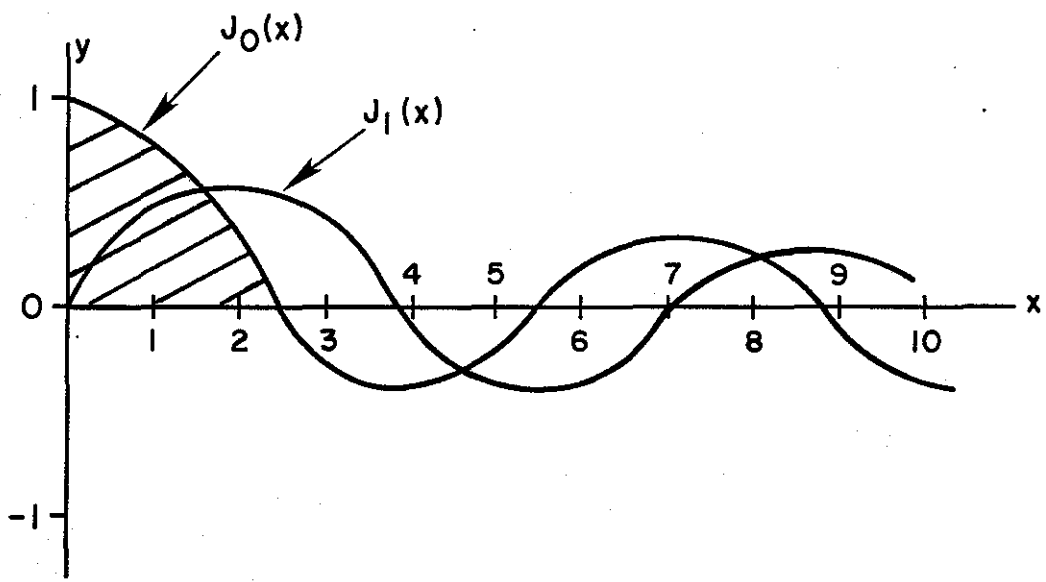


Figure 5. Graphical representation of Bessel functions of the first kind - $J_0(x)$ and $J_1(x)$.

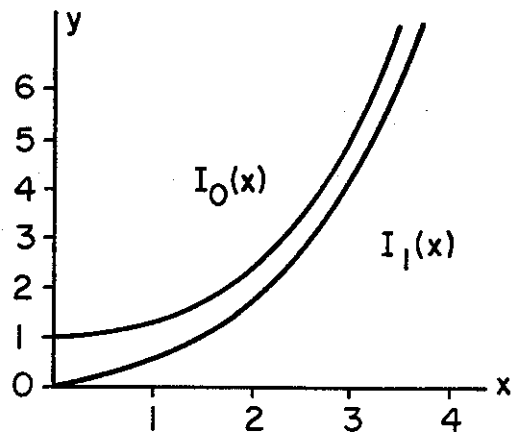


Figure 6. Graphical representation of modified Bessel functions of the first kind - $I_0(x)$ and $I_1(x)$.

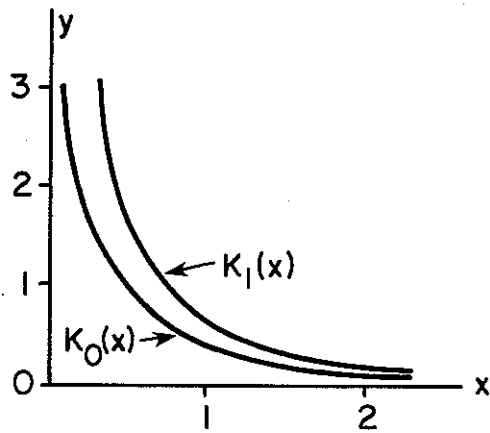


Figure 7. Graphical representation of modified Bessel functions of the second kind - $K_0(x)$ and $K_1(x)$.

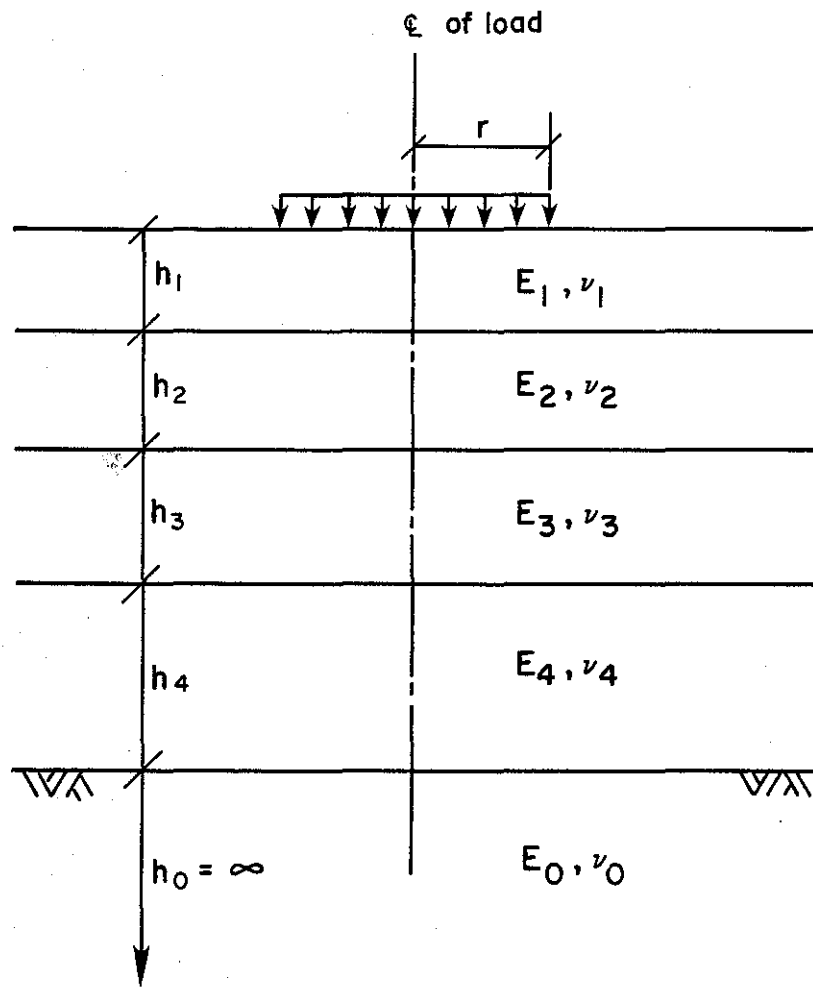
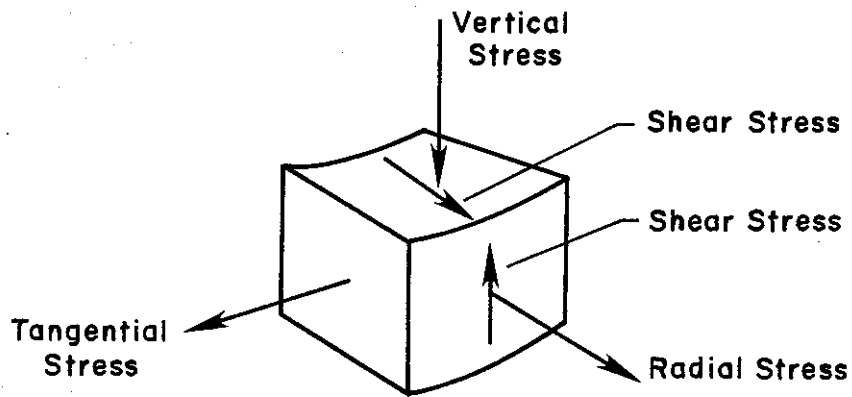


Figure 8. Schematic of multi-layered elastic system (18).



$$\text{Bulk Stress} = \text{Vertical} + \text{Radial} + \text{Tangential}$$

Figure 9. Stresses on a typical element r -inches from axis of the load and z -inches below the surface (18).

where: x = argument of the Bessel function

$n = 0, 1, 2, 3 \dots$ and

$\Gamma(n + 1)$ = gamma function with argument $n + 1$.

When n is equal to zero, the solution $J_0(x)$ is called the Bessel function of the 'first kind and order zero' and is represented by:

$$J_0(x) = 1 - \frac{x^2}{2^2(1!)^2} + \frac{x^4}{2^2(2!)^2} - \frac{x^6}{2^6(3!)^2} + \dots \quad (2-3)$$

The series represented by equation (2-3) and its derivatives are absolutely convergent for finite values of x and uniformly convergent in any bounded region of the x -plane. $J_0(x)$ is graphically represented in Figure 5. The positive range of $J_0(x)$, shown shaded in Figure 5, is particularly representative of the slope of the deflection basin. $J_0(x)$ forms the basis of this study. Figures 6 and 7 represent modified forms $I_n(x)$ and $K_n(x)$ of the Bessel function, which are the second kind of solutions to Bessel's differential equation.

2.3 Methods for Computing In-situ Elastic Moduli

2.3.1 Multi-layered Elastic Theory Approach General concepts of a multi-layered elastic system are depicted in Figures 8 and 9. The analysis of stresses, strains and deflections are primarily derived from the theory of distribution of stresses in an unstratified semi-elastic medium under the compressive action of a rigid body presented by Boussinesq in 1885 and generalized to layered systems by

Burmister in 1943. The analytical solution to the state of stress or strain has several assumptions:

1. Each layer acts as a continuous, isotropic, homogeneous and linearly elastic medium.
2. Each layer has a finite thickness except for the lower layer, and is infinite in the horizontal directions.
3. Full friction is developed between layers at each interface.
4. Surface shearing forces are not present at the surface.
5. The stress solutions are characterized by two material properties for each layer. They are Poisson's ratio, and Young's elastic modulus, E.

Computer programs developed by Shell Research N.V. namely BISTRO (BITumen Structures in Roads) and BISAR (BITumen Structures Analysis in Roads) are suited for n-layer computations and are based on an extension of the Burmister theory taking into account full three dimensional linear elasticity of the pavement layers. The effect of each load is separately calculated in a cylindrical coordinate system. Stresses, strains, and displacements are computed by integration of complex expressions involving Bessel functions (9).

McCullough and Taute (7) applied the BISAR computer program to estimate elastic moduli of layers of rigid pavement systems using a trial-and-error procedure. A similar method was utilized in this study for computing the initial values of elastic moduli for the test sections and is explained in more detail in Chapter 4.

2.3.2 "Empi" Method Swift (19) derived an empirical equation

for predicting pavement surface deflections of 2-layer elastic structures based on a Poisson's ratio value of 0.5. The concept is illustrated in Figure 10 and the equation is of the form:

$$w = \frac{3P}{4\pi} \cdot \frac{1}{rL} \left[\frac{1}{E_1} + \left(\frac{1}{E_2} - \frac{1}{E_1} \right) \left(\frac{r}{L} + \frac{rx^2}{2L^3} + \frac{3rx^4}{2L^5} \right) \right] \quad (2-4)$$

where: w = Amount of deflection on the surface at distance r ,

P = Applied load,

E_1 = Elastic modulus of the pavement layer,

E_2 = Elastic modulus of the subgrade,

h = Thickness of pavement layer,

$$x^2 = 4h^2 \cdot \left(\frac{E_1 + 2E_2}{3E_2} \right)^{2/3} \quad \text{and}$$

$$L = (r^2 + x^2)^{1/2}.$$

The results obtained from equation (2-4) were found in close agreement to solutions based on Burmister's equations of multi-layered elastic theory. Moore (20) applied a regression analysis technique to fit the entire measured Dynaflect deflection basin to deflections computed from arbitrarily selected values of elastic moduli. Reasonable values of elastic moduli E_1 and E_2 were determined by an iterative process when the "root mean square error" of measured to computed deflections was minimized. Simple computations involved in equation (2-4) permitted substantial savings in computer use time when compared to Burmister's equations and Scrivner's 'Elastic Modulus I'

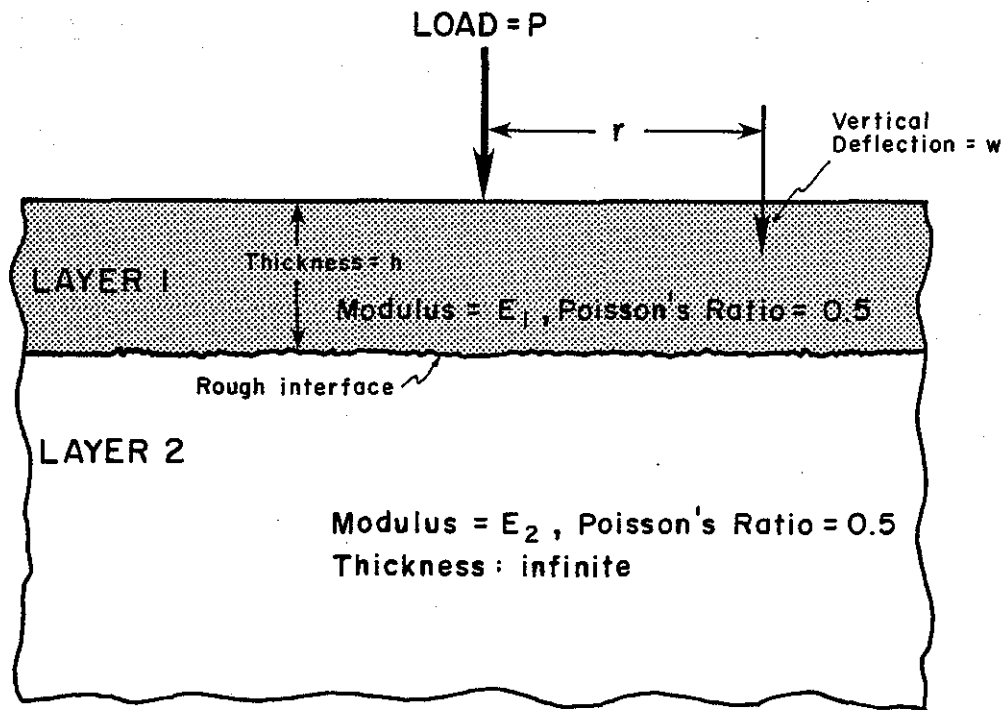


Figure 10. Schematic of a 2-layer elastic system (19).

method (16, 21).

2.3.3 "Elastic Modulus I" Method Scrivner et al., (21) applied concepts of multi-layered elastic theory to 2-layer pavement structures for determination of the in-situ material properties from Dynaflect data for the Texas flexible pavement system. For pavements of known thickness resting on homogenous subgrade of infinite depth and assuming a Poisson's ratio of 0.5, Scrivner's approximated equation is of the general form:

$$\frac{4\pi E_1}{3P} wr \cong 1 + \int_{x=0}^{x=10r/h} (V-1)J_0(x)dx \quad (2-5)$$

where: P = Point load acting vertically at the surface,

E_1 = Elastic modulus of the upper layer,

E_2 = Elastic modulus of the subgrade layer,

w = Vertical displacement of a point on the surface,

r = The horizontal distance of the measurement of the deflection w from the load P,

x = mr/h (where m is a parameter)

V = Function of m and N,

$$N = \frac{E_1 - E_2}{E_1 + E_2}, \quad (2-6)$$

$$V = \frac{1 + 4 N m e^{-2m} - N^2 e^{-4m}}{1 - 2N (1+2m^2) e^{-2m} + N^2 e^{-4m}}, \quad (2-7)$$

$J_0(x)$ = Bessel function of the first kind and zero order
with argument x and

N = a function of E_1 and E_2 .

Equation (2-5) is integrated in a converging solution process to determine values of E_1 and E_2 within desired accuracy limits. A detailed description of the solution is in reference (16). In this method also, solutions are computed by integration of complex expressions involving Bessel functions.

2.3.4 "Russian Equations" Method Equations formulated by Lytton et al., (1) are useful for predicting load induced deflections and elastic moduli in n-layer pavement structures at different Poisson's ratios. The general form of deflection equation used in this method is:

$$w(r,z) = \frac{C.P.}{\pi} \frac{1+v_0}{E_0} \cdot \frac{2m+1}{H^1} \cdot J_0(\alpha r) \cdot \left[\frac{H^1 - \bar{z}}{H^1} \right]^m \quad (2-8)$$

where: $w(r,z)$ = Deflection at radius r and depth z ,

P = Applied load (1000 lbs for Dynaflect),

E_0 = Elastic modulus of the subgrade,

v_0 = Poisson's ratio of the subgrade,

$J_0(\alpha r)$ = Bessel function of the first kind of order zero and argument αr ,

H' = Transformed depth of all layers converted to a single modulus, based on Odemark's assumption (3),

\bar{z} = Transformed depth of a point z below the surface,

$$\alpha = \frac{mB}{H'} \left[\frac{2(2mB + 1)}{(2mB - 1)(1 - \nu_0)} \right]^{1/2} \quad \text{and}$$

m, C, B = Constants determined analytically from field deflection data.

A non-linear regression analysis procedure called pattern search (22) was applied to field data and relationships of the constants to physical properties of pavement were derived. The derived relationships were used in equation (2-8) and by simple mathematical computations, deflections and elastic moduli were predicted from values of elastic moduli of the layers that were measured using wave propagation technique. Reasonably accurate values of elastic moduli of the layers were determined when the "sum of squared error" of computed to measured deflections was minimized. This method forms the basis of this study and its theoretical background is explained in more detail in Chapter 3.

3. THEORETICAL BACKGROUND AND STATISTICAL PROCEDURE

3.1 Deflection Equation for Single Elastic Layer

Vlasov and Leont'ev (3) postulated a simplified form of elastic layer theory. Figure 11 depicts the load distribution system of an elastic layer of thickness H resting on a rigid incompressible layer, where load P is applied to rigid circular plate of radius r_0 . For all radii greater than r_0 , the deflection of the elastic layer could be determined by the equation (3-1). While detailed theoretical development is given in reference (3), the forms of equation pertinent to this study are derived in the text.

$$w(r,z) = \frac{3P}{\pi} \frac{(1+\nu_1)}{E_1 H \psi_t} K_0(\alpha r) \psi_1(z) \quad (3-1)$$

where: $w(r,z)$ = vertical deflection at radius r and depth z ,

E_1 = the elastic modulus of the layer,

r = the radius,

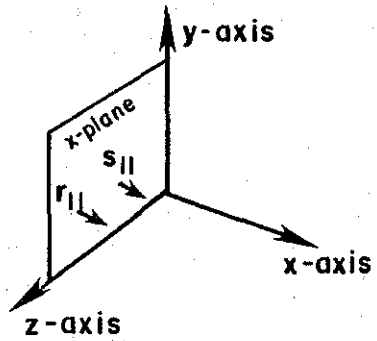
P = applied point load,

z = depth below the surface,

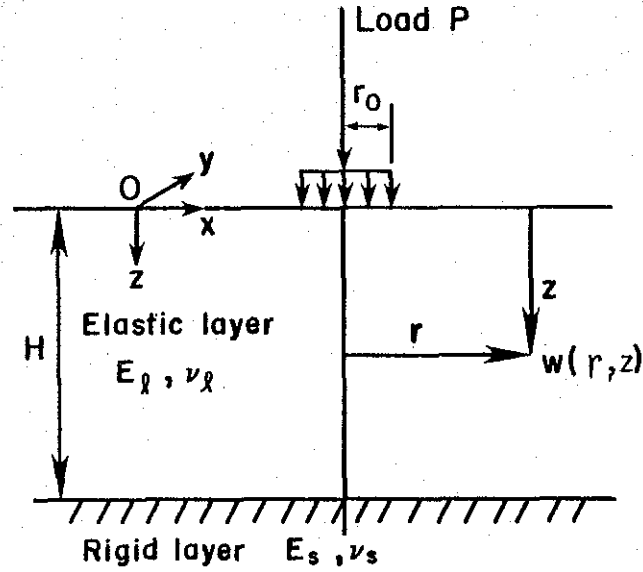
$K_0(\alpha r)$ = modified second kind Bessel function of order zero with argument r and

ν_1 = Poisson's ratio of the elastic layer.

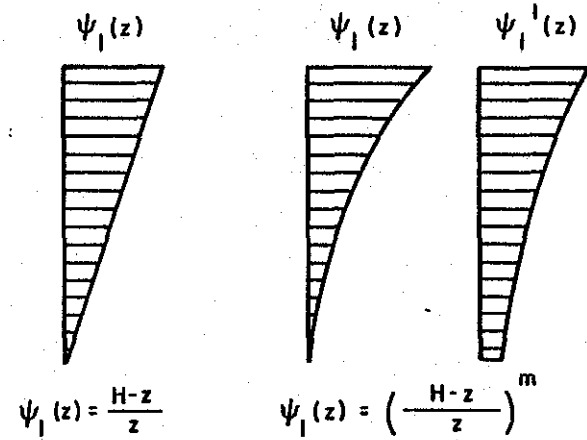
$\psi_1(z)$ signifies the distribution of vertical displacement with depth and is assumed to be related to H and z . In thin compressible



Interpretation of coefficients $r_{||}$ & $s_{||}$



Schematic of single elastic layer



Distribution forms of vertical displacements

Figure 11. Load distribution system of a single elastic layer over a rigid layer.

layers, the principal stress σ_z is assumed to be constant over the depth of the layer and therefore the displacement would decrease linearly with increasing depth, as shown in Figure 11 (page 31) and $\Psi_1(z)$ would be represented by:

$$\Psi_1(z) = \frac{H-z}{z} \cdot \quad (3-2)$$

For a thick compressible layer, Vlasov and Leont'ev (3) recommended a distribution form represented by equation (3-3) and suggested that other suitable expressions would also be appropriate:

$$\Psi_1(z) = \frac{\text{Sinh } \gamma (H-z)}{\text{Sinh } \gamma H} \cdot \quad (3-3)$$

Gamma γ , is a constant determining the rate of decrease of the displacement with depth.

Alpha α , in equation (3-1) is defined as a ratio characterizing the combined effect of compressive strain and shearing strain in the elastic layer and is represented by:

$$\alpha = \left(\frac{k}{2t}\right)^{1/2} \cdot \quad (3-4)$$

The coefficient k characterizes the compressive strain in the elastic layer:

$$k = \frac{E_1 s_{11}}{1-\nu_1^2} \cdot \quad (3-5)$$

The coefficient t characterizes the shear strain in the elastic layer:

$$t = \frac{E_1 r_{11}}{4(1 + \nu_1)} \quad (3-6)$$

In equations (3-5) and (3-6), s_{11} and r_{11} are parameters characterizing compressive strain and shear strain respectively in the X plane and the X direction.

ψ_k and ψ_t are defined as distribution forms of compressive and shear strains respectively, and are related to $\psi_1(z)$ and its derivative $\psi_1'(z)$, and s_{11} and r_{11} defined previously:

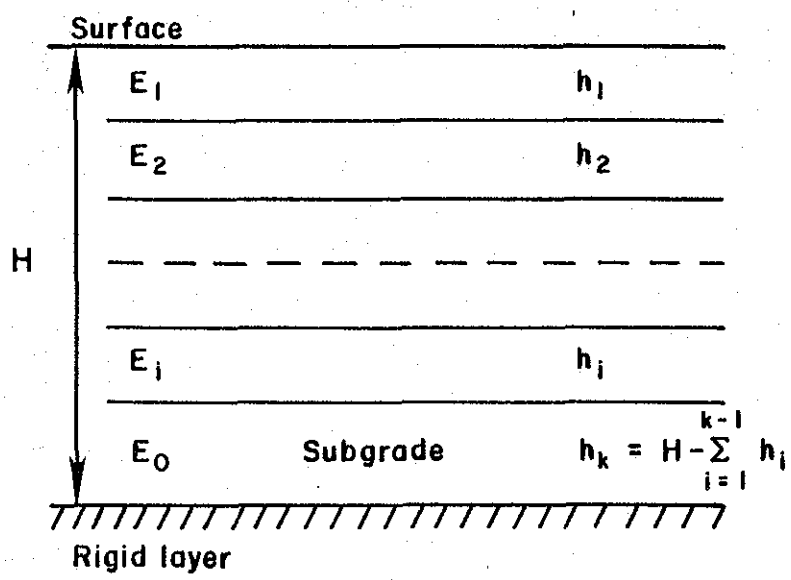
$$s_{11} = \frac{k}{H} = \int_0^H \psi_1'^2(z) dz, \quad (3-7)$$

$$r_{11} = \frac{H\psi_t}{3} = \int_0^H \psi_1^2(z) dz. \quad (3-8)$$

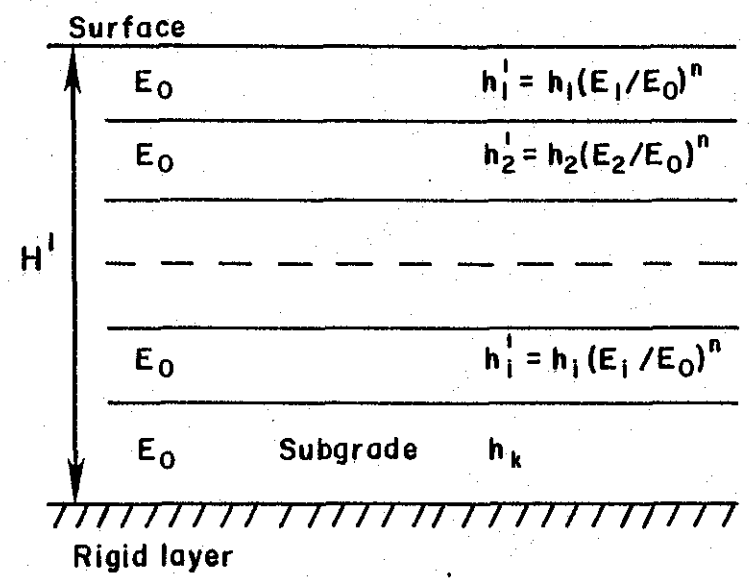
3.2 Odemark's Assumption

An assumption presented by Odemark (4) is useful in transforming the thickness of multiple elastic layers to an equivalent thickness of a material with a single datum elastic modulus. The concept as pertinent to this study is presented in Figure 12 where H is the distance of the rigid layer from the surface as in Figure 11, and h_k is the thickness of the subgrade layer assumed to behave elastically.

The transformed total thickness of all layers is of the form:



Pavement Thicknesses



Transformed Thicknesses in terms of Subgrade modulus E_0

Figure 12. Transformed thicknesses of k-layers for multi-layered pavements.

$$H' = \sum_{i=1}^k h_i \left(\frac{E_i}{E_0} \right)^n \quad (3-9)$$

where: H' = transformed depth of all layers,
 k = number of layers,
 h_i = thickness of layer i ,
 n = exponent to be found by analysis in this study,
equal to 0.33 in Odemark's assumption (4),
 E_i = Elastic modulus of layer i ,
 E_0 = Modulus of datum layer, assumed to be the subgrade
in this study and

$$h_k = H - \sum_{i=1}^{k-1} h_i \quad (3-10)$$

3.3 Derivation of Deflection Equation for Multi-layered Pavements

The distribution of vertical displacements for the single elastic layer were assumed to be represented by the exponential expression (2):

$$\psi_1(z) = \left(\frac{H-z}{H} \right)^m \quad (3-11)$$

where m is a constant dependent on the in-situ physical properties of a pavement structure.

Equations (3-1) and (3-4) are reformulated in terms of the form of the distribution of vertical displacement in the following

derivation steps. Substituting equation (3-11) in equation (3-8),

$$r_{11} = \frac{H}{3} \psi_t = \int_0^H \left(\frac{H-z}{H}\right)^{2m} dz, \quad (3-12)$$

and by integration

$$\psi_t = \frac{3}{2m+1}, \quad (3-13)$$

$$r_{11} = \frac{H}{2m+1} \quad (3-14)$$

$$\psi_{1,1}'(z) = \frac{d}{dz} \left(\frac{H-z}{H}\right)^m = \frac{-m}{H} \left(1-\frac{z}{H}\right)^{m-1} \quad \text{and} \quad (3-15)$$

$$\psi_{1,1}''(z) = \frac{m^2}{H^2} \left(\frac{H-z}{H}\right)^{2m-2} \quad (3-16)$$

Substituting equation (3-16) in equation (3-7) yields,

$$s_{11} = \frac{\psi_k}{H} = \int_0^H \frac{m^2}{H^2} \left(\frac{H-z}{H}\right)^{2m-2} dz \quad (3-17)$$

and by integration

$$s_{11} = \frac{m^2}{H(2m-1)} \quad (3-18)$$

Substituting equation (3-13) in (3-1) and replacing the K_0 Modified Bessel function by the J_0 Bessel function, which is the basis of this study, equation (3-19) is obtained:

$$w(r,z) = \frac{P}{\pi} \frac{(1 + \nu_1)}{E_1} \frac{2m + 1}{H} J_0(\alpha r) \left[\frac{H-z}{H} \right]^m \quad (3-19)$$

where, $J_0(\alpha r)$ = First order Bessel function of order zero and argument αr

By substituting equation (3-14) and (3-17) in equation (3-4), equation (3-20) is obtained:

$$\alpha = \frac{m}{H} \left[\frac{2(2m + 1)}{(2m-1)(1-\nu_1)} \right]^{1/2} \quad (3-20)$$

Equations (3-19) and (3-20) are then modified to account for multiple layers in pavements utilizing equation (3-9) and (3-21):

$$\bar{z} = \sum_{i=1}^{l-1} h_i \left(\frac{E_i}{E_0} \right)^n + \left(z - \sum_{i=1}^{l-1} h_i \right) \left(\frac{E_l}{E_0} \right)^n \quad (3-21)$$

where \bar{z} is the transformed depth of point z in terms of subgrade modulus E_0 and l the number of layer in which z falls.

The revised equations for multi-layered pavements are:

$$w(r,z) = \frac{C}{\pi} \cdot P \cdot \frac{1 + \nu_0}{E_0} \frac{2m + 1}{H'} J_0(\alpha r) \left[\frac{H' - \bar{z}}{H'} \right]^m \quad (3-22)$$

$$\alpha = \frac{mB}{H} \left[\frac{2(2mB + 1)}{(2mB-1)(1-\nu_0)} \right]^{1/2} \quad (3-23)$$

where ν_0 = Poisson's ratio of datum subgrade layer.

For multi-layered pavements, the constant B is introduced to correct the value of the power law exponent m, and constant C is introduced to correct the derived deflection value in the equation (3-22). Equation (3-22) and (3-23) are the basis of this study, and constants m, n, C, B and H are to be determined for each type of pavement construction by statistical analysis of Dynaflect measured field data.

3.4 Statistical Analysis Procedure

The regression analysis procedure followed in this study assumes a non-linear relationship between the dependent variable y and the independent variable x. A non-linear regression model would be of the form:

$$\hat{y} = \beta_0 x^{\beta_1} \quad (3-24)$$

where \hat{y} = the predicted value of the dependent variable and
 β_0 and β_1 = constants derived by regression analysis.

From principles of simple linear regression analysis the "best" values of constants β_0 and β_1 would be obtained when a "least square" criterion is employed that minimizes the summed square of differences between an observed y and the predicted \hat{y} . To meet assumed conditions of non-linearity a method called pattern search (22), explained later in the text, was incorporated in the overall statistical analysis procedure of the study. The principal steps in the analysis are

explained as follows:

1. Assume a functional relationship between x and y , and write the equation (3-24) in the form:

$$\hat{y} = f(x). \quad (3-25)$$

2. Subtract the predicted value of dependent variable \hat{y} from observed value y and obtain error ϵ . Error is squared and added to errors of all the other observations:

$$\epsilon_j^2 = \sum_{j=1} [y_j - f(x)]^2. \quad (3-26)$$

where ϵ_j = error for the j th observation and

y_j = j th observation of y .

3. Apply pattern search technique and determine set of constants in $f(x)$ that minimize the sum of squared error in equation (3-26).

In summary, the statistical procedure applied in this study in regression analyses number 1, number 2 and number 3, which will be discussed in the following section, meets "least square" criterion typically used in linear regression analysis and employs pattern search technique to account for the non-linearity of relationships. The value of $J_0(x)$ was determined by polynomial approximation in the regression analysis.

3.4.1 Pattern Search Technique

The computer base pattern search method developed by Letto (22) relies on a non-linear optimization technique based on the method of

Hooke and Jeeves. While details of the program are available in the reference (22) a brief description follows:

If the problem has the objective function of two variables $z(X_1, X_2)$ and a base function $c(X_1, X_2)$ then at any point in question, the objective gradient is the vector sum of $|\frac{\partial z}{\partial X_1}| + |\frac{\partial z}{\partial X_2}|$ and the base gradient is the vector sum of $|\frac{\partial c}{\partial X_1}| + |\frac{\partial c}{\partial X_2}|$. Figure 13 illustrates the method in which the pattern search proceeds. The objective function is assumed circular with an optimum at point t_z at the center of the circle. This implies that the closer a point is to t_z the more nearly optimal it is. In simple terms a point is "better" than another point if the objective function evaluated at the first point is nearer to t_z than objective function evaluated at the second point. The program makes a series of exploratory searches around the starting point to find a direction that will lead to better points in the search. The incremental amount is assumed to be small and for purposes of discussion can be referred to as one unit.

Starting at the initial point of search, the program does an exploratory search by incrementing the variable X_1 by one unit positive reaching the point t_{oa} . Since t_{oa} is "better" than t_o , the incrementation of variable X_2 is conducted about point t_{oa} . Addition of one unit of variable X_2 leads to "poorer" point t_{ob} . The point t_{ob} is discarded and one unit of X_2 is subtracted from t_{oa} leading to t_o' which is "better" than t_{oa} . The program then conducts an accelerated

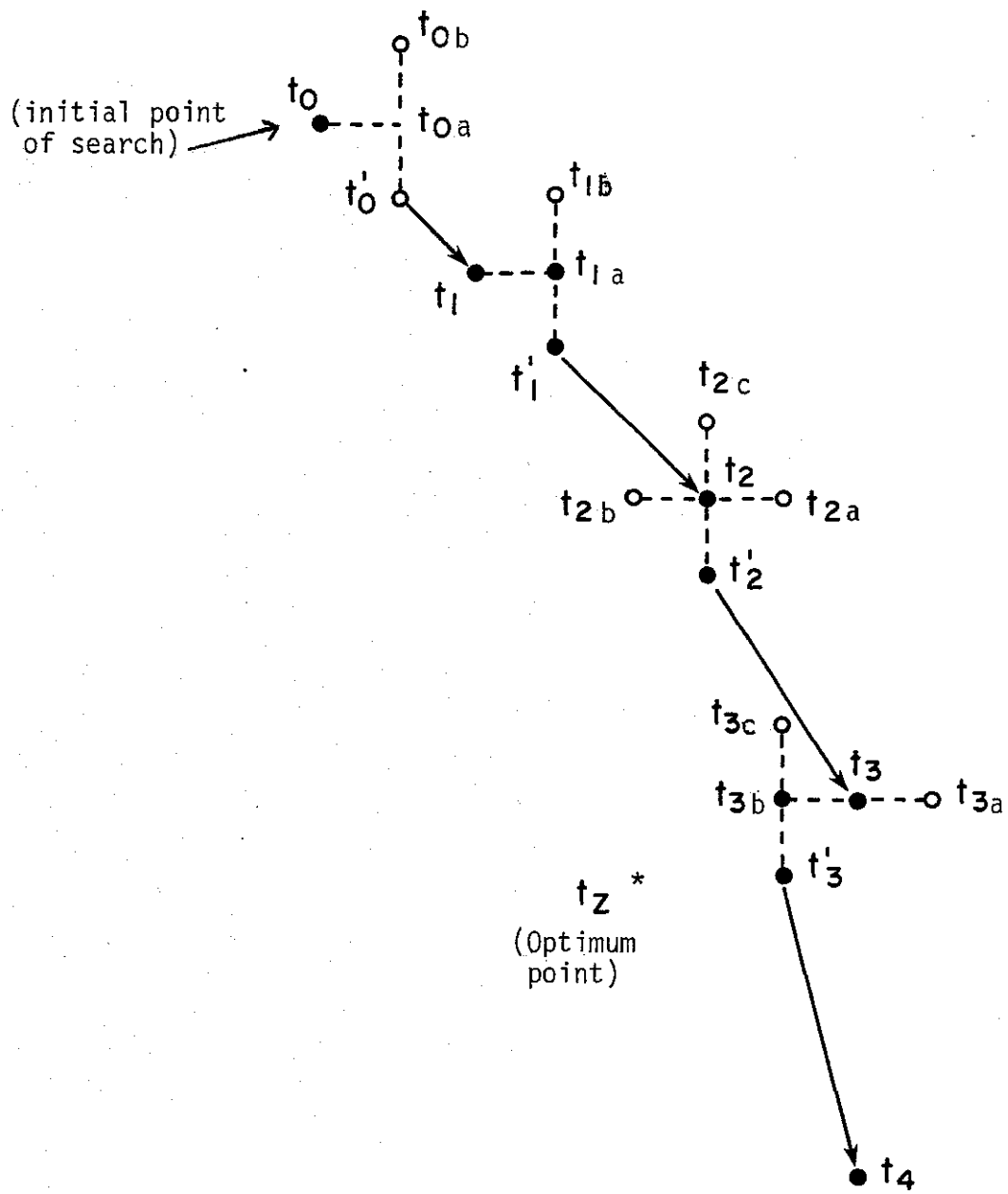


Figure 13. Pattern search technique (28).

search in direction $t_0 t_0'$ and determines point t_1 which is "better" than t_0' . Exploratory search is started again at point t_1 with values of variables X_1 and X_2 incremented again one-at-a-time. After the effect is evaluated the pattern is allowed to move to t_1' and accelerated to t_2 . By repeat processing the "best" point t_3' is obtained. A further pattern move to point t_4 is observed to be deleterious to optimization. Therefore the program rejects the pattern move.

In summary, the application of the pattern search procedure to the statistical analysis technique, provides the capability of evaluating the effect of several variables in a mathematical model. For example, if the models of deflection equations (3-22) and (3-23) are used, the constants m , n , C , B and H would be individually iterated, and evaluated after each iteration, until a "computed deflection basin" that closely resembles the shape of the "field measured deflection basin" is obtained.

3.4.2 Regression Analysis Number 1 to Determine the Constant m

In this analysis, illustrated in Figure 14, the variation of vertical displacement of the pavement structure with depth was studied on the basis of the concept introduced in equation (3-2) and modified in equation (3-22) for multi-layered pavements. The form of the deflection relationship is affected by depth is assumed to be:

$$w(r, \bar{z}) = w(r, 0) \left[\frac{H - \bar{z}}{H} \right]^m \quad (3-27)$$

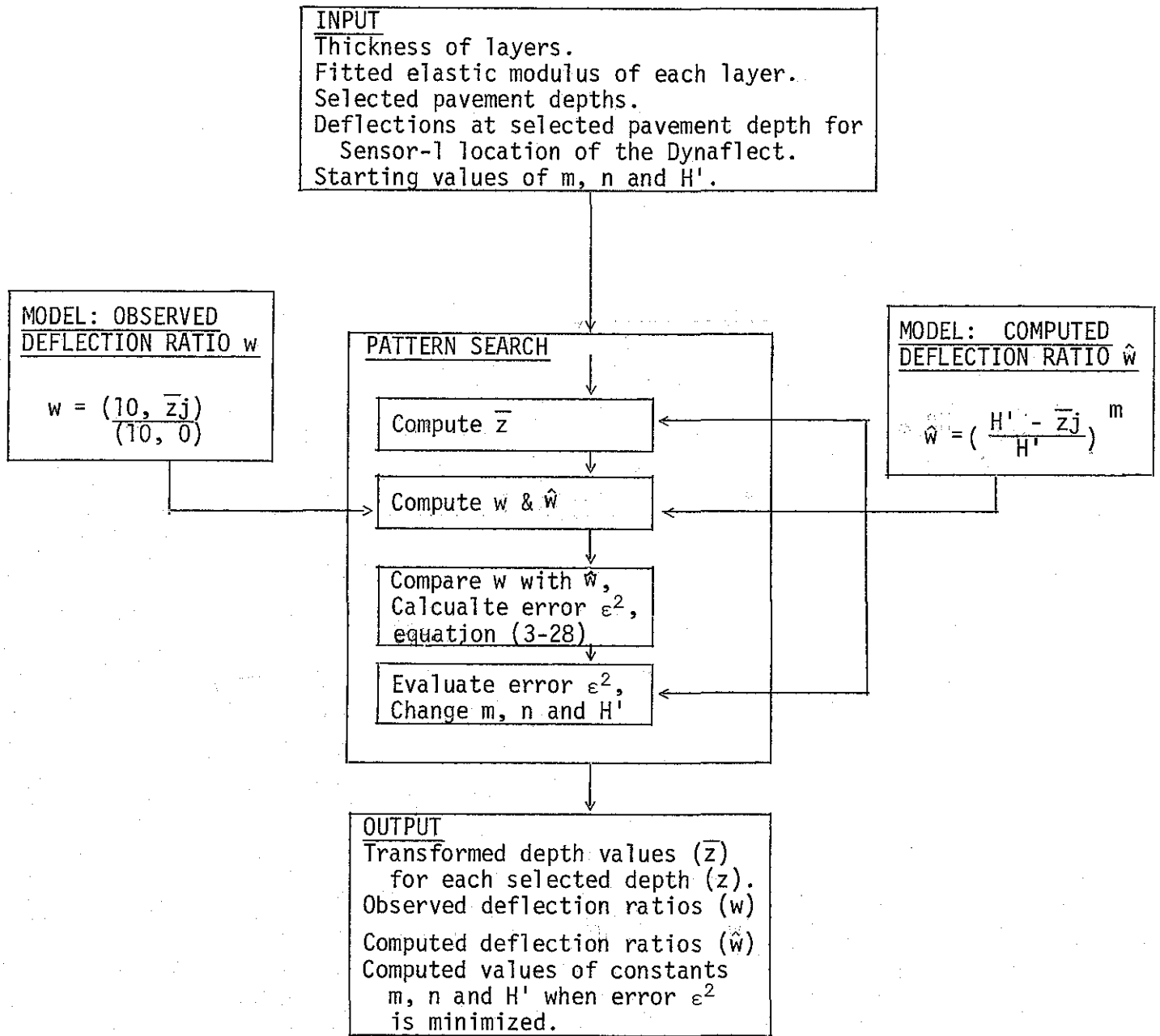


Figure 14. Flow chart for Regression Analysis Number 1.

where: $w(r,z)$ = the deflection at transformed depth z of the pavement and

$w(r,0)$ = observed deflection at the pavement surface at geophone location W_1 .

The objective of this study was to determine the values of constants m , n and H' for each test section, and establish relationships between the exponential constant m and physical properties of pavement layers for each type of construction.

The procedure utilizes the "squared error" criterion defined by equation (3-28). The regression was accomplished employing starting values of constants m , n and H' of 1.0, 0.33 and 70 inches respectively:

$$\epsilon_j^2 = \left[\frac{w(10, \bar{z}_j)}{w(10,0)} - \left(\frac{H' - \bar{z}_j}{H'} \right)^m \right]^2 \quad (3-28)$$

where: ϵ_j = error for the j th observation

$w(10, \bar{z}_j)$ = Deflections at Dynaflect geophone location W_1 for selected depths z , determined by a separate analysis described in Chapter 5 and

$w(10,0)$ = Observed deflection at Dyanflect geophone location W_1 on the pavement surface.

3.4.3 Regression Analysis Number 2 to Determine Constants n, C, B and H

In this analysis, illustrated in Figure 15, the relationships of exponential constant m and physical properties of pavement layers,

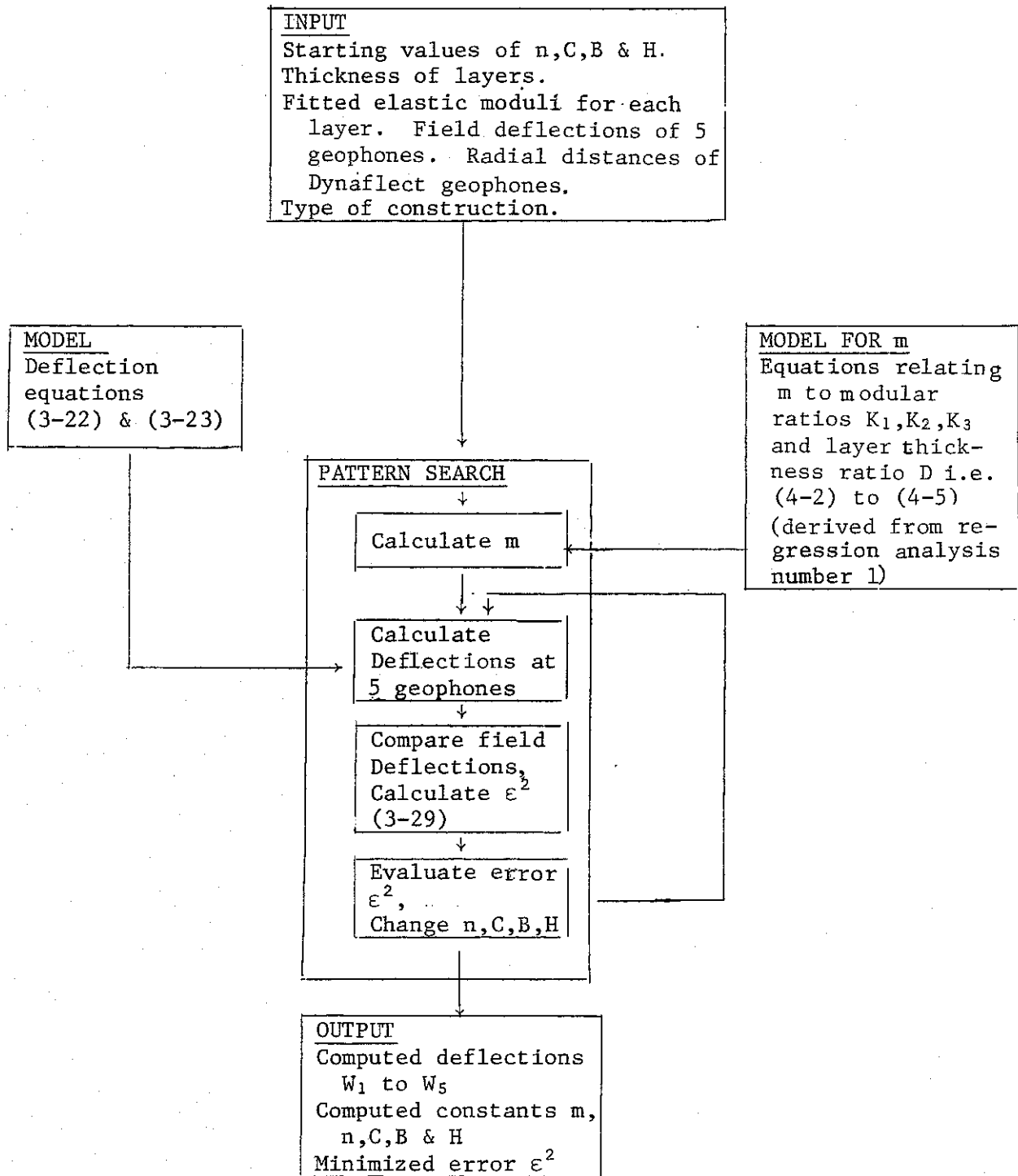


Figure 15. Flow chart for Regression Analysis Number 2.

that were derived from the vertical displacement study in regression analysis number 1, were used to determine values of constants n, C, B and H for all lime-flyash stabilized sections. The objectives were to establish relationships of these constants with the physical properties of pavements. The analysis utilized the surface deflection measurements at the five geophones locations and evaluated the entire deflection basin to minimize the "sum of squared error" in the equation:

$$\sum_{j=1}^5 \epsilon_j^2 = [w(r_j, 0) - \text{C.P.} \cdot \frac{1 + \nu_0}{E_0} \cdot \frac{2m + 1}{H^1} \cdot J_0(ar_j)]^2 \quad (3-29)$$

where: ϵ_j = error in observation at radius r_j and
 r_j = Standard radial distances of Dynaflect geophones from applied load i.e. 10, 15.62, 26, 37.3 and 49.03 inches.

The regression study was accomplished employing starting values of the constants n, C, B and H of 0.30, 1.0, 1.0 and 70 inches respectively.

3.4.4 Regression Analysis Number 3 to Predict Deflections and Elastic Moduli

This analysis constitutes the final predictive step of the study and was accomplished using the concepts illustrated in Figure 16. The relationships established from regression analysis number 1 and number 2 for constants m, n, c, B and H were utilized to compute deflections

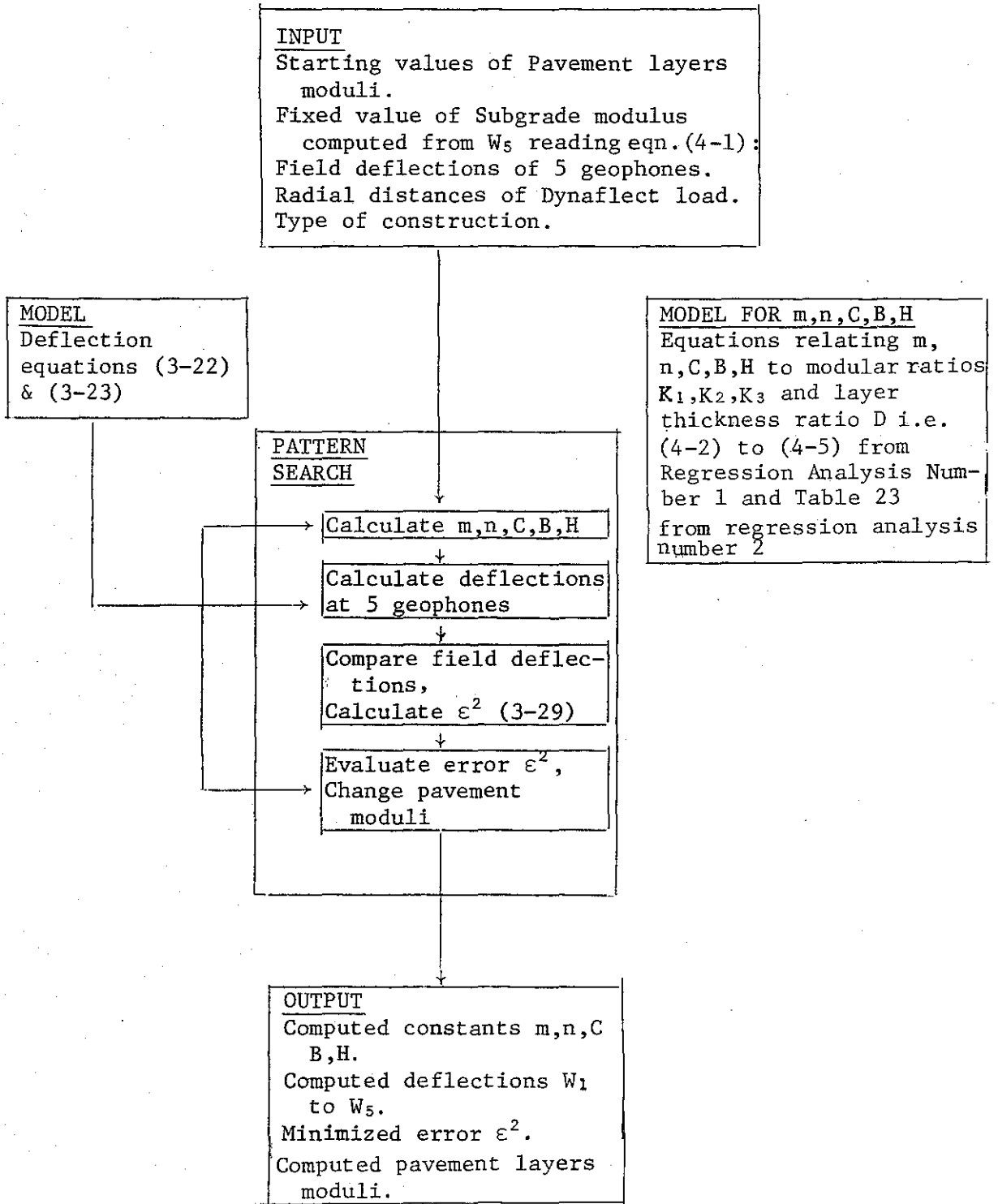


Figure 16. Flow chart for Regression Analysis Number 3.

and elastic moduli of the pavement layers. In this analysis, the deflection model of equations (3-22) and (3-23) and the error equation (3-29) were used.

4. ANALYSIS AND RESULTS

4.1 Deflection Basin Fitting Analysis

In order to study the variables that govern the behavior of pavements under an induced load, it is necessary that the stress-strain characteristics of the pavements be estimated first. In this study, the elastic moduli of the various layers of the test sections, summarized in Table 1, were estimated by a deflection basin fitting technique.

The elastic moduli of pavement layers were estimated from Dynaflect deflection measurements employing the multi-layered elastic approach with the aid of the Shell BISTRO computer program. The following steps were followed:

1. Thickness of pavement layers, initial estimates of the pavement layer elastic moduli, the Dynaflect induced load of 1000 lbs and "loading configuration" were input into the computer program and vertical deflections were analytically computed at the five geophone locations of the Dynaflect. The Poisson's ratio of layers were assumed for HMAC layer, flexible base, lime-flyash stabilized layers and the natural subgrade as 0.40, 0.45, 0.15 and 0.45, respectively (12, 13).
2. Field measured deflections were individually compared with the five computed deflections and the overall fit of the basin determined.

3. The initial layer moduli used in the computer program were adjusted to improve the fit of the computed to measured deflection basin.
4. The process was repeated until a reasonable accuracy of fit imposed by an "average percentage variation", criterion, explained later in this section, was achieved.

Observations made in application of the procedure are generally in agreement with the findings of McCullough and Taute (7) on rigid pavements as follows:

1. Variations in the elastic moduli of the base or subbase influences sensor-1 deflection significantly but has only a minor effect on sensor-5 deflections, implying that the slope of the basin is affected.
2. Variations in the elastic moduli of the subgrade significantly affects both sensor-1 and sensor-5 deflections. This effect is generally proportional and thus has a minimal effect on the slope of the basin.

Sensor-5 deflection is observed to be a unique indicator of the stiffness of the subgrade and predicts the elastic modulus of the subgrade accurately.

The slope of the deflection basin is observed to be dependent on the stiffness of the layers above the subgrade. For 2-layer pavements the predicted elastic moduli of these layers were observed to be fairly accurate. In pavement structures of more than two layers, it must be recognized that several combinations of base and subbase

moduli may predict approximately the same basin slope. Therefore, for greater accuracy in predicting the modulus of the top layers the deflection basin fitting procedure applied in this study was restricted to "stiffer on top" solutions only.

4.1.1 "Average Percentage Variation" Criterion

A simple acceptance criterion was imposed to evaluate the overall fit of the computed to measured deflection basin. The elastic moduli of the layers were adjusted repeatedly until the average percentage variation of the computed deflections at the five geophone locations were within five percent of the field measure deflections.

If Wf_1, Wf_2, Wf_3, Wf_4 and Wf_5 are field measured deflections and Wa_1, Wa_2, Wa_3, Wa_4 and Wa_5 are analytically derived deflections, then the percentage variation at the i th geophone location is given by

$$\text{Variation}_i = \frac{|Wf_i - Wa_i|}{Wf_i} \times 100$$

The average percentage variation of the entire deflection basin is given by

$$\text{Variation}_{\text{basin}} = \frac{\sum_{i=1}^5 \text{Variation}_i}{5}$$

where: $i = 1, 2, 3, 4, 5$.

4.1.2 Fitted Elastic Moduli Results

The values of layer elastic moduli obtained by the basin fitting technique for 51 sections including "lime only" control sections, are presented in Tables B-1 to B-16 in Appendix B.

Sensor-5 deflections are observed to be highly correlated to the stiffness of the subgrade and capable of predicting the subgrade modulus accurately. Figure 17 depicts graphically the log-log relationship between the subgrade modulus and W_5 deflections, established from multi-layered elastic theory for all lime-flyash stabilized sections of this study. The relationship was tested by applying the general linear model (GLM) procedure. Equation (4-1) describes the relationship:

$$E_{sg} = \frac{e^{8.64}}{W_5} \quad (4-1)$$

where: E_{sg} = Elastic modulus of subgrade in psi,

W_5 = Sensor-5 field reading of the Dynaflect in mils.

The equation established a significant relationship between E_{sg} and W_5 at the level of α equal to 0.1. The R-Square value was 0.99.

4.2 Regression Analysis Number 1

The first step of this analysis was the analytical determination of the vertical displacement with depth. All sections containing lime-flyash stabilized layers as summarized in Table 2 were analyzed at Dynaflect geophone location W_1 for eight depths selected at the pavement surface, at the interfaces of the layers and at one foot

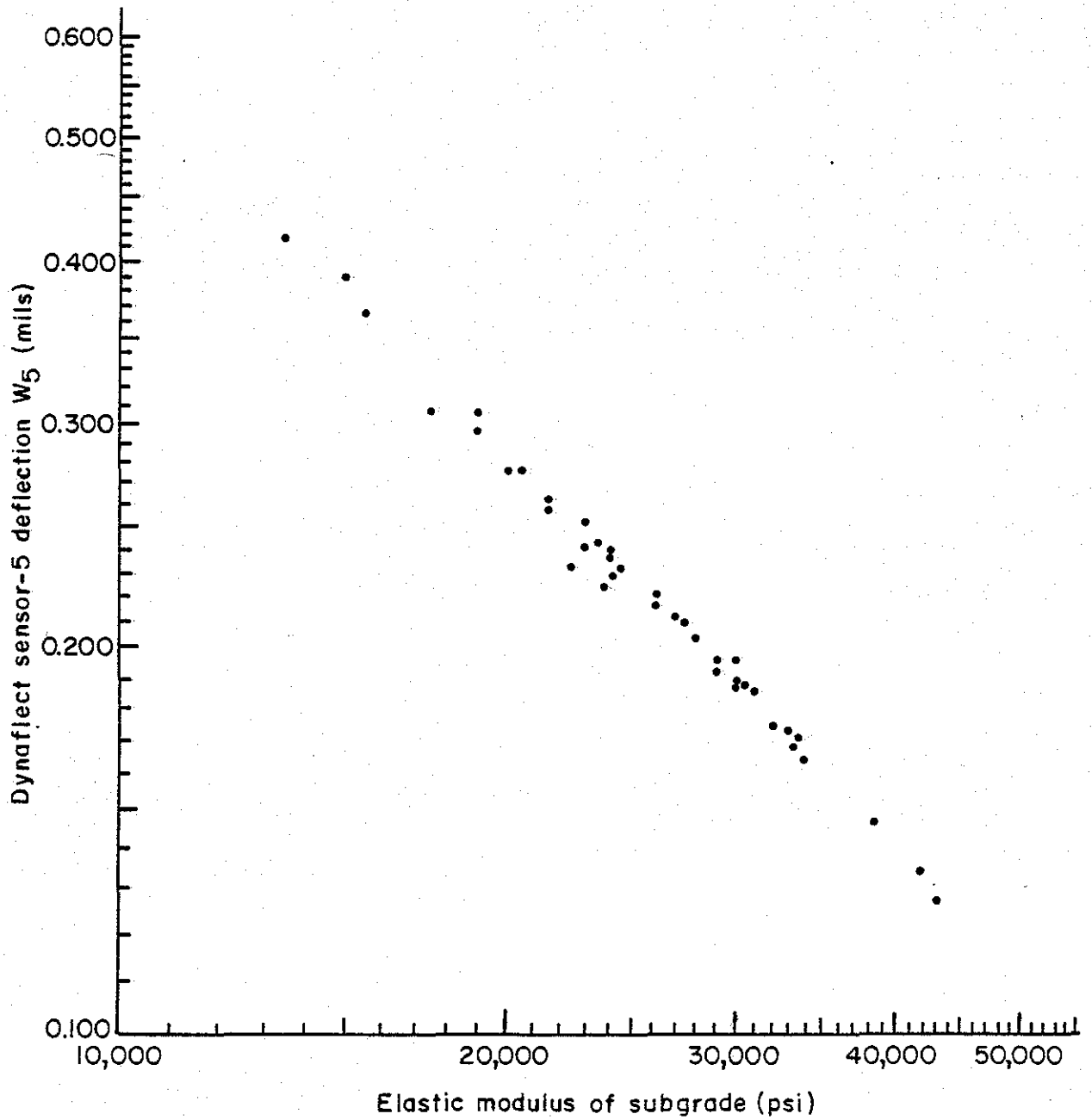


Figure 17. Subgrade modulus as a function of Sensor-5 reading of the Dynaflect, in the log-log form.

depth thereafter. The Shell BISTRO computer program was used to determine vertical displacement values given in Tables C-1 to C-7 in Appendix C.

Regression analysis number 1, explained in Chapter 3 (see Figure 14), was applied to all sections containing lime-flyash stabilized layers employing the results of elastic moduli from basin fitting analyses, the results of vertical displacements with depth analysis, the deflection model according to equation (3-27) and the error model according to equation (3-28).

From this procedure the values of constants m , n and H' were obtained for each test section, as were computed values of transformed depth \bar{z} at each selected depth z . The results of the analysis and "sum of squared error" between computed and field deflections are given in Tables 3 to 9. In Figure 18, the values of the constant m are plotted versus values of \bar{z} , where z is based on the total pavement thickness above the subgrade for each test site. The constant m was observed to be dependent on the type of construction of the pavement sections.

4.2.1 Effect of Physical Properties of Pavements on Constant m

The pavement sections of this study were of the same thickness for all construction types except construction type 3*, therefore, two physical properties, namely "modular ratios K_1 , K_2 and K_3 " and "layer thickness ratio D ", were investigated as predictors of the constant m .

*The construction types are defined on page 11.

Table 3. Values of Constants m, n and H' determined by Regression Analysis
 Number 1 - Site 1^a.

Section No	Transformed depth \bar{z} at depth z (in inches):							Values of constants		
	8	16	28	40	52	64	76	m	n	H'
2	12.19	20.56	32.56	44.56	56.56	68.56	80.56	1.80460	0.30001	132.49
3	16.45	30.36	42.36	54.36	66.36	78.36	90.36	0.65666	0.30000	96.011
4	16.45	29.41	41.41	53.41	65.41	77.41	89.41	0.73517	0.30004	99.586
6	12.29	21.13	33.13	45.13	57.13	69.13	81.13	1.50040	0.30000	121.13
7	11.89	19.99	31.99	43.99	55.99	67.99	79.99	2.09940	0.30004	143.97
8	13.72	21.80	33.80	45.80	57.80	69.80	81.80	1.67090	0.30000	126.14
9	12.43	20.83	32.83	44.83	56.83	68.83	80.83	1.69700	0.30001	127.83
10	12.97	21.31	33.31	45.31	57.31	69.31	81.31	1.69800	0.30002	128.09

Note: For analytically determined vertical displacement with pavement depth used in this analysis refer to Table C-1 Appendix C.

^aConstruction type 1 - L-FA base over L or FA subbase.

Table 4. Values of Constants m, n and H' determined by Regression Analysis
 Number 1 - Site 2^a.

Section No	<u>Transformed depth \bar{z} at depth z (in inches):</u>							<u>Values of constants</u>		
	2	14	22	34	46	58	70	m	n	H'
2	4.21	19.79	30.18	42.18	54.18	66.18	78.18	0.74735	0.30002	92.801
3	4.18	23.23	33.97	45.97	57.97	69.97	81.97	0.55430	0.30001	86.238
4	4.07	22.26	32.94	44.94	56.94	68.94	80.94	0.59032	0.30002	87.754
5	4.38	25.29	36.77	48.77	60.77	72.77	84.77	0.46849	0.30000	83.851
6	4.98	23.72	35.59	47.59	59.59	71.59	83.59	0.51152	0.30001	85.404
7	4.88	26.68	39.92	51.92	63.92	75.92	87.92	0.39341	0.30000	82.452
8	4.68	23.21	34.98	46.98	58.98	70.98	82.98	0.51646	0.30001	85.580
9	5.31	26.86	40.80	52.80	64.80	76.80	88.80	0.37234	0.30001	81.505

Note: For analytically determined vertical displacements with pavement depth used in this analysis, refer to Table C-2 Appendix C.

^a Construction type 2 - HMAc layer over flexible base and L-FA subbase.

Table 5. Values of Constants m, n and H' determined by Regression Analysis
 Number 1 - Site 3^a.

Section No	<u>Transformed depth \bar{z} at depth z (in inches):</u>							<u>Value of constants</u>		
	10	16	28	40	52	64	76	m	n	H'
1	14.08	21.82	33.82	45.82	57.82	69.82	81.82	0.89691	0.30002	100.55
2	13.76	21.02	33.02	45.02	57.02	69.02	81.02	0.97493	0.30003	101.85
3	14.56	22.69	34.69	46.69	58.69	70.69	82.69	0.81282	0.30004	97.342
5	15.33	23.66	35.66	47.66	59.66	71.66	83.66	0.78100	0.30002	97.092
6	18.09	27.25	39.25	51.25	63.25	75.25	87.25	0.63120	0.30001	91.951

Note: For analytically determined vertical displacements with pavement depth used in this analysis, refer to Table C-3 Appendix C.

^aConstruction type 3 - Flexible base over L-FA subbase.

Table 6. Values of Constants m, n and H' determined by Regression Analysis
Number 1 - Site 4^a.

Section No	Transformed depth \bar{z} at depth z (in inches):							Value of constants		
	14	20	32	44	56	68	80	m	n	H'
2	24.26	31.74	43.74	55.74	67.74	79.74	91.74	0.68139	0.30000	99.736
3	23.16	30.08	42.08	54.08	66.08	78.08	90.08	0.78976	0.30000	103.54
4	21.48	28.20	40.20	52.20	64.20	76.20	88.20	0.87473	0.30002	105.41
5	19.61	26.92	38.92	50.92	62.92	74.92	86.92	0.87005	0.30003	104.97
6	24.57	33.61	45.61	57.61	69.61	81.61	93.61	0.57538	0.30001	97.144

Note: For analytically determined vertical displacement with pavement depth used in this analysis, refer to Table C-4 Appendix C.

^a Construction type 3 - Flexible base over L-FA subbase.

Table 7. Values of Constants m, n and H' determined by Regression Analysis
 Number 1 - Site 5^a.

Section No	Transformed depth \bar{z} at depth z (in inches):							Value of constants		
	12	18	30	42	54	66	78	m	n	H'
1	19.35	27.79	39.79	51.79	63.79	75.79	87.79	0.66525	0.30001	94.918
2	17.52	24.25	36.25	48.25	60.25	72.25	84.25	0.96215	0.30002	104.24
3	20.07	27.20	39.20	51.20	63.20	75.20	87.20	0.81885	0.30001	101.08
4	21.26	30.25	42.25	54.25	66.25	78.25	90.25	0.60385	0.30001	94.363
6	18.41	25.69	37.69	49.69	61.69	73.69	85.69	0.86540	0.30004	102.44
7	19.57	25.60	37.60	49.60	61.60	73.60	88.60	0.97020	0.30002	103.33
8	19.65	28.07	40.07	52.07	64.07	76.07	88.07	0.70100	0.30001	98.318

Note: For analytically determined vertical displacements with pavement depth used in this analysis, refer to Table C-5 Appendix C.

^aConstruction type 3 - Flexible base over L-FA subbase.

Table 8. Values of Constants m , n and H' determined by Regression Analysis
 Number 1 - Site 8^a.

Section No	Transformed depth \bar{z} at depth z (in inches):							Value of constants		
	12	18	30	42	54	66	78	m	n	H'
2	21.20	30.73	42.73	54.73	66.73	78.73	90.73	0.58438	0.30001	94.838
3	21.26	29.97	41.97	53.97	65.97	77.97	89.97	0.61751	0.30001	94.473
4	21.76	30.86	42.86	54.86	66.86	78.86	90.86	0.56607	0.30000	92.336
5	20.99	29.25	41.25	53.25	65.25	77.25	89.25	0.68918	0.30001	98.113
6	20.51	28.30	40.30	52.30	64.30	76.30	88.30	0.75772	0.30001	100.790

Note: For analytically determined vertical displacements with pavement depth used in this analysis, refer to Table C-6 Appendix C.

^aConstruction type 3 - Flexible base over L-FA subbase.

Table 9. Values of Constants m, n and H' determined by Regression Analysis

Number 1 - 12^a.

Section No	Transformed depth \bar{z} at depth z (in inches):							Value of constants		
	6	18	30	42	54	66	78	m	n	H'
1	12.36	24.36	36.36	48.36	60.36	72.36	84.36	1.7347	0.30001	128.82
2	22.36	34.36	46.36	58.36	70.36	82.36	94.36	0.91132	0.30001	107.39
3	17.38	29.36	41.38	53.38	65.38	77.38	89.38	1.1512	0.30001	109.85
4	16.07	28.07	40.07	52.07	64.07	76.07	88.07	1.2526	0.30000	112.20
5	21.32	33.32	45.32	57.32	69.32	81.32	93.32	0.93963	0.30000	105.99

Note: For analytically determined vertical displacements with pavement depth used in this analysis, refer to Table C-7 Appendix C.

^aConstruction type 4 - FA base over natural subgrade.

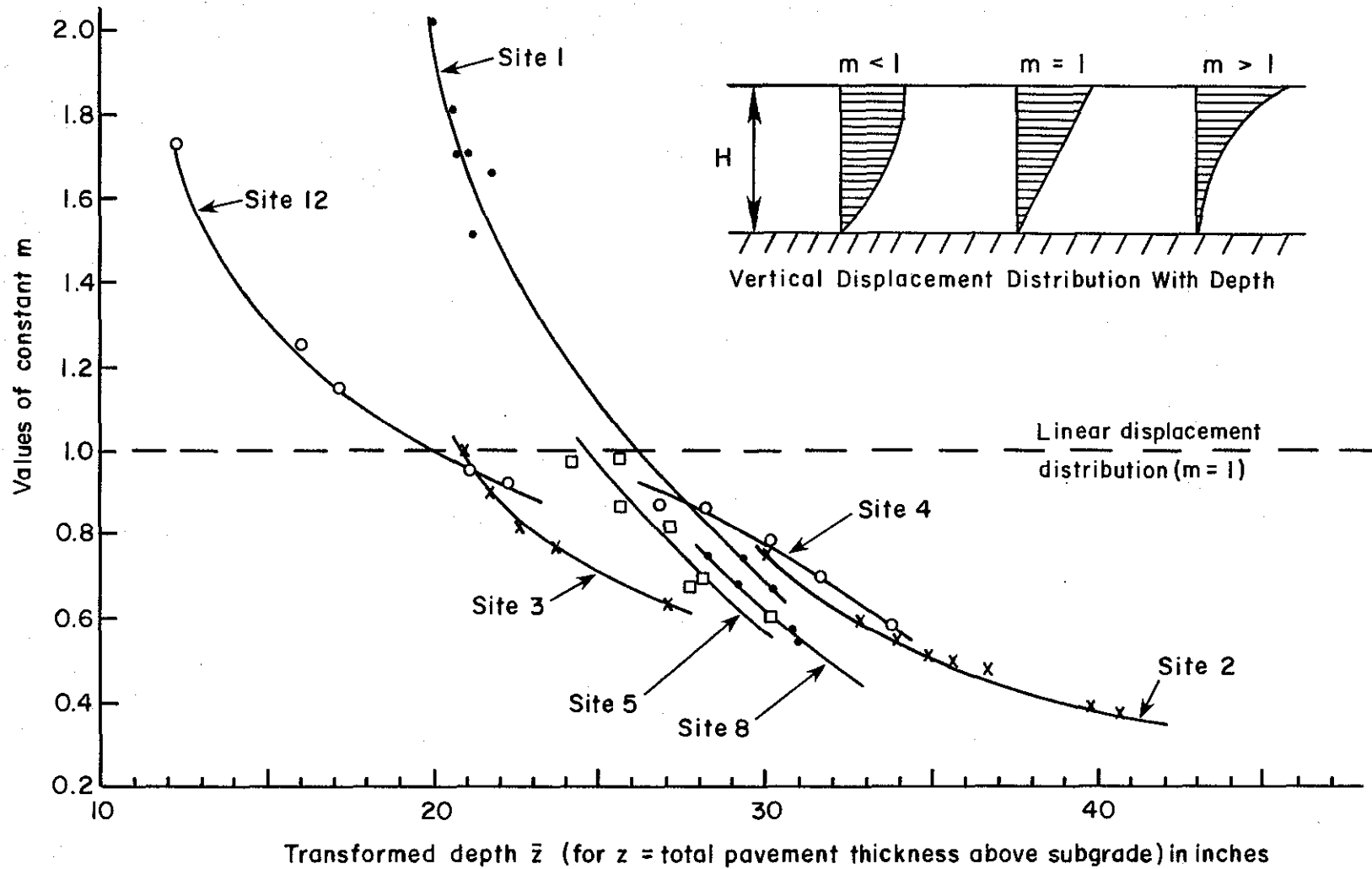


Figure 18. Trends in variation of exponential constant m for lime-flyash stabilized test sections.

The analytically determined values of both these properties are given in Tables B-1 to B-16 in Appendix B. The dependence of constant m on these properties was tested by applying general linear model (GLM) regression procedure using m values of Tables 3 to 9, and both linear and loglinear relationships were derived. The results of this analysis are given in Table 10.

Study of the statistical parameters, in Table 10, suggests that the mathematical model fits the data well and the independent variables significantly account for the behavior of the dependent variable. Therefore, on basis of the statistical evaluation, the following loglinear relationships were established for each type of construction*:

Type 1,

$$\text{Log}_e m = 0.4717 + 0.0684 K_1 - 1.427 K_2 \quad (4-2)$$

Type 2,

$$\text{Log}_e m = 0.6713 - 0.0322 K_1 - 0.3916 K_2 - 0.1714 K_3 \quad (4-3)$$

Type 3,

$$\text{Log}_e m = 0.7732 - 0.0421 K_1 - 0.1908 K_2 - 0.2324 D \quad (4-4)$$

Type 4,

$$\text{Log}_e m = 0.6125 - 0.092 K_1 \quad (4-5)$$

4.3 Regression Analysis Number 2

The relationships for m as defined by equations (4-2) to (4-5) were utilized in regression analysis number 2, explained in Chapter 3 (see Figure 15). Values of constants n , C , B and H were derived for

*The construction types are defined on page 11.

Table 10. List of Regression coefficients of Linear and Log-linear relationships between Constant m versus modular ratios K_1 , K_2 and K_3 and layer thickness ratio D .

Constr. ^a Type	Dependent Variable	<u>Independent Variables Coefficients</u>					F- Value	R- Square	Significant Difference @ $\alpha = 0.1$
		Intercept	K_1	K_2	K_3	D			
1	m	1.6799	0.0684	-0.1648	5.19	0.675	Significant
	$\log_e m$	0.4717	0.0654	-1.427	6.82	0.732	Significant
2	m	1.2985	-0.0251	-0.2563	-0.0905	...	18.53	0.933	Significant
	$\log_e m$	0.6173	-0.0322	-0.3916	-0.1714	...	43.86	0.970	Significant
3	m	1.5528	-0.0287	-0.1405	...	-0.1787	63.81	0.914	Significant
	$\log_e m$	0.7732	-0.0421	-0.1908	...	-0.2324	89.67	0.937	Significant
4	m	1.6541	-0.0103	13.09	0.814	Significant
	$\log_e m$	0.6125	-0.0092	21.81	0.879	Significant

^aConstruction types are defined on page 11.

each lime-flyash stabilized test section. The regression procedure utilized elastic moduli values obtained from basin fitting analysis, the deflection model according to equations (3-22) and (3-23), the error equation (3-29) and field measured Dynaflect deflections at all five locations of the geophones.

The results of the analysis and the "sum of squared error" of computed versus field deflections are given in Tables D-1 to D-4, in Appendix D, for each type of construction. Figures 19 to 22 depict graphically the values of constants determined for the test sections. From the analysis of results, the following trends in behavior of the constants were noted:

1. The computed values of the constant n were observed to be realistic in all test sections when compared to the value of 0.33 based on Odemark's assumption (4). Variations were the smallest in construction type 2* with values in the range of 0.301 to 0.385, while the largest variations were observed in construction type 3 with values in the range of 0.293 to 0.532. In general, the computed values of n were reasonable for all test sections when compared to Odemark's assumption, which is widely used in the analysis and design of multi-layered pavement systems.
2. The constant C in the deflection equation was an overall correction factor for multi-layered pavements. The computed

*Construction types are defined on page 11.

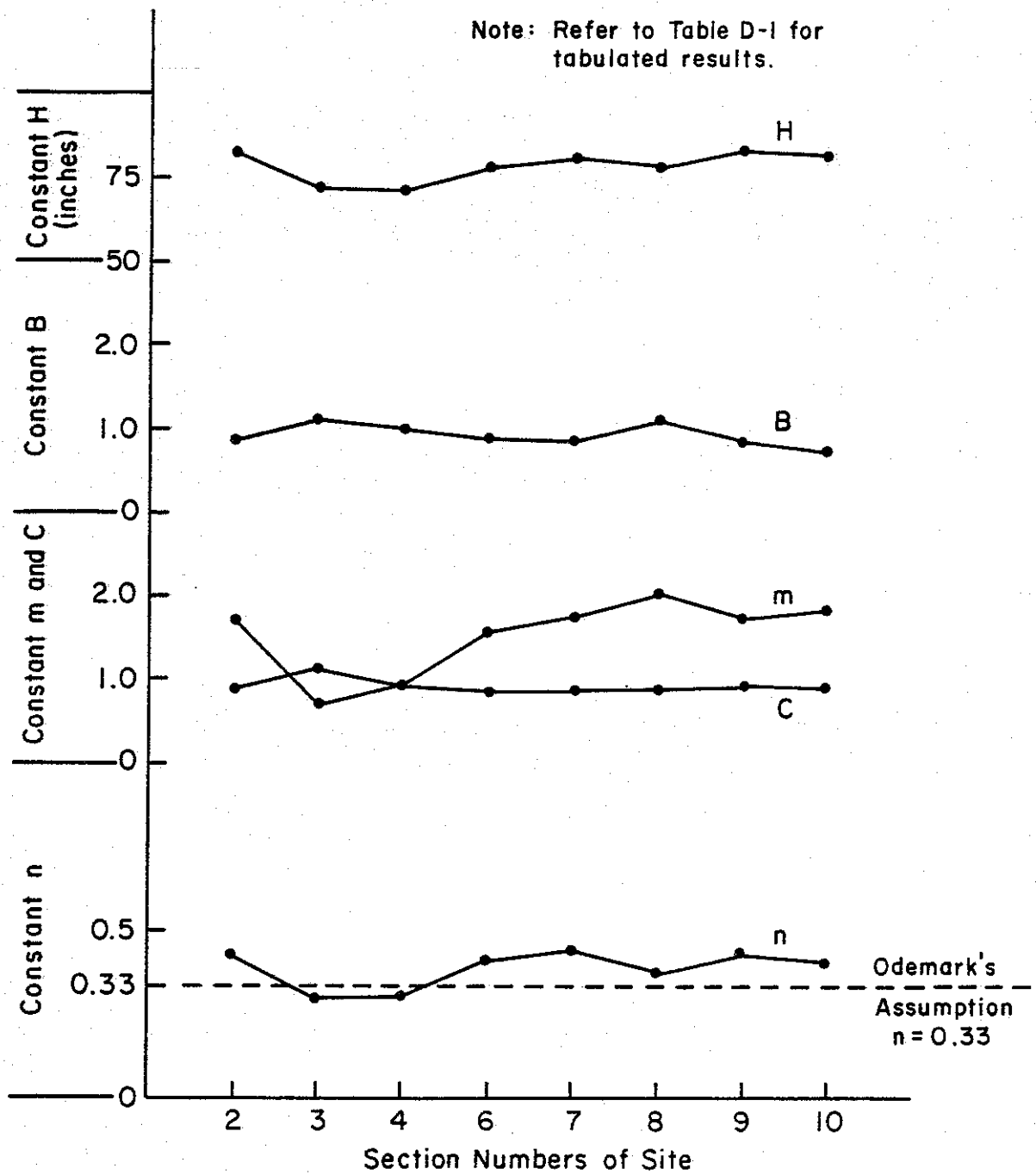


Figure 19. Graphical representation of the computed constants m, n, C, B and H - Site 1.

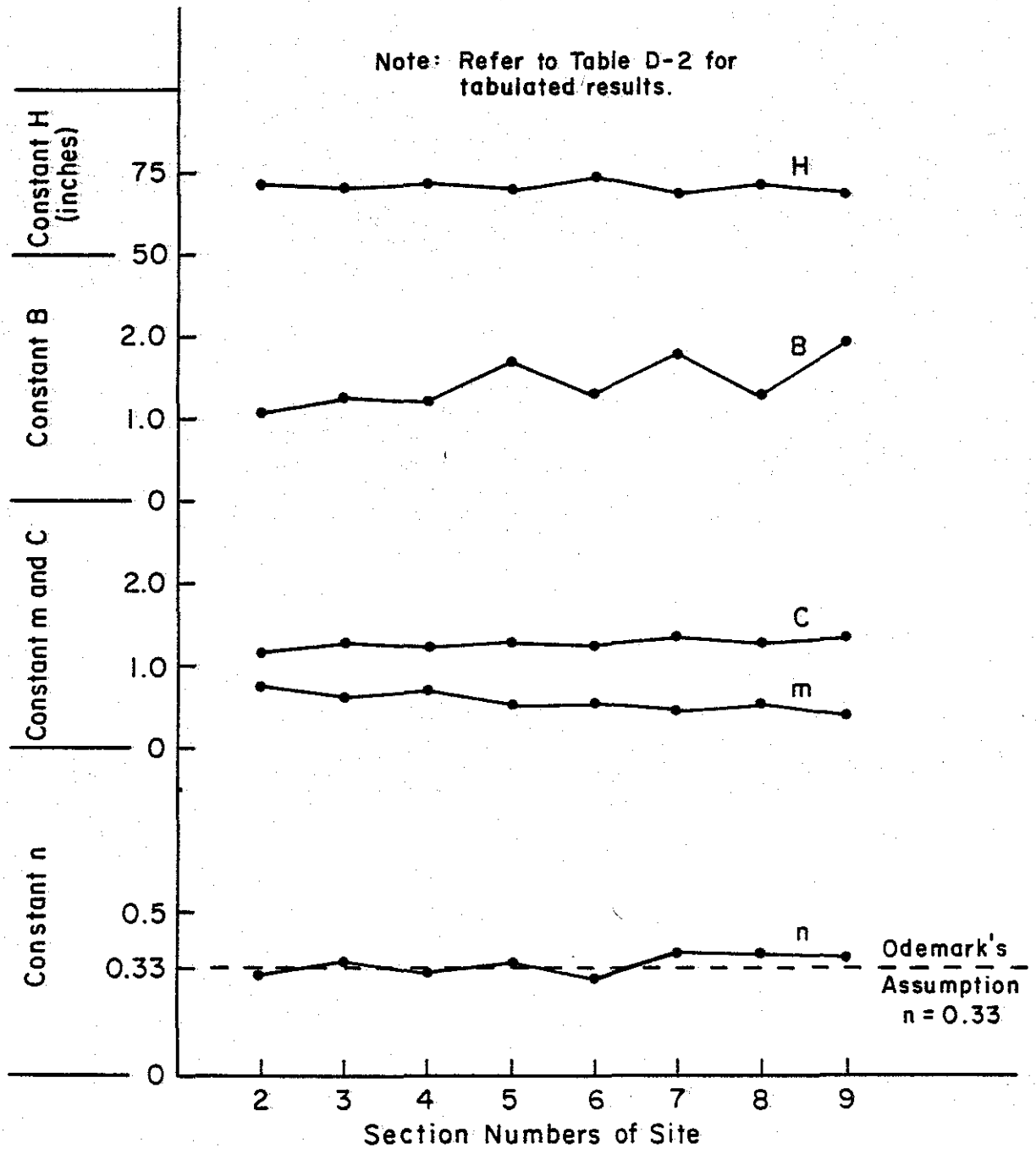


Figure 20. Graphical representation of the computed constants m, n, C, B and H - Site 2.

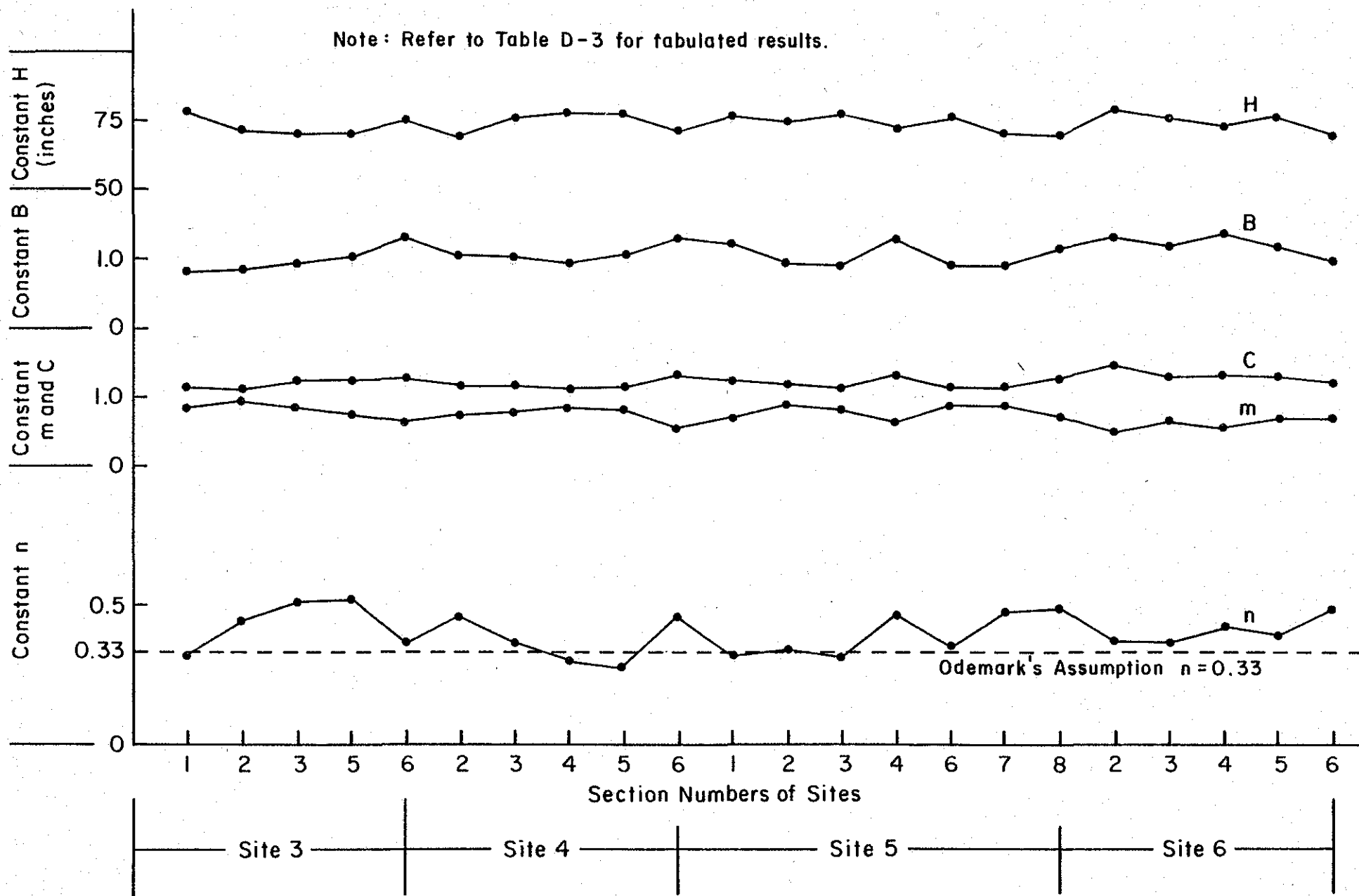


Figure 21. Graphical representation of the computed constants m , n , C , B and H - Sites 3, 4, 5 and 8.

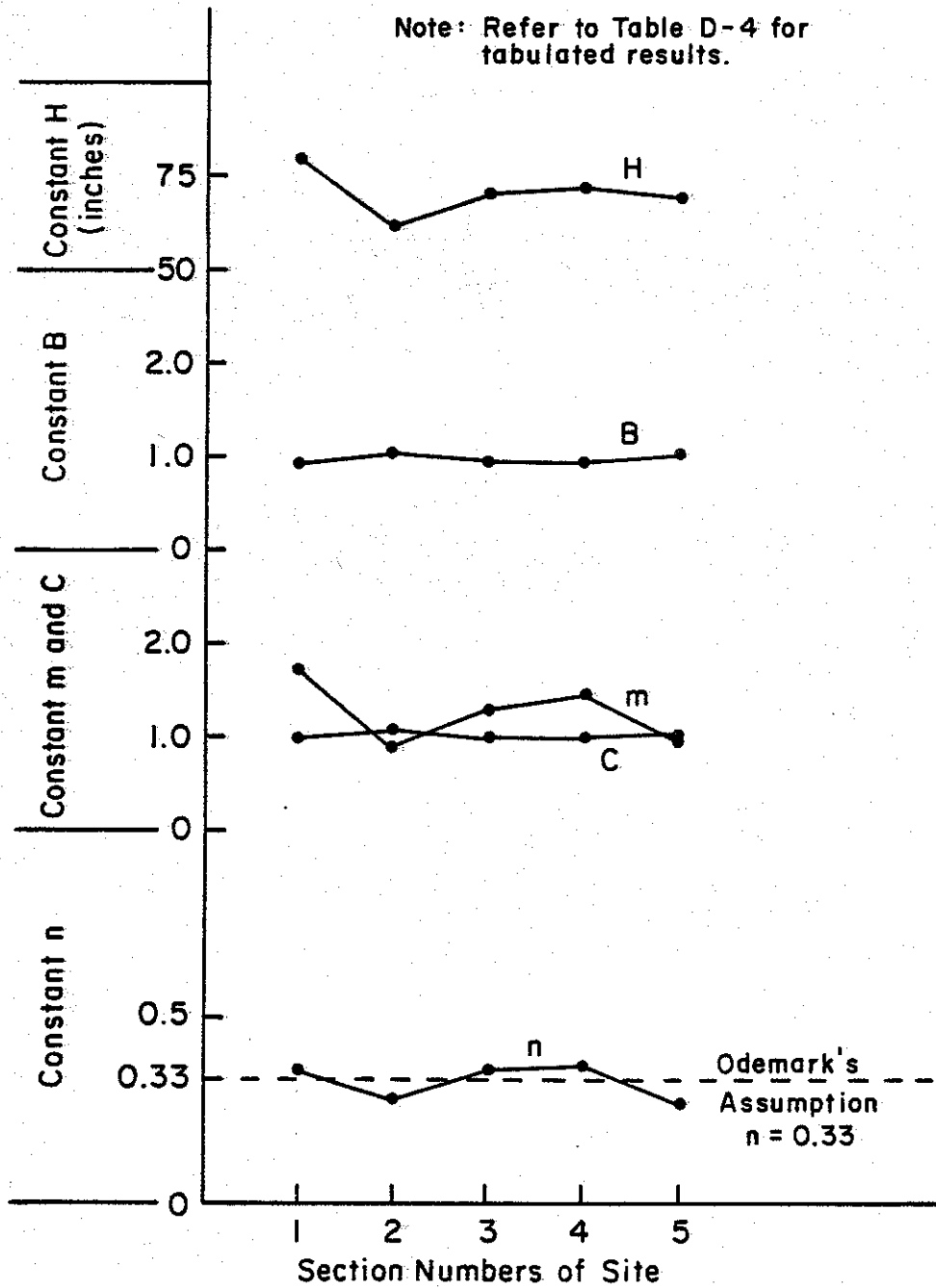


Figure 22. Graphical representation of the computed constants m, n, C, B and H - Site 12.

values of constant C were reasonable for all test sections. The variations in the values were the smallest in construction types 1* and 4 with values in the range of 0.882 to 1.111. The largest variations were in construction types 2 and 3 with values in the range of 1.129 to 1.477.

3. The constant B which was assumed originally as a correction factor for the power law constant m in multi-layered pavements with a starting value of 1, generally followed the trend of the constant C in terms of variation and also attained realistic values for all test sections. The variations in the constant B were the smallest in construction type 1 and 4 with values in the range of 0.788 to 1.128. The variations were largest in construction type 2 with values in the range of 1.088 to 1.943. For construction type 3 the range of values was 0.814 to 1.386.
4. The constant H characterizes the depth of the rigid layer from the pavement surface and was assumed to be 70 inches at start of the analysis. The variations in the constant H were observed to be the smallest in the 4-layer system of construction type 2 with values in the range of 67.074 to 73.111, and the largest in the 2-layer system of construction type 4 with values in the range of 63.889 to 78.959. In general, constant H attained reasonable values in all sections.

*Construction types are defined on page 11.

4.3.1 Effect of Physical Properties of Pavements on Constants n, C, B and H

Similar to the procedure used to obtain relationships to describe the constant m , the dependence of constants n , C , B and H , on physical properties, were tested by applying general linear model (GLM) regression procedure. Using values of n , C , B and H from Tables D-1 to D-4, Appendix D, several linear and loglinear relationships with both single and multiple independent variables were examined. Selected loglinear relationships are summarized in Table 11.

The statistical parameters of Table 11 suggests that a varying degree of correlation exists between the dependent and the independent variables for constants n , C , B and H . The correlation of constant C to the modular ratios and layer thickness ratios was found consistently higher than the correlations exhibited by n , B and H . In construction type 3* insignificant correlation was noted between the constants n and H with the physical properties.

4.4 Investigation using K_0 Bessel Function

The deflection equation proposed by Vlasov and Leont'ev (3) utilized the modified $K_0(x)$ form of the Bessel function illustrated in Figure 7. In this study, the capability of K_0 Bessel function to predict deflections was also investigated. Regression analysis number 2 was applied using a procedure similar to that previously explained for J_0 function, except that $J_0(\alpha r)$ was replaced with $K_0(\alpha r)$ in the deflection equation models (3-22) and (3-23). The results obtained for computed deflections, "sum of squared error" and the values of

*Construction types are defined on page 11.

Table 11. List of Regression Coefficients of Loglinear Relationships between Constants n, C, B & H versus Modular ratios K_1 , K_2 and K_3 and layer thickness ratio D.

Constr. ^a Type	Dependent Variable	Independent Variables Coefficients					F- Value	R- Square	Significant Difference @ $\alpha = 0.1$
		Intercept	K_1	K_2	K_3	D			
1	$\log_e n$	-0.6815	-0.0280	-0.0719	4.01	0.616	Significant
	$\log_e C$	0.0654	-0.0364	0.0093	13.26	0.841	Significant
	$\log_e B$	-0.4738	0.0691	0.0603	1.79	0.418	Not Significant
	$\log_e H$	4.4239	-0.0008	-0.0233	2.55	0.505	Not Significant
2	$\log_e n$	-0.7075	-0.0759	-0.1045	0.0107	1.23	0.480	Not Significant
	$\log_e C$	-0.1085	0.0053	0.1078	0.0447	23.35	0.946	Significant
	$\log_e B$	-1.0297	0.0409	0.4382	-0.2573	19.52	0.936	Significant
	$\log_e H$	4.1297	0.0248	0.0464	0.0088	3.49	0.723	Not Significant
3	$\log_e n$	-0.7355	0.0673	0.0680	-0.2535	1.13	0.158	Not Significant
	$\log_e C$	-0.0233	0.0395	0.0757	0.0156	16.06	0.728	Significant
	$\log_e B$	-0.9724	0.0352	0.1740	-0.2573	63.05	0.913	Significant
	$\log_e H$	4.2325	-0.0199	-0.0062	0.0686	0.72	0.108	Not Significant

Table 11 cont'd. List of regression coefficients

Constr. ^a Type	Dependent Variables	<u>Independent Variables Coefficients</u>					F-Value	R-Square	Significant Difference @ $\alpha = 0.1$
		Intercept	K ₁	K ₂	K ₃	D			
4	log _e n	-0.9438	-0.0045	8.57	0.741	Significant
	log _e C	-0.0393	0.0014	38.38	0.928	Significant
	log _e B	-0.1352	0.0019	27.18	0.901	Significant
	log _e H	4.3631	-0.0024	14.67	0.830	Significant

^aConstruction types are defined on page 11.

constants were analyzed.

The K_0 function was observed to predict deflections with substantially higher accuracy with smaller "sum of squared error" than was the J_0 function. However, in the case of the K_0 function, the computed values of constants n and H were of questionable physical significance. The values of constant n exceeded 1.0 in all sections of construction types 1, 2 and 3* and in one section of construction type 4, whereas with the J_0 equation model the computed values of n were reasonably close to Odemark's assumption of 0.33. In the case of the K_0 function, the constant H , which signifies the location of the rigid layer below the pavement surface achieved values in the range of 119.96 to 199.44 inches for all types of construction. These values unrealistically exceeded the values of H' , obtained in the vertical displacement study, conducted in regression analysis number 1 and given in Tables 3 to 9.

On the basis of these findings, further investigation using K_0 function was discontinued in the study.

4.5 Regression Analysis Number 3

In this analysis, the relationships derived for constants m , n , C , B and H with modular ratios and layer thickness ratios were utilized to predict deflections and elastic moduli of pavement layers from field deflections according to the procedure explained in Chapter 3 and illustrated in Figure 16. The listing of the computer program developed at Texas Transportation Institute and modified in this study

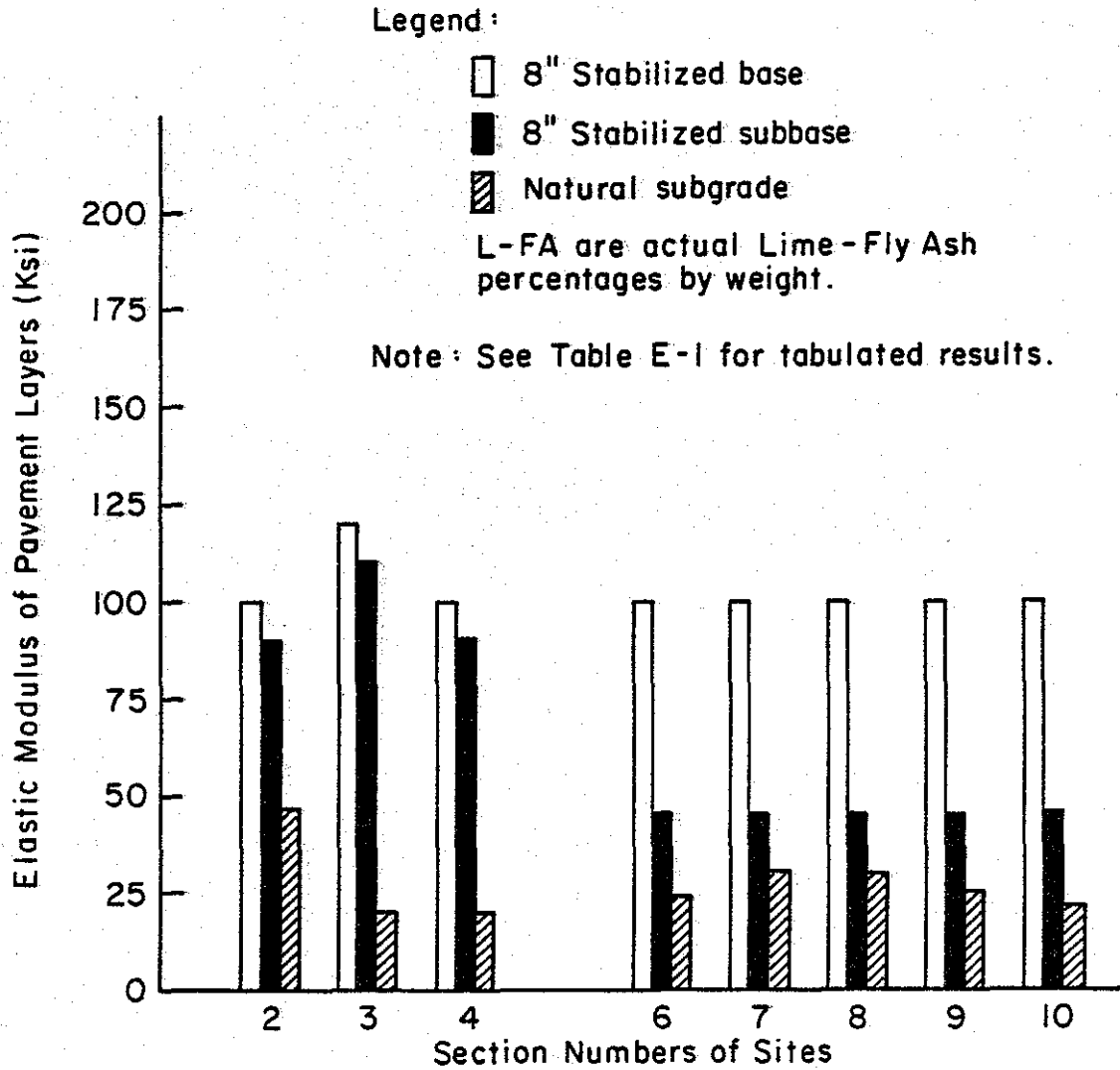
*Construction types are defined on page 11.

for regression analysis number 3 is given in Reference (1). In the study, the pattern search technique was modified, as follows:

1. The search for elastic moduli of pavement structural layers was restricted to n-1 layers by eliminating the subgrade modulus from the search. This was based on the knowledge that the subgrade modulus is capable of being accurately determined from the W_5 reading of the Dynaflect. Equation (4-1) substantiates this. This equation was utilized to compute the subgrade modulus in regression analysis number 3.
2. The accuracy of the analysis was increased substantially by reducing the incremental amount by which the variables, namely elastic moduli for layers 1 through n-1, were incremented during the pattern search process (22). The incremental amounts used were 30 psi. in the exploratory search and 10 psi. in the adaptive search.

4.5.1 Predicted Elastic Moduli Results





The elastic moduli of the pavement layers computed, by application of regression analysis number 3, are given in Tables E-1 to E-9, Appendix E, with the "sum of squared error". The results of Tasks E-1 to E-9 are also graphically illustrated in Figures 23 to 29. From the analyses of these results, the observations listed below on the condition of lime-flyash stabilized layers were noted. In analyzing these results emphasis was placed on evaluating the size of the error ϵ^2 , the accuracy of individual computed deflections were



L-FA base	4/4	4/8	4/15	6/6	6/11	7/18	5/23	6/6
L-FA subbase	4/0	4/0	4/0	0/6	0/6	0/6	0/6	0/6

Figure 23. Predicted elastic modulus values of pavement layers - Site 1.

Legend:

-  2" HMAC surface
-  12" Flexible base
-  8" Stabilized subbase
-  Natural subgrade

L-FA are actual Lime- Fly Ash percentages by weight.

Note: See Table E-3 for tabulated results.

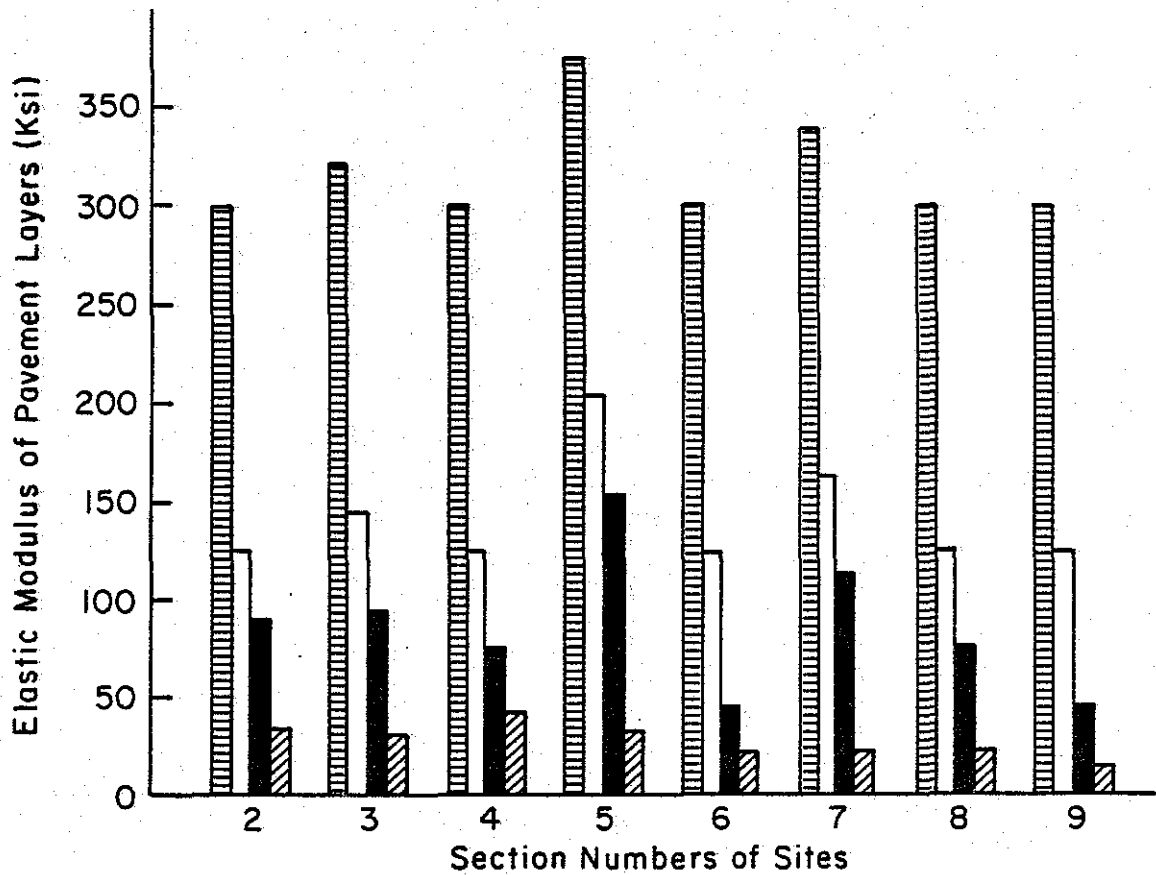


Figure 24. Predicted elastic modulus values of pavement layers - Site 2.

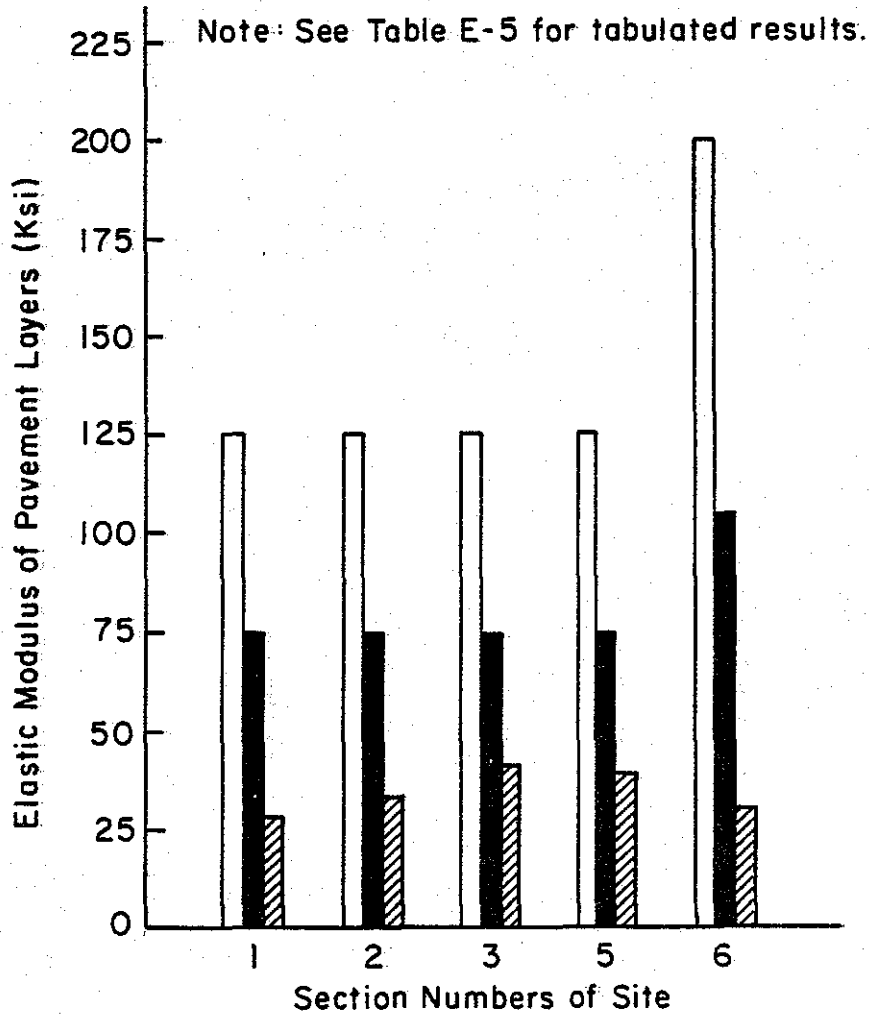
Legend:

□ 10" Flexible base

■ 6" Stabilized subbase

▨ Natural subgrade

L-FA are actual Lime-Fly Ash percentages by weight.



L-FA subbase 3/6 3/9 1½/5 2/8 0/12

Figure 25. Predicted elastic modulus values of pavement layers - Site 3.

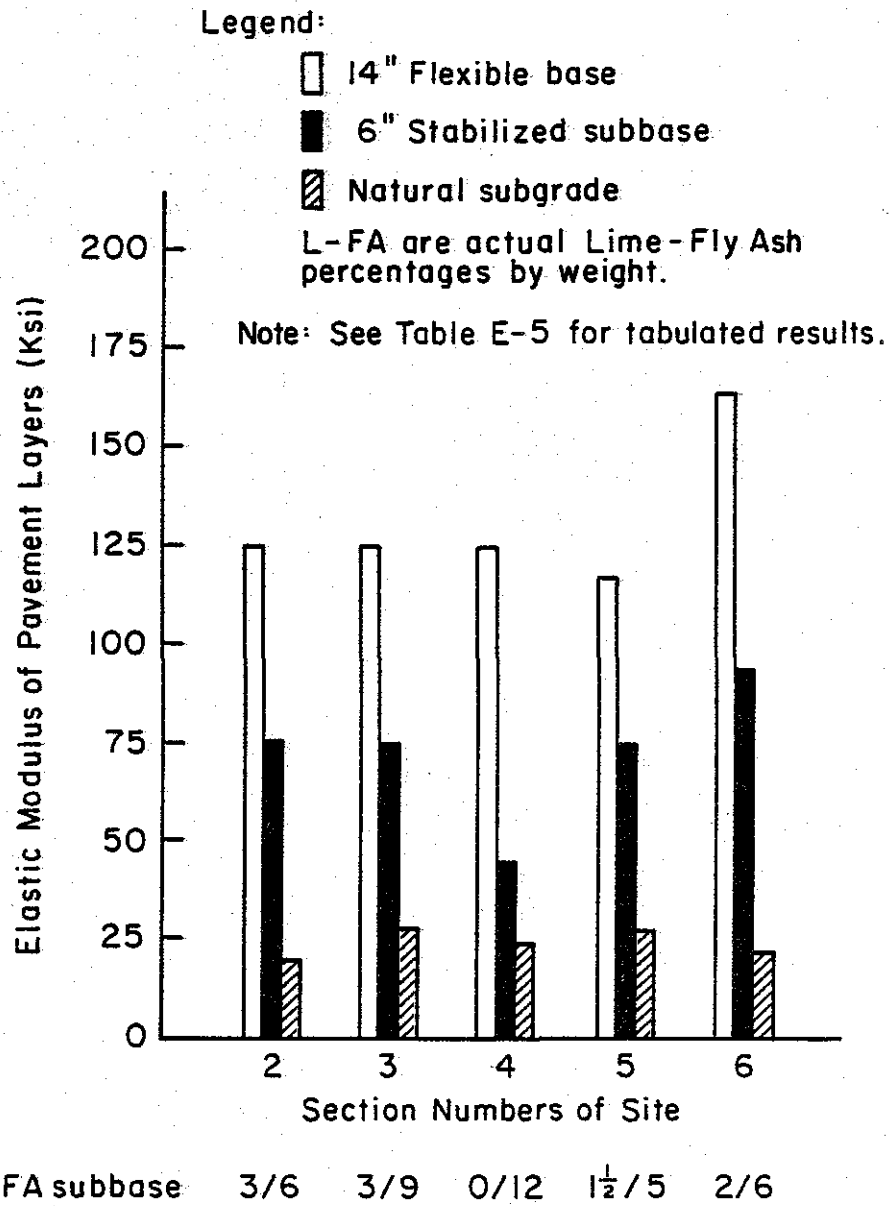


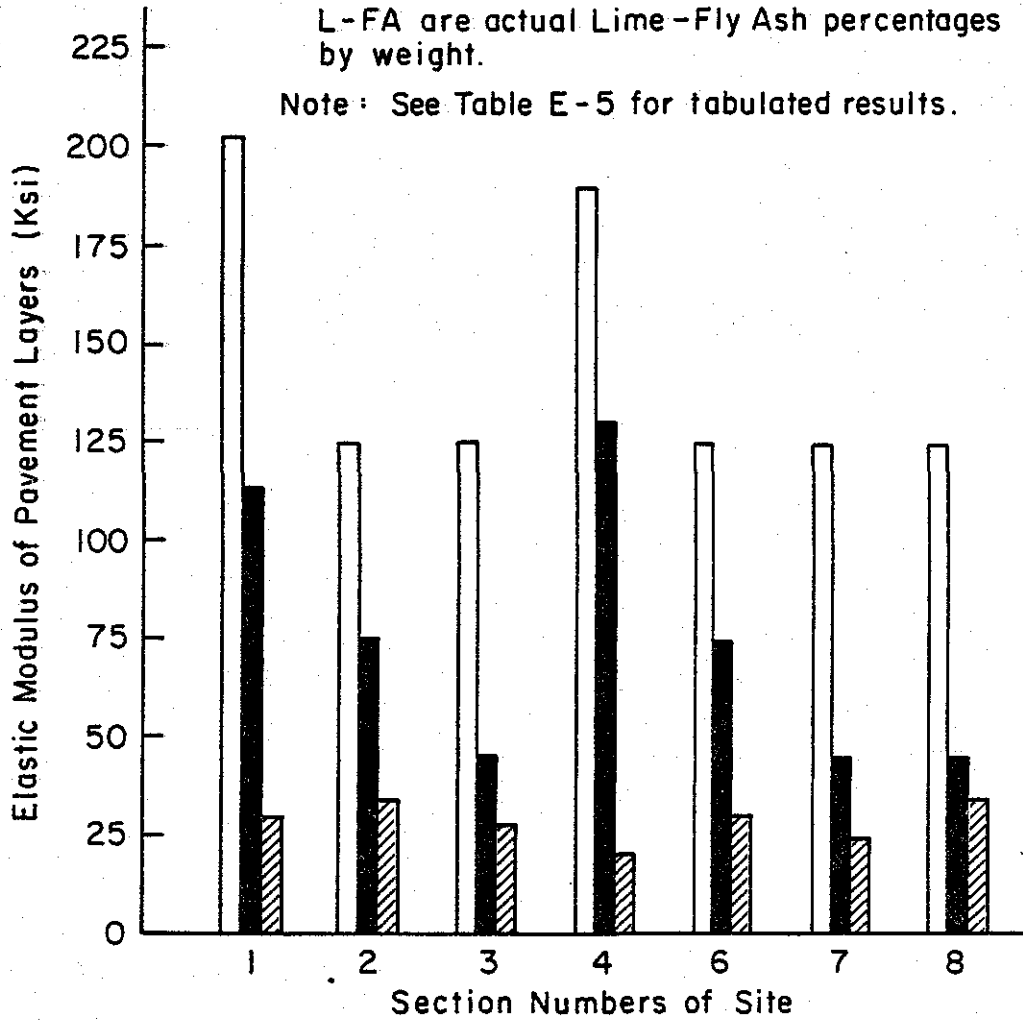
Figure 26. Predicted elastic modulus values of pavement layers - Site 4.

Legend :

- 12" Flexible base
- 6" Stabilized subbase
- ▨ Natural subgrade

L-FA are actual Lime - Fly Ash percentages by weight.

Note : See Table E - 5 for tabulated results.



L-FA subbase 3/6 3/9 0/12 2/8 1½/5 0/25 0/30

Figure 27. Predicted elastic modulus values of pavement layers - Site 5.

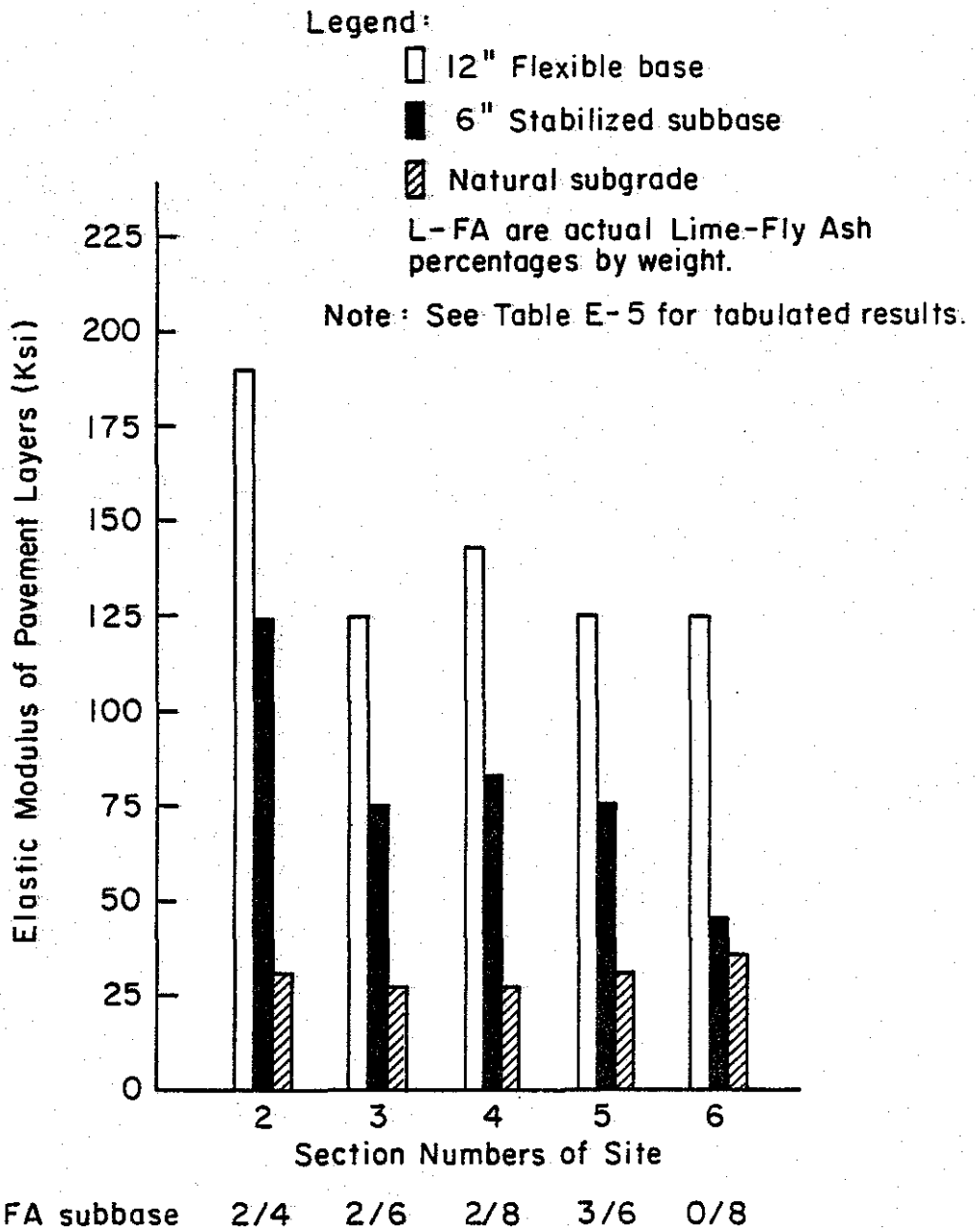


Figure 28. Predicted elastic modulus values of pavement layers - Site 8.

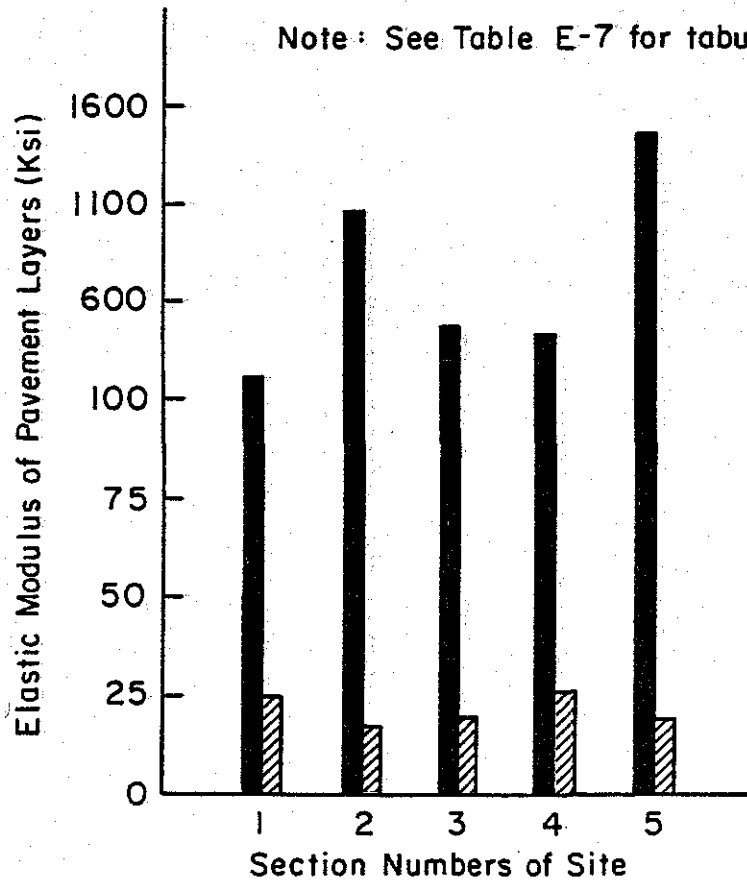
Legend:

■ 6" Stabilized base

▨ Natural subgrade

L-FA are actual Lime - Fly Ash percentages by weight.

Note: See Table E-7 for tabulated results.



L-FA base 0/20 0/30 0/40 0/20 0/40

Figure 29. Predicted elastic modulus values of pavement layers - Site 12.

compared to field deflections and the values of the derived constants were evaluated.

1. In site 1, constructed of lime-flyash stabilized base over lime or flyash stabilized subbase (Construction type 1), the lime stabilized subbases of sections 2, 3 and 4 appear to have gained distinctly higher stiffness than flyash stabilized subbases in sections 6, 7, 8, 9 and 10. The base layers of all sections exhibited comparable stiffnesses, except for section 3 (L-FA ratio 4/8) which was higher. Low prediction errors were noted in sections 2, 3, 4, 8 and 9 and higher errors in sections 6, 7 and 10.
2. In site 2, constructed of HMAC overlay over flexible base and L-FA stabilized subbase (Construction type 2), the subbase gained varying levels of stiffness. Sections 2, 3, 4, 5, 7 and 8 utilizing both lime and flyash as stabilized agents exhibited higher stiffnesses than sections 6 and 9 that employed flyash only. Highest stiffnesses were noted in sections 3, 5 and 7 that employed L-FA ratios of 2/8, 4/4 and 2/24. Low prediction errors were noted in all sections of this site.
3. In site 3, constructed of flexible base over lime-flyash stabilized subbase (Construction type 3), comparable stiffnesses were noted in sections 1, 2, 3 and 5 in the subbase. Section 6, that utilized only flyash as a stabilizing agent in the ratio 0/12, interestingly gained the

maximum stiffness in this site. Fitted results for this section substantiates this observation. Low prediction errors were noted in all sections.

4. In site 4, constructed of flexible base over lime-flyash stabilized subbase (Construction type 3), comparable stiffnesses were noted in sections 2, 3 and 5 in the subbase. Section 6 (L-FA ratio 2/6) exhibited the highest degree of stiffnesses. The stiffness of "flyash only" section 4 was observed lower than other sections. Low prediction errors were noted in all the sections of this site.
5. In site 5, constructed of flexible base over lime-flyash stabilized subbase (Construction type 3), varying levels of stiffnesses were noted in the subbase layers. Sections 1 and 4 that utilized lime-flyash ratios of 3/6 and 2/8 respectively seemed to have gained the maximum stiffnesses in this site. The stiffnesses of sections 2 and 6 were comparable and the three "flyash only" sections 3, 7 and 8 exhibited lower stiffnesses than the others. Low prediction errors were noted in all the sections of this state.
6. In site 8, constructed of flexible base over lime-flyash stabilized subbase (Construction type 3), the subbase of section 2 (L-FA ratio 2/4) gained the highest stiffness. Sections 3, 4 and 5 were comparable and section 6 stabilized with only flyash as the stabilizing agent indicated lower stiffness. Low prediction errors were noted in all the

sections.

7. In site 12, constructed of flyash stabilized base over natural subgrade (Construction type 4), stiffnesses in the range of 200.4 to 1465.8 Ksi. were observed in the base layer. This finding indicates that all sections of the site have benefited from the effect of soil reactions between the very low PI sandy soil and flyash. Flyash was effective in filling voids in coarser soils and promoting stiffness gain. The highest stiffnesses were noted in sections 2 and 5; stiffnesses were comparable in sections 3 and 4; and section 1 exhibited lower stiffness. Low prediction errors were observed in sections 2, 3, 4 and 5 and high error in section 1.

In general, the computed deflections and elastic moduli were reasonably accurate. Low prediction error were observed in the majority of computations and the computed values of the constants m , n , C , B and H of the simplified elastic theory model were reasonable for all the test sections. Significant savings, in terms of computational costs, were observed in applying the simplified elastic theory model to predict deflections and elastic moduli, as compared to the basin fitting technique using multi-layered elastic theory.

Stabilization with only flyash was found to be ineffective in promoting stiffness gains in the low PI clayey soils of the sites 1, 2, 3, 4, 5 and 8 (Construction types 1, 2 and 3*) but effective

*The construction types are defined on page 11.

stiffness gains were observed in the sections that were stabilized with both lime and flyash. In comparing the stiffness gains of the test sections constructed on clayey soils, the optimum lime-flyash ratios appear to be 0.08 to 0.50, using a minimum of 2% lime.

Very significant stiffness gains were observed in all the sections constructed on the very low PI coarse sandy soil of site 12 (Construction type 4) indicating that stabilization with 20 to 40% flyash was highly effective for this type of soil.

4.6 Effect of Time on Lime-Flyash Stabilized Layers

In an attempt to evaluate the effect of time on the stiffnesses of lime-flyash pavement layers the predictive equations formed in this study were applied to field measured data obtained at different periods after the construction of sites 1, 2, 3, 4, 5, 8 and 12. The Dynaflect measured field data are given in Appendix F.

The predicted elastic moduli results obtained from the analysis are given in Tables E-10 to 17, Appendix E, with the "sum of squared error". These results were analyzed for the size of prediction error, the individual accuracy of computed versus field deflections and the values of the derived constants were evaluated.

The computed values of the subgrade modulus and the elastic modulus of lime-flyash stabilized layers were plotted versus the time of the deflection measurement surveys, and are presented in Figures 30 to 36. In these figures, a temperature correction has been made in the elastic modulus values that were computed from deflections measured at the mean air temperatures of 70⁰F and above. The

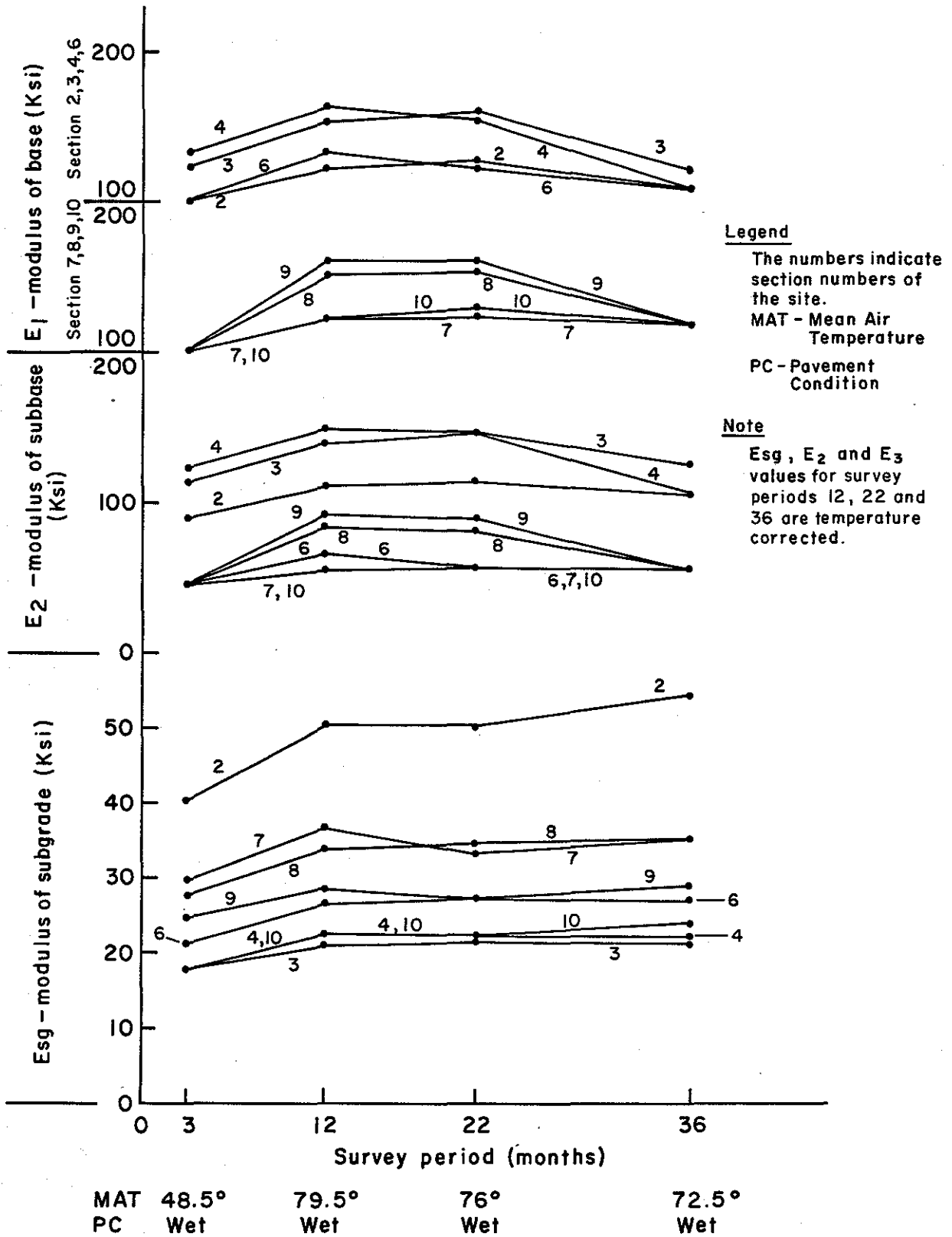


Figure 30. Variation in the base modulus E_1 , subbase modulus E_2 and subgrade modulus E_{sg} with time - Site 1.

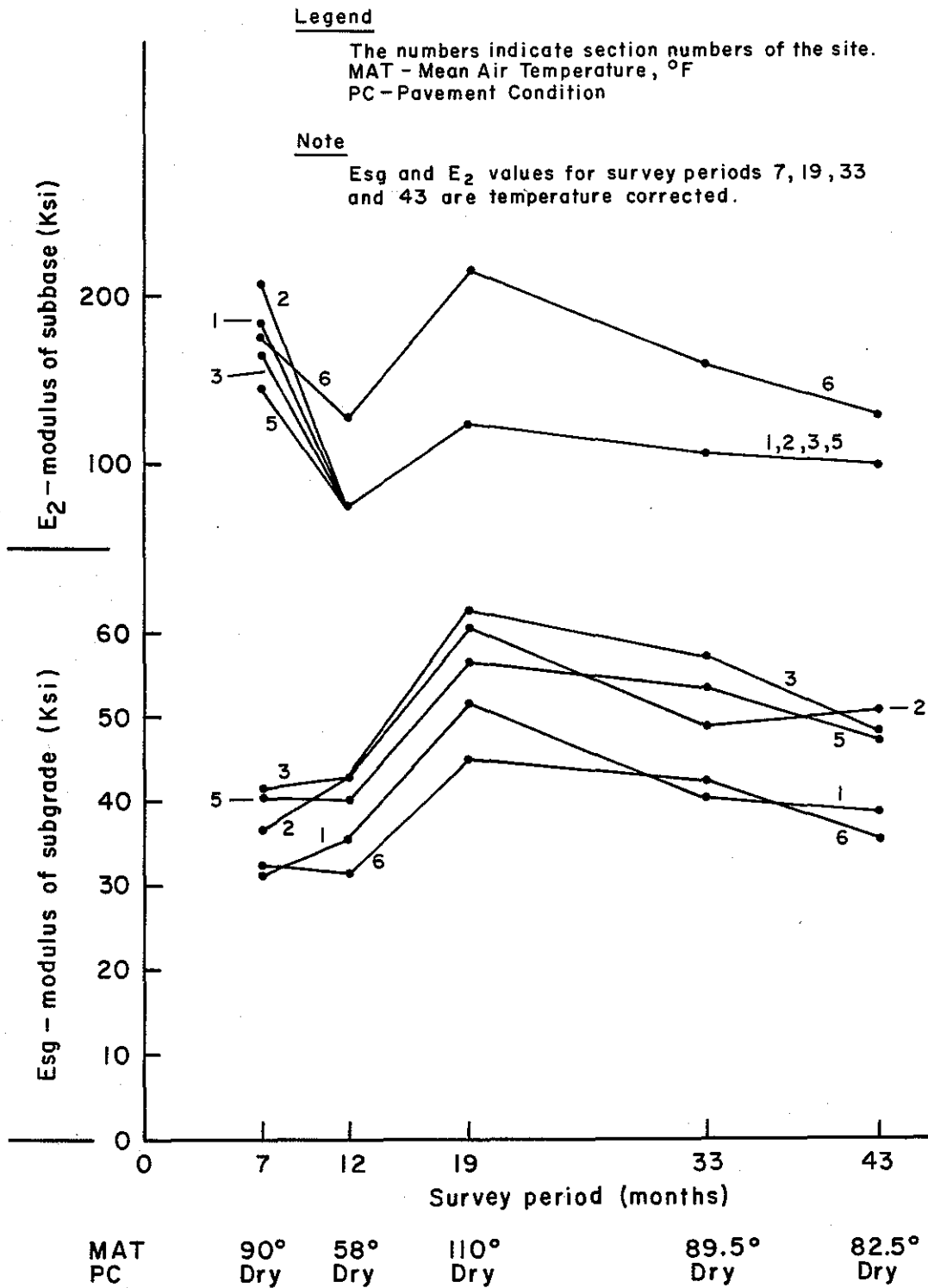


Figure 32. Variation in the subbase modulus E₂ and subgrade modulus E_{sg} with time - Site 3.

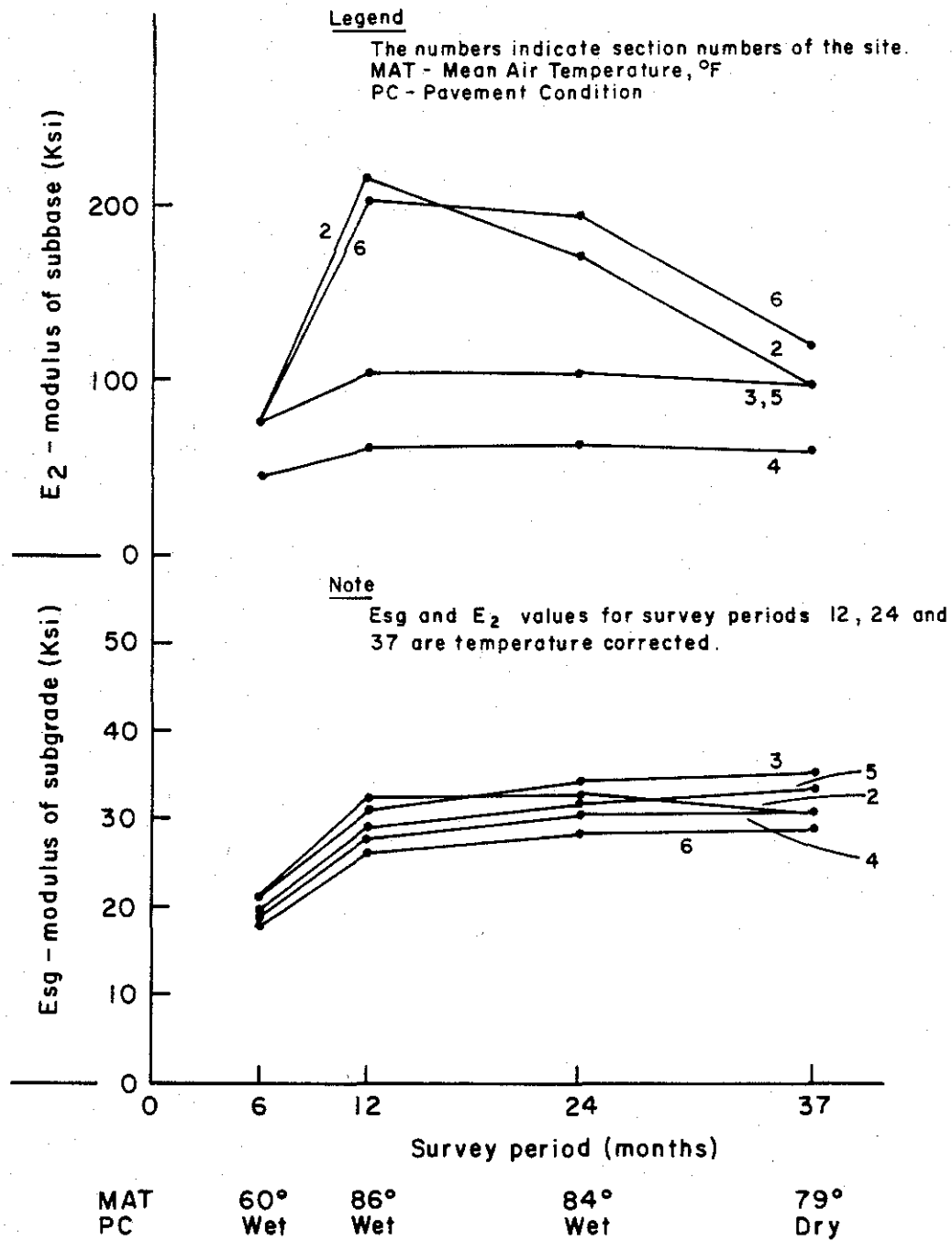


Figure 33. Variation in the subbase modulus E₂ and subgrade modulus Esg with time - Site 4.

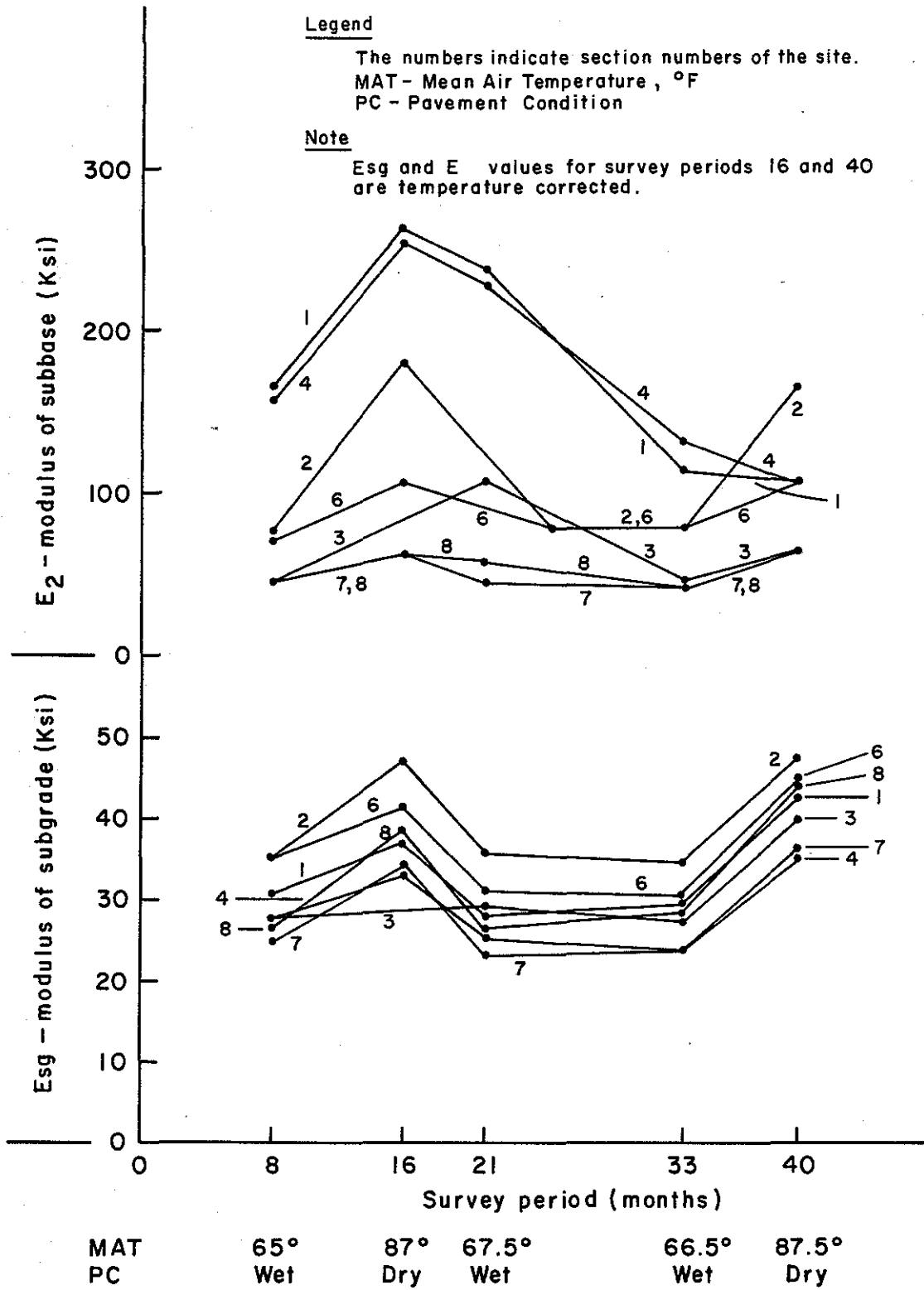


Figure 34. Variation in the subbase modulus E_2 and subgrade modulus E_{sg} with time - Site 5.

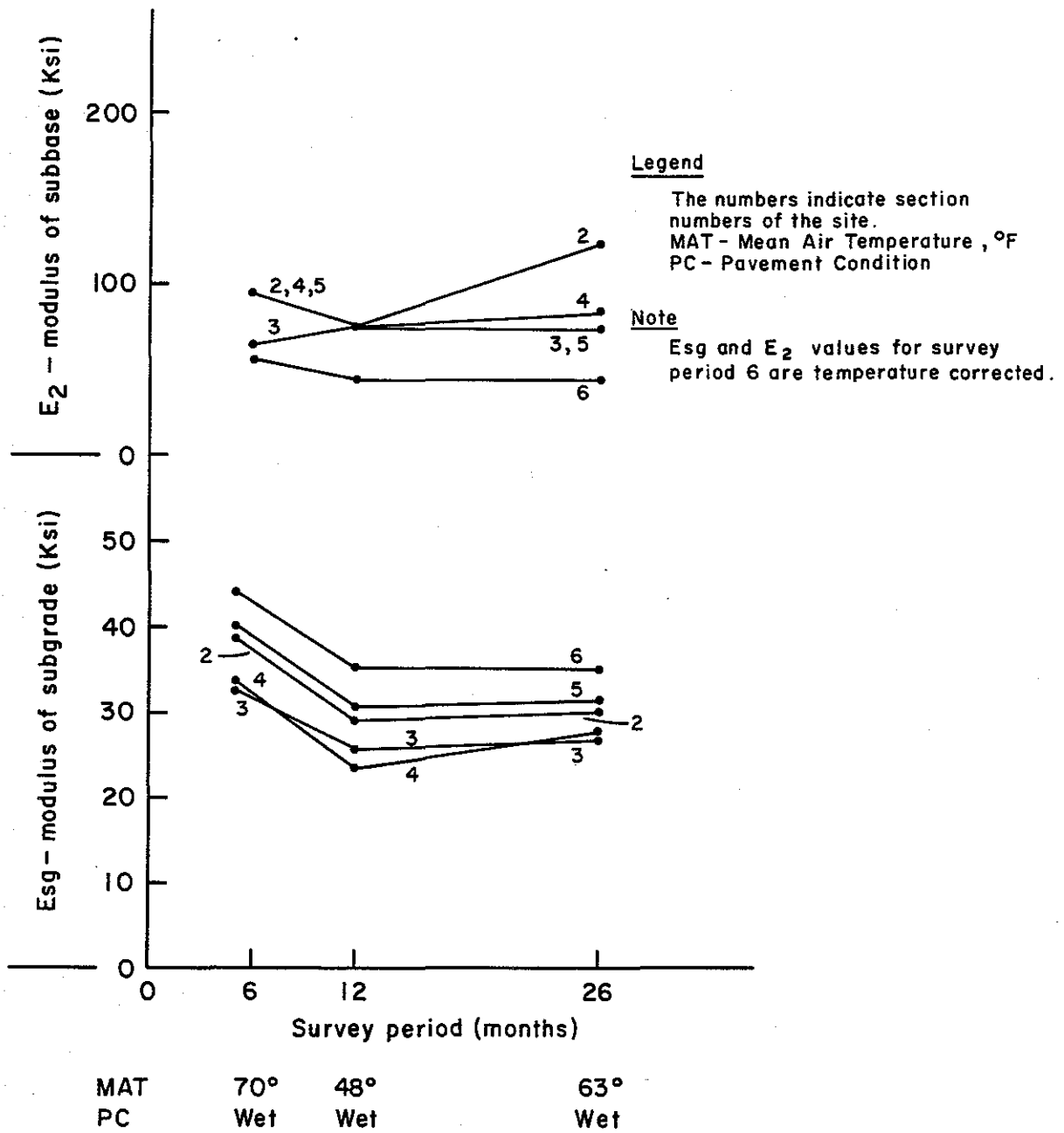


Figure 35. Variation in the subbase modulus E₂ and subgrade modulus Esg with time - Site 8.

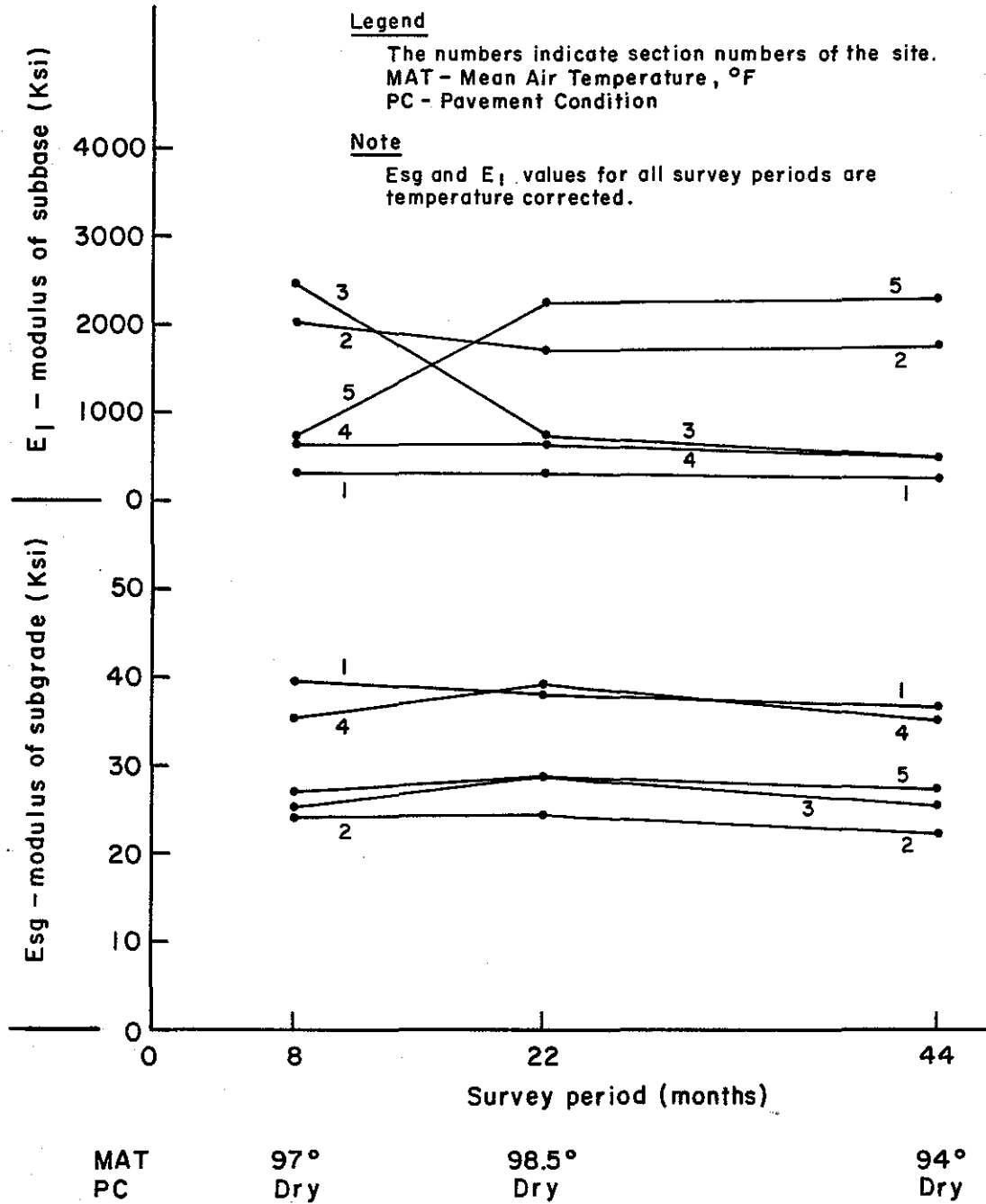


Figure 36. Variation in the base modulus E_1 and subgrade modulus Esg with time - Site 12.

procedure used for the temperature correction was based on the method given in reference (26). The pavement temperature, inclusive of the subgrade layer, was assumed to be equal to the mean air temperature on the survey data. The assumed pavement temperatures were used in Figure 37 and the 'deflection adjustment factors' were derived. The 'deflection adjustment factors' were used as multipliers to adjust the sensor-5 deflections and the subgrade modulus values were corrected utilizing equation (4-1). The elastic modulus values of the stabilized pavement layers were then adjusted in proportion to the new datum subgrade modulus.

From the Figures 30 to 36, the following trends were observed in the stiffness behavior of the sections:

1. In site 1, constructed of the lime-flyash stabilized base over lime or flyash stabilized subbase (Construction type 1), the survey data of month 3, 12, 22 and 36 were utilized. The stiffnesses of the base layers of the sections 2, 3, 7, 8, 9 and 10 increased progressively from the month 3 until the month 22. The sections 4 and 6 exhibited stiffness gains until the month 12. The base layer stiffnesses of all the sections indicated a decline after the month 22. The subbase layers, of the sections 2, 3, 4, 7, 8, 9 and 10 exhibited stiffness gains until the month 22, and section 6 indicated stiffness gain until the month 12. The subbase layer stiffnesses of all the sections indicated a decline after the month 22. In general, the base and the subbase layers of the

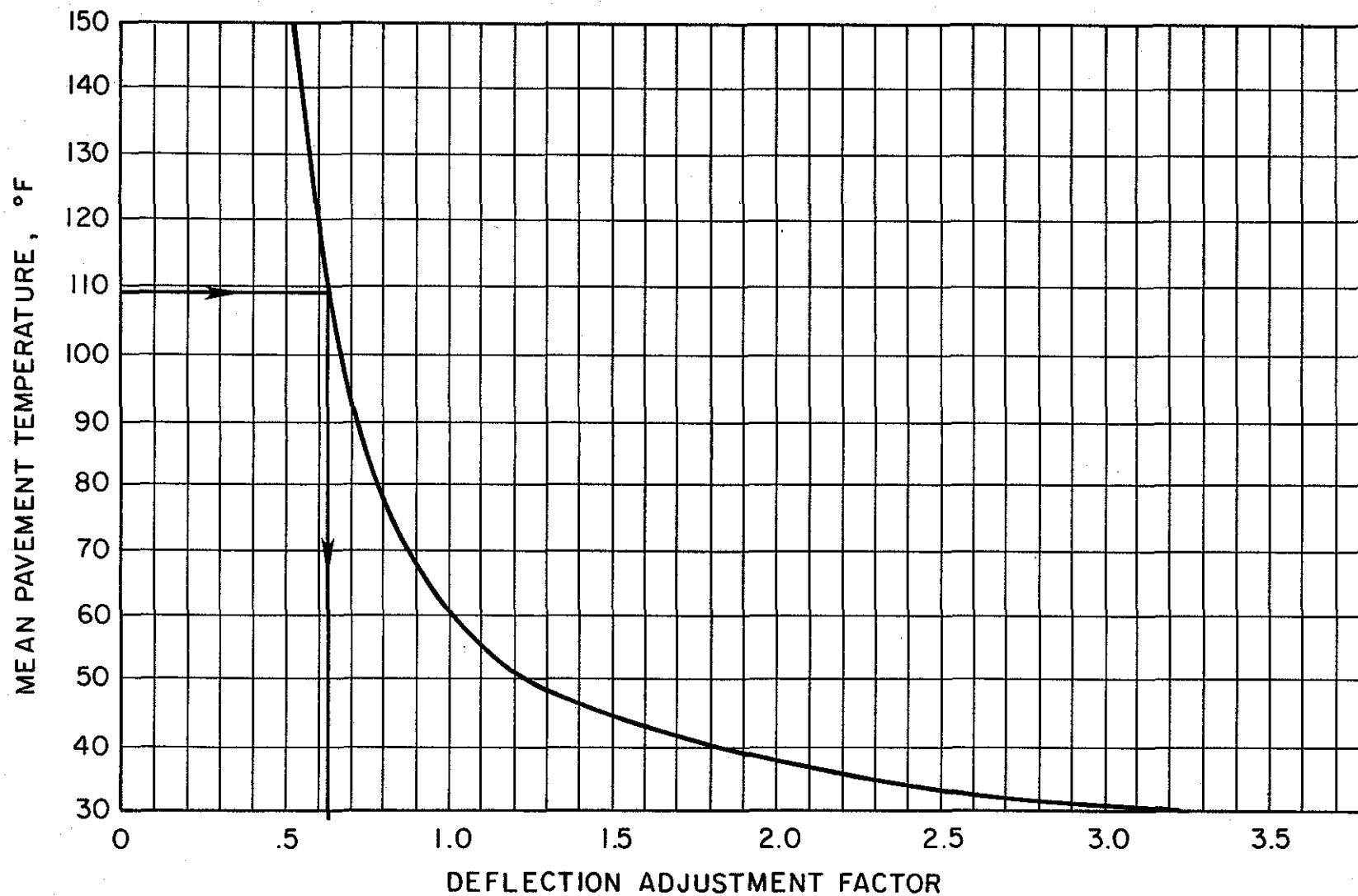


Figure 37. Mean pavement temperature versus Deflection adjustment factor (37).

site, exhibited similar stiffness behavior over time. The surveys of this site were made under wet pavement conditions, therefore, increased moisture may have caused the loss of stiffness after month 22.

2. In site 2, constructed of HMAC overlay over flexible base and lime-flyash stabilized subbase (Construction type 2), the survey data of months 24 and 27 were utilized. In the subbase layers, the sections 2, 3, 4, 6, 7, 8 and 9 indicated a small decline in the stiffness; and a larger decline in stiffness was noted in the section 5. The increased pavement moisture in the survey of month 37 would have caused the stiffness loss.
3. In site 3, constructed of flexible base over lime-flyash stabilized subbase (Construction type 3), the survey data of months 7, 12, 19, 33 and 43 were utilized. All the sections exhibited a decline in the subbase stiffness from the month 7 to the month 12. Significant stiffness gains were noted in all the sections between month 12 and month 19 and a decline thereafter. In the survey of month 19, the observed high 'mean air temperature' of 110⁰F would have caused the stiffening. Interestingly, the section 6 treated with only flyash, and no lime, exhibited better stiffness behavior over time than the lime-flyash stabilized sections.
4. In site 4, constructed of flexible base over lime-flyash stabilized subbase (Construction type 3), the survey data of

months 6, 12, 24 and 37 were utilized. The subbase layers of sections 3, 4 and 5 indicated a stiffening trend between the month 6 and the month 12, no change in stiffness between the month 12 and month 24, and declined somewhat thereafter. Significant stiffness gains were noted in the sections 2, 3, 4, 5 and 6 between the month 6 and the month 12, and decline thereafter. The subgrades of all the sections exhibited a progressive stiffening trend.

5. In site 5, constructed of flexible base over lime-flyash stabilized subbase (Construction type 3), the survey data of months 8, 16, 21, 33 and 40 were utilized. The subbase layers of all the sections exhibited stiffening between the month 8 and the month 16, and a decline until month 33. The section 3 exhibited stiffness gains until the month 21. The sections 2, 6, 7 and 8 indicated stiffness gains after the month 33. The subgrades of all the sections indicated higher stiffnesses in the month 16 and the month 40. Large variations with time in the stiffness behavior of the subbase layers of this site were noted.
6. In site 8, constructed of flexible base over lime-flyash stabilized subbase (Construction type 3), the survey data of months 6, 12 and 26 were analyzed. The subbase layers of the sections 2, 4, 5 and 6 exhibited a decline in stiffness between the month 6 and the month 12, whereas section 3 stiffened in the same period of time. The subbase layers of

the sections 2 and 4 indicated significant stiffness gains after the month 12 and the sections 3, 5 and 6 exhibited stiffness gains also, but to a lesser degree. The stiffness of the subgrade, in all the sections, was noted to be high in the month 6 and declined thereafter.

7. In site 12, constructed of flyash stabilized base over natural subgrade, the survey data of months 8, 22 and 44 were utilized. The section 1 and 4 exhibited insignificant changes in the stiffness of the base layers; the sections 2 and 3 indicates a stiffness decline between the month 8 and the month 22; and the section 5 stiffened progressively from the month 8 to the month 44.

It was recognized for the time study that the stiffnesses of the lime-flyash stabilized layers and the subgrade, that were computed from field measured deflections, could be significantly affected by the 'pavement temperature' and the 'moisture' in the sections at the time of the surveys. In this study, the effects of the pavement temperatures were quantified and the computed moduli were adjusted to account for the temperature variations in the survey periods. A quantitative adjustment in the moduli due to the 'moisture' was not practically feasible.

In general, the computed deflections and the elastic modulus values were reasonably accurate in the time study, and low prediction errors were observed. The computed values of the constants m , n , C , B and H of the simplified elastic theory model were also reasonable.

For low PI clayey soils (Construction types 1, 2, and 3*), effective long term structural support was found in the sections that were stabilized with both the lime and the flyash. Generally, flyash by itself was ineffective in promoting stiffness gains. The optimum lime-flyash ratios, for long term stiffness gains were found to be in the range of 0.08 to 0.5, using a minimum of 2% lime.

For very low PI coarse sandy soil (Construction type 4), soil stabilization with 20-40% flyash, and no lime, was highly effective.

*The construction types are defined on page 11.

5. CONCLUSIONS AND RECOMMENDATIONS

5.1 Conclusions

In this study, a new approach for characterizing the stress-strain behavior of n-layer lime-flyash stabilized pavement structures from field measured deflections, was developed. This method employed a simplified form of elastic theory and utilized the J_0 Bessel functions. A major benefit of this method as opposed to the conventional methods, employing multi-layered elastic theory, is that the need for mathematical integration of complex expressions involving Bessel functions is eliminated in the computational process. This in turn results in very significant savings in computational costs and makes it practicable to analyze a large number of field measurements to infer structural stiffness of layers with reasonable accuracy. This study provides the theoretical background and experimental support for this method.

A new approach for relating 'modular ratios' and 'layer thickness ratios' to the constants of the simplified elastic theory model was introduced in this study. Both of these parameters are commonly used in pavement design. The parameters correlated very well with the exponential constant m which signifies vertical displacement behavior of pavement structures.

Comparison between the deflection basin fitting technique, using multi-layered elastic theory, and this method indicates that while both methods rely on reasonable 'starting values', a higher accuracy in the computed deflections is achievable with the deflection basin

fitting technique. In general, similar trends were observed in the layer elastic moduli computed using both the methods. For cost considerations in terms of computer use time, the use of the basin fitting technique must be restricted to applications where a limited number of field deflections are to be analyzed. Low prediction errors and a high accuracy in the predicted deflections were achieved with the new method, in the majority of computations done in this study for the flyash experimental test sites. The conclusions drawn from the study are summarized as follows:

1. The method, developed in this study, was very cost effective and capable of predicting layer stiffnesses, of lime-flyash stabilized pavement structures, from Dynaflect measured field deflections with reasonable accuracy.
2. Flyash, by itself, was found to be generally ineffective in promoting stiffness gains in low PI clayey soils, but provided effective structural support when used with lime. The only significant exception to this finding was section 6, in site 3, that exhibited high stiffness with 12% flyash and no lime.
3. For very low PI coarse sandy soil, stabilization with 'flyash only' was effective and resulted in substantial stiffness gains in the base layers of all the sections.
4. In comparing the test sections constructed on the low PI clayey soils, the optimum lime-flyash ratios were found to be in the range of 0.08 to 0.5, using a minimum of 2% lime.

5. The time study has indicated the progressive stiffening of several sections, and signified the importance of temperature and moisture adjustments in the computed moduli, for determining clear trends over a period of time.

Based on the conclusion reached in this study, the following recommendations are made:

1. Apply the new method developed in this study to individual readings taken in the surveys to determine layer elastic moduli at the individual points of the test sections (as opposed to averages), and statistically analyze these values. The benefit of this approach is that the informations provided by individual deflection basins would be evaluated and more accurate trends in the stiffness behavior of each test section would be determined.
2. Compute stresses in the pavement structures and attempt to predict performance life of these sections with the aid of fatigue based methods such as PDMAP (35) and VESYS IIM (36).
3. Implement the equations developed in this study for lime-flyash stabilized bases and subbases in the Texas Flexible Pavement System (FPS).
4. Continue to monitor the experimental test sites and observe performance with time.
5. Attempt to correlate the results obtained from this study using the Dynaflect data with the Benkleman beam field

measured data of these sites.

REFERENCES

1. Alam, S. M., "Equations for Predicting the Layer Stiffness Moduli in Pavement Systems Containing Lime-flyash Stabilized Materials", Master of Science Thesis, Texas A&M University, College Station, Texas, May, 1984.
2. Lytton, R. L. and Michalak, C. H., "Flexible Pavement Deflection Equation Using Elastic Moduli and Field Measurements", Research Report 207-7F, Texas Transportation Institute, Texas A&M University, College Station, Texas, August, 1979.
3. Vlasov, V. Z. and Leont'ev, N. N., "Beams, Plates and Shells on Elastic Foundation", (Translated from Russian), Israel Program for Scientific Translations, Jerusalem, 1966.
4. Odemark, N., "Investigations as to the Elastic Properties of Soils and Design of Pavements According to the Theory of Elasticity", Staten Vaeginstitut, Stockholm, 1949.
5. McKerall, W. C., Ledbetter, W. B. and Teague, D. J., "Analysis of Flyashes Produced in Texas", Research Report 240-1, Texas Transportation Institute, Texas A&M University, College Station, Texas.
6. Ledbetter, W. B., Teague, D. J., Long, R. L. and Banister, B. N., "Construction of Flyash Test Sites and Guidelines for Construction", Research Report 240-2, Texas Transportation Institute, Texas A&M University, College Station, Texas, October, 1981.
7. McCullough, F. and Taute, A., "Use of Deflection Measurements for Determining Pavement Material Properties", University of Texas at Austin, Transportation Research Record 852.
8. Scrivner, F. H. and Moore, W. M., "Evaluation of the Stiffness of Individual Layers in a Specially Designed Pavement Facility From Surface Deflections", Research Report 32-8, Texas Transportation Institute, Texas A&M University, College Station, Texas, June, 1966.
9. Izatt, J. O., Lettier, J. A. and Taylor, C. A., "The Shell Group Methods for Thickness Design of Asphalt Pavements", Report presented to National Asphalt Paving Association, January, 1967.
10. Raba, G. W., "Evaluation of Lime-flyash Stabilized Bases and Subgrades Using Static and Dynamic Deflection Systems", Master of Science Thesis, Texas A&M University, College Station, Texas, December, 1982.

11. Meyers, J. F., Pichumani, R. and Kapples, B. S., "Flyash as a Construction Material for Highways", Report FHWA-IP-76-16, GAI Consultants, May, 1976.
12. Terrel, R. L., Epps, J. A., Barenburg, E. J., Mitchell, J. K. and Thompson, M. K., "Soil Stabilization in Pavement Structures, A User's Manual, Volume 1 - Pavement Design and Construction Considerations", Report FHWA-IP-80-2, October, 1979.
13. Terrel, R. L., Epps, J. A., Barenburg, E. J., Mitchell, J. K. and Thompson, M. K., "Soil Stabilization in Pavement Structures, A User's Manual, Volume 2 - Mixture Design Considerations", report FHWA-IP-80-2, October, 1979.
14. Moore, W. M. and Swift, G., "A Technique for Measuring the Displacement Vector throughout the Body of a Pavement Structure Subject to Cyclic Loading", Research Report 136-2, Texas Transportation Institute, Texas A&M University, College Station, Texas, August, 1971.
15. Scrivner, F. H. and Moore, W. M., "An Empirical Equation for Predicting Pavement Deflections", Research Report 32-12, Extension of AASHO Road Test Results, Texas Transportation Institute, Texas A&M University, College Station, Texas, October, 1968.
16. Michalak, C. H., Lu, D. Y. and Turman, G. W., "Determining Stiffness Coefficients and Elastic Moduli of Pavement Materials from Dynamic Deflections", Research Report 207-1, Texas Transportation Institute, Texas A&M University, College Station, Texas, November, 1976.
17. Scrivner, F. H. and Moore, W. M., "Some Recent Findings in Pavement Research", Research Report 32-9, Extension of AASHO Road Test Results, Texas Transportation Institute, Texas A&M University, College Station, Texas, July, 1967.
18. Terrel, R. L., "Mechanistic Behavior of Pavement Systems", Research Report 17-2, prepared for Washington State Highway Commission, University of Washington, Olympia, Washington, July, 1976.
19. Swift, G., "An Empirical Equation for Calculating Deflections on the Surface of a Two-layer Elastic System", Research Report 136-4, Texas Transportation Institute, Texas A&M University, College Station, Texas, November, 1972.

20. Moore, W. M., "Elastic Moduli Determination for Simple Two-layer Pavement Structures based on Surface Deflections", Research Report 136-5, Texas Transportation Institute, Texas A&M University, College Station, Texas, August, 1973.
21. Scrivner, F. H., Michalak, C. H. and Moore, W. M., "Calculation of the Elastic Moduli of a Two-layer Pavement System From Measured Surface Deflections", Research Report 123-6, Texas Transportation Institute, Texas A&M University, College Station, Texas and Center for Highway Research, The University of Texas at Austin, Texas, March, 1971.
22. Letto, A. R., "A Computer Program for Function Optimization Using Pattern Search and Gradient Summation Techniques", Report submitted to the graduate college of Texas A&M University for the degree of Master of Engineering in Industrial Engineering, May, 1968. (This pattern search procedure is currently in use at Texas Transportation Institute, Texas A&M University, College Station, Texas.)
23. Vaswani, N. K., "Method for Separately Evaluating Structural Performance of Subgrades and Overlying Flexible Pavements", Highway Research Record Number 362, pp. 48-62.
24. Finn, F., Saraf, C., Kulkarni, R., Nair, K., Smith, W. and Abdullah, A., "The Use of Distress Prediction Subsystems for Design of Pavement Structures", paper presented at Fourth International Conference (1977), Structural Design of Asphalt Pavements.
25. Kenis, W. J., "Predictive Design Procedures, VESYS Users Manual - An Interim Design Method for Flexible Pavement Systems Using VESYS Structural Subsystem", Federal Highway Administration Research Report FHWA-RD-77-154, January, 1978.
26. Kinchen, R. W. and Temple, W. H., "Asphaltic Concrete Overlays of Rigid and Flexible Pavements", Louisiana Highway Research Report for Federal Highway Administration FHWA/LA-80/147, Baton Rouge, Louisiana, 70804, October, 1980.
27. NOAA, "Local Climatological Data - Monthly Summary", published by National Oceanic and Atmospheric Administration, U.S. Department of Commerce, National Climatic Data Center, Asheville, NC, 28801.

APPENDIX A.
Typical Layouts and Sections of Test Sites.



EACH TEST SECTION APPROXIMATELY 800 FT LONG

SECT 1	SECT 2	SECT 3	SECT 4	SECT 5	SECT 6	SECT 7	SECT 8	SECT 9	SECT 10
8% LIME	4% LIME	4% LIME	4% LIME	7% LIME	6% LIME	6% LIME	7% LIME	5% LIME	6% LIME
0% FA	4% FA	8% FA	15% FA	0% FA	6% FA	11% FA	18% FA	23% FA	6% FA

BASE

SUBBASE - SECTIONS 1, 2, 3, 4 & 5 4% LIME 0% FLY ASH

SECTIONS 6, 7, 8, 9, & 10 0% LIME 6% FLY ASH

Note: Construction type 1.

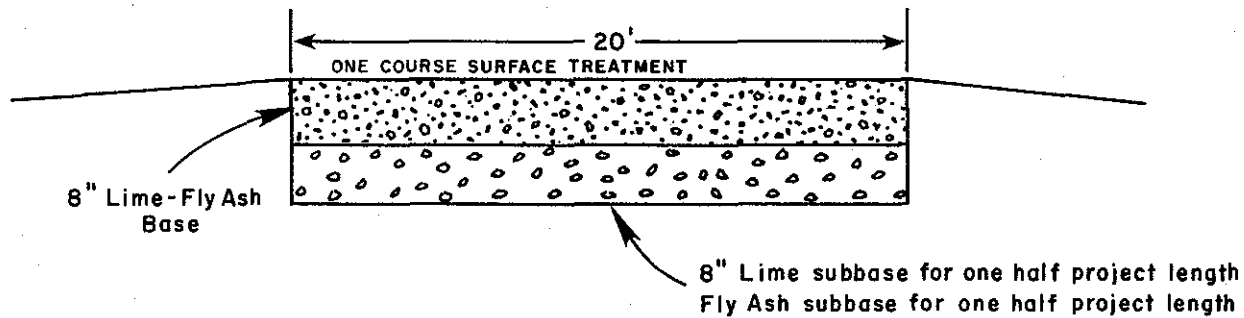


Figure A-1. Typical section and layout planview of Test sections on FM 3378 in Bowie County, Texas - Site No. 1 (6).

N →

EACH TEST SECTION APPROXIMATELY 1000 FT LONG

SECT 1	SECT 2	SECT 3	SECT 4	SECT 5	SECT 6	SECT 7	SECT 8	SECT 9	SECT 10
4% LIME	2% LIME	2% LIME	4% LIME	4% LIME	0% LIME	2% LIME	2% LIME	0% LIME	4% LIME
0% FA	4% FA	8% FA	8% FA	4% FA	22% FA	24% FA	16% FA	15% FA	16% FA

Note: Construction type 2.

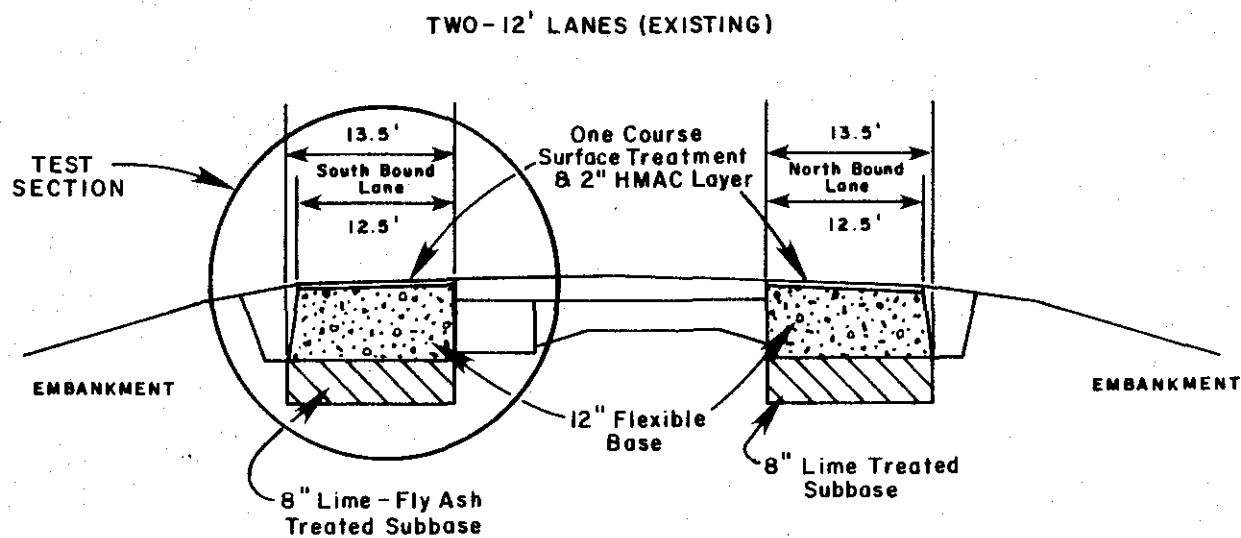


Figure A-2. Typical section and layout planview of Test sections on US 59 in Panola County, Texas - Site No. 2 (6).

EACH TEST SECTION APPROXIMATELY 800 FT LONG



SECT NO. 1 3% LIME 6% FA	TRANSITION	SECT NO 2 3% LIME 9% FA	TRANSITION	SECT NO, 3 1½% LIME 5% FA	TRANSITION	SECT NO. 4 4% LIME 0% FA	TRANSITION	SECT NO. 5 2% LIME 8% FA	TRANSITION	SECT NO. 6 0% LIME 12% FA
--------------------------------	------------	-------------------------------	------------	---------------------------------	------------	--------------------------------	------------	--------------------------------	------------	---------------------------------

Note: Construction type 3.

110

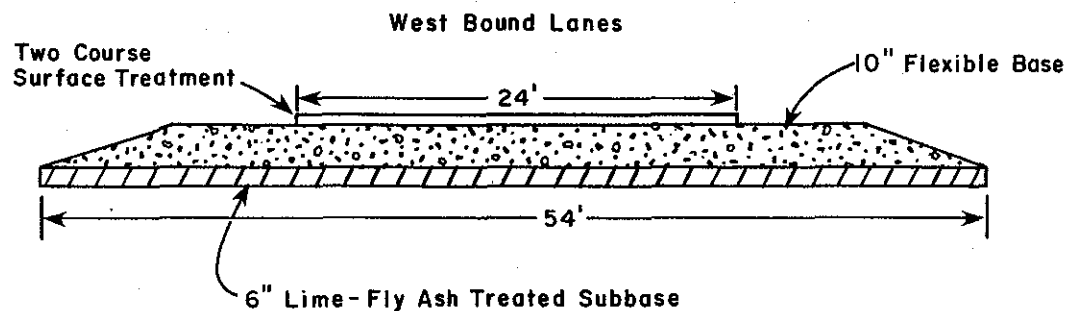


Figure A-3. Typical section and layout planview of Test sections on westbound lanes of FM 1604 in Bexar County, Texas - Site 3 (6).



EACH TEST SECTION APPROXIMATELY 800 FT LONG

SECTION NO. 1 4% LIME 0% FA	650' TRANSITION SECTION	SECTION NO. 2 3% LIME 6% FA	TRANSITION	SECT NO. 3 3% LIME 9% FA	TRANSITION	SECT NO. 4 0% LIME 12% FA	TRANSITION	SECT NO. 5 1.5% LIME 5% FA	TRANSITION	SECT NO. 6 2% LIME 6% FA
-----------------------------------	-------------------------------	-----------------------------------	------------	--------------------------------	------------	---------------------------------	------------	----------------------------------	------------	--------------------------------

Note: Construction type 3.

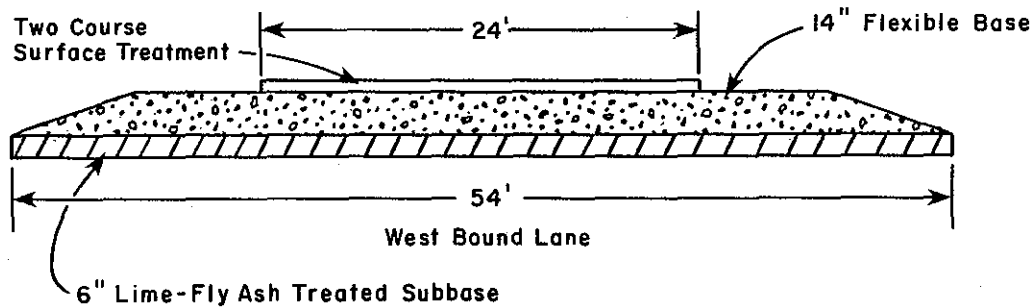


Figure A-4. Typical section and layout planview of Test sections on west bound lanes of FM 1604 in Bexar County, Texas - Site No. 4 (6).

TEST
SECTION
No. 1

2



3

4

5

6

7

8

Each Test Section Approximately 800 ft. long

3% Lime 6% FA	TRANSITION	3% Lime 9% FA	TRANSITION	0% Lime 12% FA	TRANSITION	2% Lime 8% FA	TRANSITION	4% Lime 0% FA	TRANSITION	1½% Lime 5% FA	0% Lime 25% FA	0% Lime 30% FA
------------------	------------	------------------	------------	-------------------	------------	------------------	------------	------------------	------------	-------------------	-------------------	-------------------

Note: Construction type 3.

112

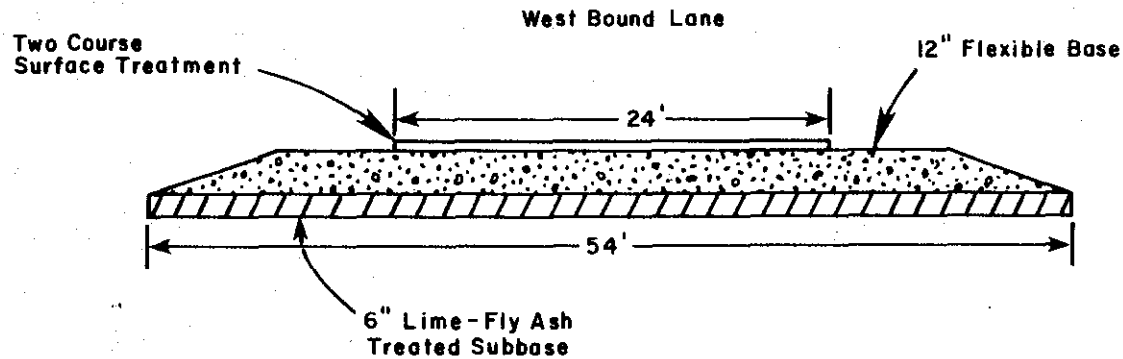
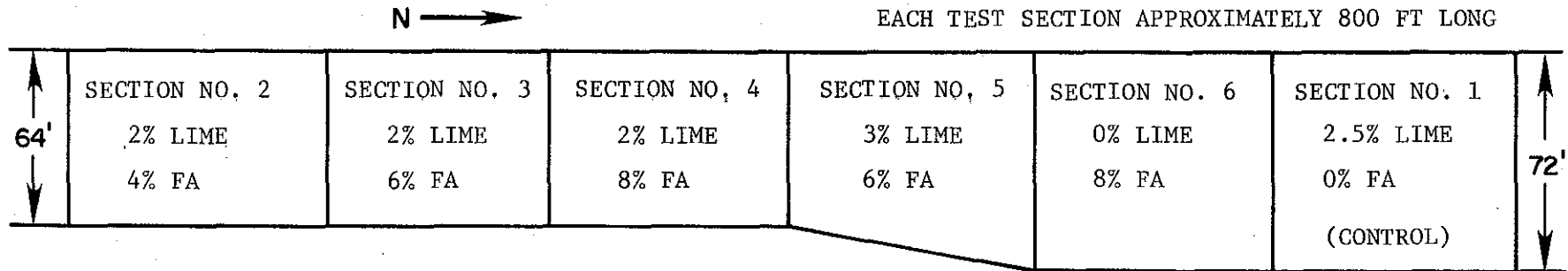


Figure A-5. Typical section and layout planview of test sections on westbound lane of FM 1604 in Bexar County, Texas - Site No. 5 (6).



Note: Construction type 3.

113

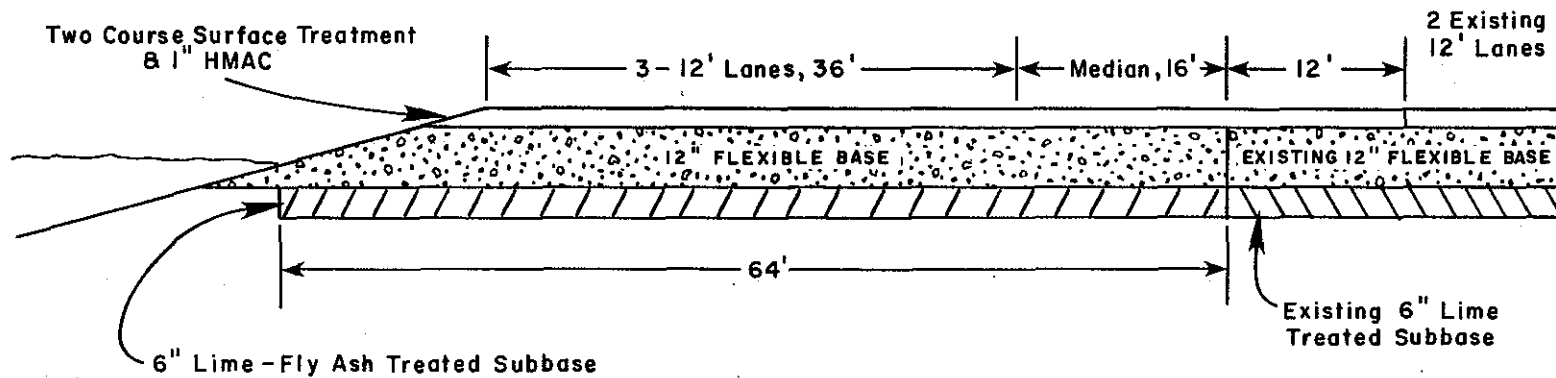
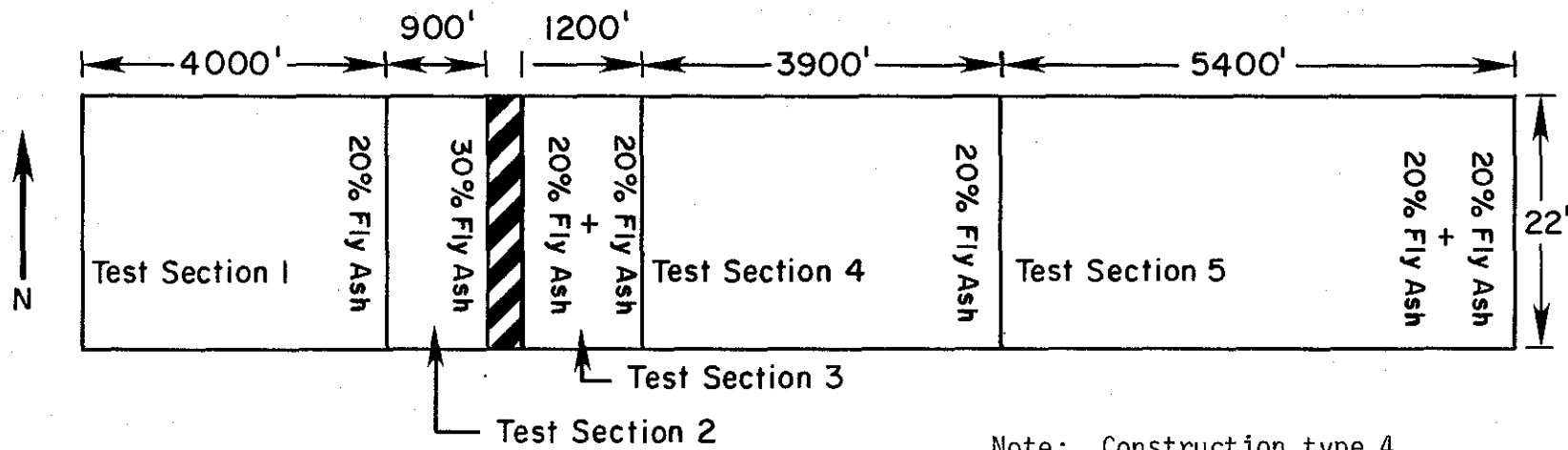


Figure A-6. Typical section and layout planview of Test sections on SH 335 in Potter County, Texas - Site No. 8 (6).



114

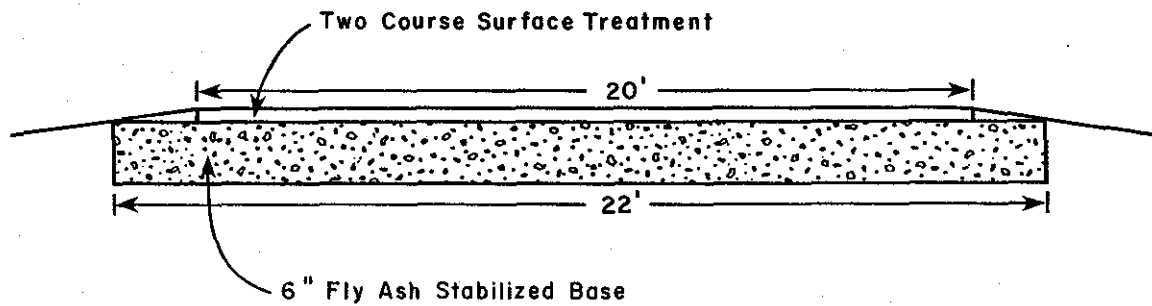
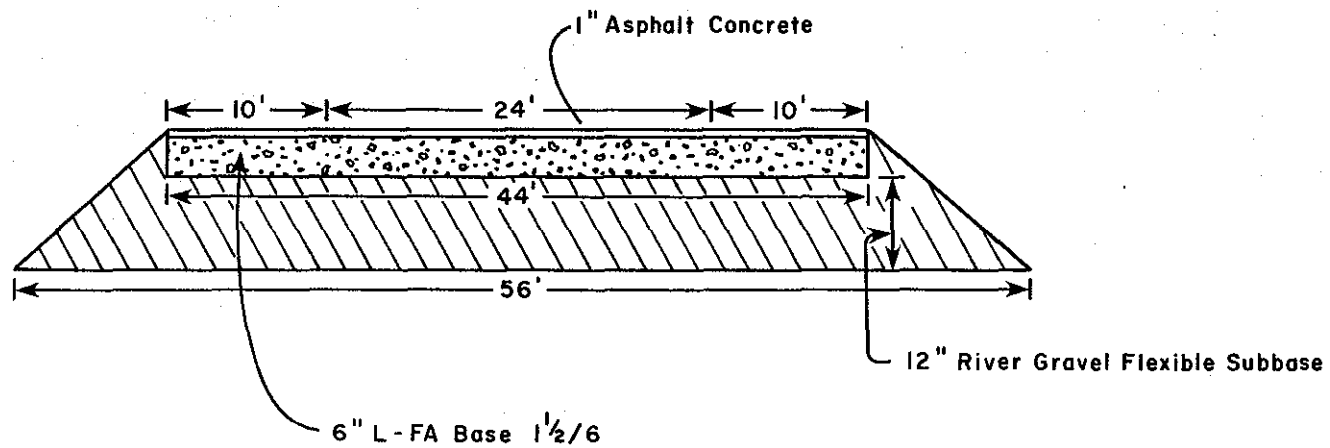


Figure A-7. Typical section and layout planview of Test sections on FM 2697 in Wheeler County, Texas - Site No. 12 (6).



ONE SECTION - 1 1/2 MILES LONG

Figure A-8. Typical section of US 87 in Wilson County, Texas - Site No. 13 (6).

APPENDIX B.
Elastic Modulus of Pavement Layers
Determined by Basin Fitting Technique.

Table B-1. Fitted elastic modulus of pavement layers - Site 1.

Section No	Lime-flyash ratio ^a		Elastic moduli of layers (Ksi)			Modular ratios		Deflection basin fitting criterion	
	8 in. L-FA Base	8 in. L or FA Subbase	E ₁ Base	E ₂ Subbase	E _{sg} Subgrade	K ₁ (E ₁ /E ₂)	K ₂ (E ₂ /E _{sg})	Ave. % variation	Summed Error ε ² (10 ⁻⁸ in ²)
1	8/0	4/0	210	140	39.5	1.5	3.54	4.06	0.1402
2	4/4	4/0	175	50	43	3.5	4.07	4.89	0.2187
3	4/8	4/0	210	120	19	1.75	6.32	2.00	0.2117
4	4/15	4/0	210	95	19	2.21	5.00	2.72	0.1619
5	7/0	4/0	200	100	15	2.00	6.67	8.69	1.9688
6	6/6	0/6	90	30	21.5	3.00	1.40	2.85	0.2249
7	6/11	0/6	90	25	24	3.60	1.04	7.11	1.0167
8	7/18	0/6	175	30	29	5.83	1.03	4.14	0.3081
9	5/23	0/6	100	27	23	3.70	1.17	3.39	0.5985
10	6/6	0/6	100	23	20	4.35	1.15	2.33	0.2446

Note: Refer to Table B-2 Appendix B for fitting results of field deflections to analytically determine deflections of this site.

^aActual percentage by weight

Table B-2. Fitted deflection basins - Site 1.

Section No.	Field basin (F) Analytic basin (A)	Dynalect deflections at different geophone locations (in mils)					Deflection basins ^b fitting criterion	
		W ₁	W ₂	W ₃	W ₄	W ₅	Ave.% varia- tion	Summed Error $\epsilon^2(10^{-8} \text{ in}^2)$
1	F	0.478	0.369	0.271	0.203	0.140	4.06	0.1402
	A	0.503	0.395	0.273	0.194	0.144		
2	F	0.559	0.414	0.272	0.182	0.121	4.89	0.2187
	A	0.601	0.429	0.262	0.175	0.128		
3	F	0.828	0.712	0.534	0.400	0.307	2.00	0.2117
	A	0.870	0.728	0.543	0.404	0.307		
4	F	0.877	0.726	0.532	0.395	0.299	2.72	0.1619
	A	0.904	0.748	0.549	0.404	0.305		
5	F	1.051	0.824	0.593	0.503	0.465	8.69*	1.9688
	A	1.070	0.902	0.680	0.510	0.390		
6	F	1.163	0.810	0.487	0.355	0.238	2.85	0.2249
	A	1.140	0.830	0.519	0.350	0.258		
7	F	1.030	0.807	0.484	0.316	0.190	7.11	1.0167
	A	1.120	0.788	0.471	0.312	0.229		
8	F	0.836	0.610	0.400	0.279	0.187	4.14	0.3081
	A	0.877	0.642	0.394	0.261	0.191		
9	F	1.036	0.817	0.493	0.332	0.228	3.39	0.5985
	A	1.110	0.799	0.489	0.327	0.240		
10	F	1.236	0.925	0.568	0.405	0.278	2.33	0.2446
	A	1.270	0.918	0.565	0.377	0.276		

^aThis table is cross referenced to Table B-1.

^bSections exceeding fitting criterion are marked with an asterisk.

Table B-3. Fitted elastic modulus of pavement layers - Site 2.

Section No	Lime-flyash ratio ^a		Elastic moduli of layers (Ksi)				Modular ratios			Deflection basin fitting criterion		
	2in.HMAC Surf.	12in.Flex Base	8in.L-FA Subbase	E ₁ Surf.	E ₂ Base	E ₃ Sbase	E _{sg} Subgrade	K ₁ (E ₁ /E ₂)	K ₂ (E ₂ /E ₃)	K ₃ (E ₃ /E _{sg})	Ave.% variation	Summed Error $\epsilon^2(10^{-8} \text{ in}^2)$
1			4/0	450	120	120	21.5	3.75	1.00	5.58	3.63	0.2272
2			2/4	400	80	80	33.5	5.00	1.00	2.39	3.11	0.0911
3			2/8	350	140	80	30	2.50	1.75	2.67	2.05	0.0594
4			4/8	450	168	110	42	2.68	1.53	2.62	2.38	0.0411
5			4/4	450	210	110	33	2.14	1.91	3.33	2.63	0.0787
6			0/22	450	95	80	21.5	4.74	1.19	3.72	2.68	0.1470
7			2/24	400	150	110	20.5	2.67	1.36	5.37	2.07	0.0557
8			2/16	400	100	85	23.5	4.00	1.18	3.62	3.48	0.1889
9			0/15	350	95	86	13.5	3.68	1.10	6.37	3.42	0.8150

Note: Refer to Table B-4 Appendix B for fitting results of field deflections to analytically determined deflections of this site.

^aActual percentage by weight.

Table B-4. Fitted Deflection Basins - Site 2^a.

Section No.	Field basin (F) Analytic basin (A)	Dynalect deflections at different geophone locations (in mils)					Deflection basins fitting criterion	
		W ₁	W ₂	W ₃	W ₄	W ₅	Ave.% variation	Summed Error $\epsilon^2(10^{-8}\text{in}^2)$
1	F	0.658	0.495	0.396	0.334	0.268	3.63	0.2272
	A	0.620	0.518	0.411	0.327	0.263		
2	F	0.543	0.426	0.293	0.222	0.171	3.11	0.0911
	A	0.534	0.399	0.287	0.215	0.167		
3	F	0.543	0.426	0.310	0.249	0.191	2.05	0.0594
	A	0.521	0.423	0.318	0.243	0.190		
4	F	0.394	0.323	0.225	0.178	0.135	2.38	0.0411
	A	0.383	0.307	0.228	0.173	0.135		
5	F	0.450	0.365	0.259	0.218	0.174	2.63	0.0787
	A	0.434	0.364	0.282	0.219	0.174		
6	F	0.720	0.564	0.413	0.343	0.265	2.68	0.1470
	A	0.687	0.556	0.426	0.331	0.263		
7	F	0.641	0.538	0.411	0.351	0.273	2.07	0.0557
	A	0.630	0.537	0.430	0.344	0.278		
8	F	0.669	0.537	0.404	0.321	0.243	3.48	0.1889
	A	0.637	0.515	0.393	0.305	0.241		
9	F	1.011	0.821	0.612	0.517	0.415	3.42	0.8150
	A	0.929	0.791	0.638	0.515	0.418		

^aThis table is cross referenced to Table B-3.

Table B-5. Fitted elastic modulus of pavement layers - Site 3.

Section No	Lime-flyash ratio ^a		Elastic moduli of layers (Ksi)			Modular ratios		Deflection basin fitting criterion	
	10 in. Flex Base	6 in. L-FA Subbase	E ₁ Base	E ₂ Subbase	E _{sg} Subgrade	K ₁ (E ₁ /E ₂)	K ₂ (E ₂ /E _{sg})	Ave. % variation	Summed Error $\epsilon^2 (10^{-8} \text{ in}^2)$
1		3/6	100	75	32	1.33	2.34	9.04	0.4770
2		3/9	100	65	34.5	1.54	1.88	7.70	0.7015
3		1½/5	140	110	40	1.27	2.75	2.51	0.1488
4		4/0	300	275	34.5	1.09	7.97	5.31	0.2198
5		2/8	160	115	38.5	1.39	2.99	3.59	0.1064
6		0/12	220	125	30.5	1.76	4.10	2.61	0.0711

Note: Refer to Table B-6 Appendix B for fitting results of field deflections to analytically determined deflections of this site. Layer thickness ratio D = 1.67.

^aActual percentage by weight.

Table B-6. Fitted deflection basins - Site 3^a.

Section No.	Field basin (F)/ Analytic basin (A)	Dynalect deflections at different geophone locations (in mils)					Deflection basin ^b fitting criterion	
		W ₁	W ₂	W ₃	W ₄	W ₅	Ave.% variation	Summed Error $\epsilon^2(10^{-8}\text{in}^2)$
1	F	0.647	0.480	0.271	0.213	0.196	9.04*	0.4770
	A	0.621	0.480	0.328	0.232	0.174		
2	F	0.676	0.470	0.274	0.193	0.163	7.70*	0.7015
	A	0.603	0.457	0.306	0.215	0.160		
3	F	0.518	0.381	0.259	0.188	0.137	2.51	0.1488
	A	0.480	0.376	0.262	0.187	0.140		
4	F	0.461	0.344	0.263	0.213	0.169	5.31*	0.2198
	A	0.437	0.375	0.288	0.219	0.169		
5	F	0.506	0.368	0.255	0.192	0.147	3.59	0.1064
	A	0.485	0.386	0.272	0.195	0.146		
6	F	0.573	0.445	0.326	0.245	0.185	2.61	0.0711
	A	0.555	0.460	0.338	0.248	0.188		

^aThis table is cross referenced to Table B-5.

^bSections exceeding fitting criterion are marked with an asterisk.

Table B-7. Fitted elastic modulus of pavement layers - Site 4.

Section No	Lime-flyash ratio ^a		Elastic moduli of layers (Ksi)			Modular ratios		Deflection basin fitting criterion	
	14in.Flex Base	6in.L-FA Subbase	E ₁ Base	E ₂ Subbase	E _{sg} Subgrade	K ₁ (E ₁ /E ₂)	K ₂ (E ₂ /E _{sg})	Ave.% variation	Summed Error ε ² (10 ⁻⁸ in ²)
1		4/0	180	170	23	1.06	7.39	1.88	0.0613
2		3/6	150	50	24	3.00	2.08	2.00	0.0859
3		3/9	150	45	28	3.33	1.61	3.02	0.1574
4		0/12	100	35	24	2.86	1.46	4.98	0.4566
5		1½/5	80	50	26	1.60	1.92	6.18	0.6734
6		2/6	150	90	23	1.67	3.91	3.25	0.1703

Note: Refer to Table B-8 Appendix B for fitting results of field deflections to analytically determined deflections of this site. Layer thickness ratio D = 2.33.

^aActual percentage by weight.

Table B-8. Fitted deflection basins - Site 4.

Section No.	Field basin (F)/ Analytic basin (A)	Dynalect deflections at different geophone locations (in mils)					Deflection basins ^b fitting criterion	
		W ₁	W ₂	W ₃	W ₄	W ₅	Ave. % variation	Summed Error $\epsilon^2 (10^{-8} \text{ in}^2)$
1	F	0.583	0.489	0.377	0.314	0.251	1.88	0.0613
	A	0.578	0.499	0.399	0.316	0.251		
2	F	0.695	0.558	0.399	0.315	0.237	2.00	0.0859
	A	0.673	0.559	0.418	0.313	0.240		
3	F	0.649	0.497	0.347	0.274	0.209	3.02	0.1574
	A	0.615	0.502	0.366	0.270	0.205		
4	F	0.794	0.572	0.385	0.308	0.238	4.98	0.4566
	A	0.762	0.608	0.432	0.314	0.237		
5	F	0.767	0.525	0.340	0.279	0.218	6.18*	0.6734
	A	0.709	0.552	0.391	0.285	0.216		
6	F	0.647	0.519	0.385	0.323	0.256	3.25	0.1703
	A	0.644	0.543	0.418	0.321	0.251		

^aThis table is cross referenced to Table B-7.

^bSections exceeding fitting criterion are marked with an asterisk.

Table B-9. Fitted elastic modulus of pavement layers - Site 5.

Section No	Lime-flyash ratio ^a		Elastic moduli of layers (Ksi)			Modular ratios		Deflection basin fitting criterion	
	12in.Flex Base	6in.L-FA Subbase	E ₁ Base	E ₂ Subbase	E _{sg} Subgrade	K ₁ (E ₁ /E ₂)	K ₂ (E ₂ /E _{sg})	Ave.% variation	Summed Error ε ² (10 ⁻⁸ in ²)
1		3/6	150	95	30.5	1.58	3.11	4.19	0.2219
2		3/9	120	50	34	2.40	1.47	2.08	0.2084
3		0/12	150	48	27	3.13	1.78	3.52	0.1641
4		2/8	175	100	26	1.75	3.85	4.47	0.1926
5		4/0	220	126	24	1.75	5.25	4.47	0.2560
6		1½/5	125	57	30	2.19	1.90	3.52	0.2648
7		0/25	125	25	24.5	5.00	1.02	2.07	0.1173
8		0/30	150	90	29	1.67	3.10	2.95	0.1876

Note: Refer to Table B-10 Appendix B for fitting results of field deflections to analytically determined deflections of this site. Layer thickness ratio D = 2.0.

^aActual percentage by weight.

Table B-10. Fitted deflection basins - Site 5^a.

Section No.	Field basin (F)/ Analytic basin (A)	Dynalect deflections at different geophone locations (in mils)					Deflection basins fitting criterion	
		W ₁	W ₂	W ₃	W ₄	W ₅	Ave. % variation	Summed Error $\epsilon^2(10^{-8} \text{ in}^2)$
1	F	0.541	0.416	0.314	0.244	0.190	4.19	0.2219
	A	0.559	0.455	0.333	0.246	0.187		
2	F	0.633	0.467	0.316	0.221	0.165	2.08	0.2084
	A	0.589	0.456	0.311	0.220	0.164		
3	F	0.675	0.517	0.360	0.272	0.208	3.52	0.1641
	A	0.675	0.545	0.388	0.280	0.211		
4	F	0.632	0.483	0.363	0.291	0.237	4.47	0.1926
	A	0.611	0.511	0.384	0.289	0.221		
5	F	0.619	0.487	0.372	0.300	0.240	4.47	0.2560
	A	0.608	0.522	0.405	0.311	0.242		
6	F	0.671	0.477	0.331	0.249	0.191	3.52	0.2648
	A	0.626	0.495	0.348	0.250	0.188		
7	F	0.854	0.649	0.430	0.316	0.234	2.07	0.1173
	A	0.825	0.654	0.447	0.313	0.231		
8	F	0.622	0.459	0.340	0.261	0.199	2.95	0.1876
	A	0.584	0.477	0.350	0.259	0.197		

^aThis table is cross referenced to Table B-9.

Table B-11. Fitted elastic modulus of pavement layers - Site 8.

Section No	Lime-flyash ratio ^a		Elastic moduli of layers (psi)			Modular ratios		Deflection basin fitting criterion	
	12in.Flex Base	6in.L-FA Subbase	E ₁ Base	E ₂ Subbase	E _{sg} Subgrade	K ₁ (E ₁ /E ₂)	K ₂ (E ₂ /E _{sg})	Ave.% variation	Summed Error ε ² (10 ⁻⁸ in ²)
1		2½/0	175	80	37	2.19	2.16	4.04	0.1456
2		2/4	200	140	30	1.43	4.67	2.50	0.0436
3		2/6	175	90	26	1.94	3.46	2.38	0.0450
4		2/8	200	110	27.5	1.82	4.00	2.56	0.0752
5		3/6	200	90	31	2.22	2.90	4.24	0.1068
6		0/8	200	80	33.5	2.50	2.39	3.91	0.0626

Note: Refer to Table B-12 Appendix B for fitting results of field deflections to analytically determined deflections of this site. Layer thickness ratio D = 2.0.

^aActual percentage by weight

Table B-12. Fitted deflection basins - Site 8.

Section No.	Field basin (F)/ Analytic basin (A)	Dynalect deflections at different geophone locations (in mils)					Deflection basins fitting criterion	
		W ₁	W ₂	W ₃	W ₄	W ₅	Ave. %	Summed
1	F	0.523	0.393	0.285	0.218	0.146	4.04	0.1456
	A	0.489	0.392	0.280	0.203	0.153		
2	F	0.520	0.421	0.331	0.264	0.187	2.50	0.0436
	A	0.516	0.434	0.330	0.249	0.192		
3	F	0.632	0.508	0.386	0.301	0.212	2.38	0.0450
	A	0.620	0.517	0.386	0.289	0.221		
4	F	0.590	0.475	0.371	0.286	0.207	2.56	0.0752
	A	0.568	0.478	0.362	0.273	0.210		
5	F	0.550	0.445	0.343	0.267	0.179	4.24	0.1068
	A	0.536	0.443	0.327	0.243	0.185		
6	F	0.527	0.416	0.313	0.242	0.160	3.91	0.0626
	A	0.515	0.422	0.307	0.225	0.171		

^aThis table is cross referenced to Table B-11.

Table B-13. Fitted elastic modulus of pavement layers - Site 12.

Section No	Lime-flyash ratio ^a		Elastic moduli of layers (Ksi)		Modular ratio	Deflection basin fitting criterion	
	6 in.FA Base	Stabilized	E ₁ Base	Esg Subgrade	K ₁ (E ₁ /Esg)	Ave.% variation	Summed Error ε ² (10 ⁻⁸ in ²)
1	0/20		250	22.5	11.11	3.67	0.3554
2	0/30		1243	15.5	80.19	2.13	0.1229
3	0/40		606	17.5	34.63	1.70	0.1570
4	0/20		632	23.7	26.67	1.02	0.0213
5	0/40		1300	19.0	68.42	1.46	0.0449

Note: Refer to Table B-14 Appendix B for fitting results of field deflections to analytically determined deflections of this site.

^aActual percentage by weight.

Table B-14. Fitted deflection basins - Site 12^a.

Section No.	Field basin (F)/ Analytic basin (A)	Dynalect deflections at different geophone locations (in mils)					Deflection basins fitting criterion	
		W ₁	W ₂	W ₃	W ₄	W ₅	Ave. % variation	Summed Error $\epsilon^2 (10^{-8} \text{ in}^2)$
1	F	1.136	0.850	0.514	0.323	0.229	3.67	0.3554
	A	1.170	0.823	0.475	0.311	0.231		
2	F	1.183	1.015	0.712	0.498	0.352	2.13	0.1229
	A	1.210	1.020	0.725	0.507	0.367		
3	F	1.250	0.979	0.643	0.411	0.307	1.70	0.1570
	A	1.280	1.000	0.645	0.426	0.307		
4	F	0.981	0.750	0.472	0.299	0.224	1.02	0.0213
	A	0.939	0.757	0.472	0.309	0.224		
5	F	1.024	0.836	0.592	0.408	0.308	1.46	0.0449
	A	1.030	0.852	0.595	0.410	0.296		

^aThis table is cross referenced to Table B-13.

Table B-15. Fitted elastic modulus of pavement layers - Site 13.

Sect. No.	Lime-flyash ratio ^a		Elastic moduli of layers (Ksi)				Modular ratios			Deflection basin fitting criterion		
	1 in. AC Surf.	6 in. L-FA Base	12 in. Flex Subbase ^b	E ₁ Surf.	E ₂ Base	E ₃ Sbase ^b	Esg Subg.	K ₁ (E ₁ /E ₂)	K ₂ (E ₂ /E ₃)	K ₃ (E ₃ /Esg)	Ave. % variation	Summed Error ε ² (10 ⁻⁸ in ²)
1		1½/6		500	200	50	17	2.5	4.00	2.94	4.95	0.3185

Note: Refer to Table B-16 Appendix B for fitting results of field deflections to analytically determined deflections of this site.

^aActual percentage by weight.

^bRiver gravel Flexible subbase.

Table B-16. Fitted results of field measured Dynaflect deflection basin to analytically determined basin - Test site No. 13

Section No.	Field basin (F)/ Analytic basin (A)	Dynaflect deflection at different geophone locations (in mils)					Deflection basins fitting criterion	
		W_1	W_2	W_3	W_4	W_5	Ave. % variation	Summed Error $\epsilon^2 (10^{-8} \text{ in}^2)$
1	F	1.098	0.804	0.554	0.414	0.343		
	A	1.040	0.833	0.595	0.437	0.333	4.95	0.3185

^aThis table is cross referenced to Table B-15. For field deflections refer to Table F-27, Appendix F.

APPENDIX C.
Vertical Deflections at Selected Pavement Depths,
Computed at Dynaflect Sensor-1 Location.

Table C-1. Vertical deflections at selected pavement depths - Site 1^a.

Depth z (inch)	Deflections at Sensor-1 Location of Dynaflect (in mil) for Section No:							
	2	3	4	6	7	8	9	10
0	0.601	0.870	0.904	1.140	1.120	0.877	1.110	1.270
8	0.593	0.871	0.903	1.130	1.100	0.868	1.100	1.250
16	0.467	0.827	0.847	0.924	0.849	0.667	0.867	0.984
28	0.342	0.638	0.648	0.677	0.621	0.492	0.636	0.722
40	0.262	0.512	0.517	0.520	0.475	0.379	0.488	0.555
52	0.210	0.425	0.427	0.418	0.380	0.305	0.392	0.447
64	0.175	0.361	0.362	0.348	0.315	0.254	0.325	0.372
76	0.149	0.313	0.314	0.297	0.268	0.217	0.277	0.317

^aThis table is cross referenced to Table 3.

Table C-2. Vertical deflections at selected pavement depths - Site 2^a.

Depth z (inch)	Deflections at Sensor-1 location of Dynaflect (in mil) for Section No:							
	2	3	4	5	6	7	8	9
0	0.534	0.521	0.383	0.434	0.687	0.630	0.637	0.929
2	0.537	0.526	0.387	0.439	0.692	0.636	0.643	0.936
14	0.518	0.517	0.380	0.434	0.677	0.632	0.630	0.929
22	0.451	0.460	0.337	0.394	0.618	0.592	0.574	0.877
34	0.338	0.353	0.257	0.306	0.475	0.467	0.441	0.695
46	0.269	0.285	0.207	0.250	0.386	0.386	0.358	0.576
58	0.223	0.239	0.173	0.211	0.325	0.325	0.301	0.492
70	0.190	0.206	0.148	0.183	0.280	0.280	0.259	0.428

^aThis table is cross referenced to Table 4.

Table C-3. Vertical deflections at selected pavement depths - Site 3^a.

Depth z (inch)	Deflections at Sensor-1 location of the Dynaflect (in mil) for Section No:				
	1	2	3	5	6
0	0.621	0.603	0.480	0.485	0.555
10	0.651	0.629	0.503	0.507	0.573
16	0.590	0.558	0.462	0.469	0.540
28	0.431	0.405	0.340	0.346	0.408
40	0.332	0.311	0.263	0.269	0.323
52	0.269	0.251	0.213	0.219	0.266
64	0.224	0.209	0.178	0.184	0.225
76	0.192	0.179	0.153	0.158	0.194

^aThis Table is cross referenced to Table 5.

Table C-4. Vertical deflections at selected pavement depths - Site 4^a.

Depth z (inch)	Deflections at Sensor-1 location of the Dynaflect (in mil) for Section No:				
	2	3	4	5	6
0	0.673	0.615	0.762	0.709	0.644
14	0.676	0.615	0.761	0.711	0.654
20	0.610	0.541	0.659	0.631	0.614
32	0.466	0.411	0.495	0.469	0.474
44	0.375	0.329	0.393	0.370	0.384
56	0.313	0.273	0.324	0.304	0.321
68	0.268	0.232	0.275	0.257	0.276
80	0.233	0.202	0.239	0.222	0.241

^aThis table is cross referenced to Table 6.

Table C-5. Vertical deflections at selected pavement depths - Site 5^a.

Depth Z (inch)	Deflections at Sensor-1 location of Dynaflect (in mil) for Section No:						
	1	2	3	4	6	7	8
0	0.559	0.589	0.675	0.611	0.626	0.825	0.584
12	0.574	0.599	0.684	0.627	0.638	0.831	0.600
18	0.532	0.516	0.606	0.588	0.567	0.685	0.555
30	0.399	0.380	0.454	0.448	0.420	0.514	0.418
42	0.316	0.297	0.359	0.359	0.330	0.405	0.331
54	0.261	0.242	0.295	0.298	0.270	0.331	0.273
66	0.221	0.203	0.250	0.254	0.228	0.279	0.232
78	0.191	0.175	0.216	0.220	0.196	0.241	0.201

^aThis table is cross referenced to Table 7.

Table C-6. Vertical deflections at selected pavement depths - Site 8^a.

Depth z (inch)	Deflections at Sensor-1 location of the Dynaflect (in mil) for Section No:				
	2	3	4	5	6
0	0.516	0.620	0.568	0.536	0.515
12	0.532	0.634	0.583	0.547	0.525
18	0.504	0.592	0.548	0.505	0.477
30	0.386	0.450	0.419	0.382	0.359
42	0.310	0.360	0.336	0.304	0.285
54	0.257	0.298	0.280	0.252	0.235
66	0.220	0.254	0.239	0.214	0.200
78	0.191	0.221	0.208	0.186	0.173

^aThis table is cross referenced to Table 8.

Table C-7. Vertical deflections at selected pavement depths - Site 12^a.

Depth z (inch)	Deflections (in mil) for Section No.:				
	1	2	3	4	5
0	1.170	1.210	1.280	0.989	1.030
6	1.170	1.210	1.280	0.986	1.020
18	0.863	0.963	0.974	0.745	0.807
30	0.624	0.756	0.735	0.556	0.629
42	0.476	0.610	0.577	0.433	0.505
54	0.382	0.505	0.470	0.351	0.417
66	0.317	0.429	0.394	0.293	0.353
78	0.270	0.371	0.338	0.251	0.304

^aThis table is cross referenced to Table 9.

APPENDIX D.
Values of Constants n , C , B and H
Determined by Regression Analysis Number 2.

Table D-1. Values of Constants m, n, C, B and H determined by Regression Analysis Number 2 - Site 1^a.

Sect No	Values of Constants					Sum of squared error
	m	n	C	B	H	ϵ^2 (10^{-8} in ²)
2	1.7069	0.42653	0.94985	0.86013	83.317	1.7648
3	0.72971	0.29159	1.1116	1.1087	71.012	1.5973
4	0.90735	0.29925	0.99256	1.0048	69.988	2.3571
6	1.5980	0.41803	0.95843	0.88196	78.889	10.870
7	1.7480	0.44157	0.96281	0.85843	81.987	5.7135
8	2.0250	0.36877	0.88208	1.1288	77.00	21.759
9	1.7270	0.43308	0.95431	0.86444	82.986	6.2273
10	1.8075	0.39034	0.91281	0.78855	81.667	9.7403

^aConstruction type 1 - L-FA base over L or FA subbase.

Table D-2. Values of Constants m, n, C, B and H determined by Regression Analysis Number 2 - Site 2^a.

Sect No	Values of Constants					Sum of squared error
	m	n	C	B	H	ϵ^2 (10^{-8} in ²)
2	0.74780	0.31226	1.1292	1.0880	71.00	1.4342
3	0.57605	0.38545	1.2654	1.2288	69.333	1.2350
4	0.63006	0.31972	1.2031	1.1964	71.00	0.6089
5	0.48839	0.34487	1.2758	1.7018	69.012	0.85689
6	0.55765	0.30148	1.2316	1.3114	73.111	2.1924
7	0.41968	0.37198	1.3189	1.8184	67.963	1.0719
8	0.583820	0.36059	1.2406	1.2406	70.037	1.4739
9	0.37840	0.35365	1.3838	1.9439	67.074	3.6524

^a Construction type 2 - HMAC layer over flexible base and L-FA subbase.

Table D-3. Values of Constants m, n, C, B and H determined by Regression Analysis Number 2 - Sites 3, 4, 5 and 8^a.

Site No	Sect No	Values of Constants					Sum of Squared error
		m	n	C	B	H	ϵ^2 (10^{-8} in ²)
3	1	0.88849	0.32666	1.1765	0.81444	78.986	4.1454
3	2	0.96160	0.45467	1.1577	0.8420	71.00	4.4572
3	3	0.82433	0.51901	1.2465	0.97902	70.332	1.5778
3	5	0.78395	0.53276	1.2320	1.0672	70.002	1.5840
3	6	0.62440	0.36347	1.3580	1.2957	75.014	1.3579
4	2	0.74670	0.46585	1.2037	1.0941	70.00	1.8726
4	3	0.80633	0.37063	1.1940	1.0033	76.039	2.1540
4	4	0.84635	0.30851	1.1484	0.99159	78.554	4.3590
4	5	0.81663	0.29394	1.1749	1.0361	78.664	5.0807
4	6	0.55707	0.47436	1.3516	1.3506	72.629	1.5867
5	1	0.70302	0.33349	1.2378	1.2355	81.999	1.2182
5	2	0.92939	0.34777	1.1948	0.91853	75.666	2.3885
5	3	0.85013	0.31259	1.1418	0.92271	78.00	2.3227
5	4	0.60706	0.46594	1.3533	1.3674	72.667	1.8473
5	6	0.86377	0.35767	1.1791	0.91844	75.996	2.9981
5	7	0.90774	0.47551	1.2036	0.89158	70.033	4.1386
5	8	0.70194	0.49881	1.2827	1.1974	69.964	1.9651
8	2	0.52616	0.38772	1.4774	1.3577	79.037	0.64382
8	3	0.64796	0.35801	1.3136	1.2336	76.888	1.1242
8	4	0.58781	0.42185	1.3936	1.3869	73.00	0.90458
8	5	0.71242	0.39561	1.3051	1.2343	76.00	0.7169
8	6	0.77686	0.48025	1.2287	1.0694	70.00	0.82822

^a Construction type 3 - Flexible base over L-FA subbase.

Table D-4. Values of Constants m, n, C, B and H determined by Regression Analysis Number 2 - Site 12^a.

Sect No	Values of Constants					Sum of Squared error
	m	n	C	B	H	ϵ^2 (10^{-8} in ²)
1	1.6658	0.34996	0.98882	0.87005	78.959	8.6988
2	0.88225	0.28750	1.0792	1.0125	63.889	3.8735
3	1.3417	0.35033	0.99093	0.94960	70.00	8.1049
4	1.4436	0.36285	0.99615	0.93701	71.963	5.9134
5	0.98317	0.255361	1.0603	0.99032	68.996	3.8430

^aConstruction type 4 - FA base over natural subgrade.

APPENDIX E.
Predicted Elastic Modulus of Pavement
Layers Computed by Regression Analysis Number 3.

Tabel E-1. Predicted elastic modulus of pavement layers (36 month survey) - Site 1.

Section No	Lime-Flyash ^a Ratio		Elastic modulus of layers (Ksi) ^b			Modular Ratios		Deflection basin fit:
	8 in. L-FA Base	8 in. L or FA Subbase	E ₁ Base	E ₂ Subbase	E _{sg} Subbase	K ₁ (E ₁ /E ₂)	K ₂ (E ₂ /E _{sg})	ε ² (10 ⁻⁸ in ²)
2	4/4	4/0	99.9	90.0	46.5	1.11	1.93	2.6208
3	4/8	4/0	118.8	108.8	18.3	1.09	5.92	1.6195
4	4/15	4/0	100.0	90.0	18.8	1.11	4.77	2.9155
6	6/6	0/6	99.9	45.0	23.7	2.22	1.90	15.716*
7	6/11	0/6	99.9	45.0	29.6	2.22	1.52	15.58*
8	7/18	0/6	99.9	45.0	30.1	2.22	1.49	4.723
9	5/23	0/6	99.9	45.0	24.7	2.22	1.82	9.347
10	6/6	0/6	99.9	45.0	20.3	2.22	2.22	14.546*

Note: Refer to Table E-2, Appendix E for predicted deflections and values of constants. High error ε² marked with asterisk. Construction type 1 - L-FA base over L or FA subbase.

^aActual percentage by weight.

^bElastic modulus values given in table are uncorrected values.

Table E-2. Predicted deflection basins and values of Constants (36 month survey) - Site 1.

Section No	Predicted deflections at geophone locations (in mils):					Values of constants					Error
	W_1	W_2	W_3	W_4	W_5	m	n	C	B	H	$\epsilon^2 (10^{-8} \text{ in.}^2)$
2	0.422	0.399	0.335	0.238	0.126	1.31	0.427	1.044	0.755	79.68	2.6208
3	0.761	0.721	0.608	0.437	0.237	0.74	0.32	1.084	0.96	72.6	1.6195
4	0.802	0.763	0.651	0.483	0.282	0.873	0.348	1.072	0.896	74.58	2.9155
6	0.809	0.764	0.635	0.443	0.221	1.414	0.415	1.002	0.814	79.67	15.716*
7	0.679	0.638	0.524	0.355	0.162	1.492	0.427	0.999	0.795	80.38	15.58*
8	0.670	0.630	0.517	0.349	0.158	1.498	0.427	0.998	0.794	80.43	4.723
9	0.783	0.738	0.612	0.425	0.209	1.43	0.417	1.002	0.81	79.82	9.347
10	0.910	0.861	0.721	0.513	0.270	1.35	0.405	1.005	0.83	79.08	14.546*

Note: Refer to Table E-1 for predicted elastic moduli and to Table F-4, Appendix F, for field-measured deflections. High error ϵ^2 marked with asterisk.

Table E-3. Predicted elastic modulus of pavement layers (37 month survey) - Site 2.

Section No:	Lime-flyash ratio		Elastic modulus of layers (Ksi) ^b					Modular Ratios			Deflection basin fit
	2in.HMAC Surf.	12in.Flex Base	8in.L-FA Sbase	E ₁ Surf.	E ₂ Base	E ₃ Sbase	Esg Sgrade	K ₁ (E ₁ /E ₂)	K ₂ (E ₂ /E ₃)	K ₃ (E ₃ /Esg)	ε ² (10 ⁻⁸ in ²)
2			2/4	300.0	125.0	90.2	32.9	2.40	1.38	2.74	1.495
3			2/8	318.9	143.9	93.9	29.5	2.22	1.53	3.18	1.2393
4			4/8	300.0	125.0	75.0	41.7	2.40	1.67	1.80	0.7687
5			4/4	378.8	203.7	153.8	32.4	1.86	1.32	4.75	0.8653
6			0/22	300.0	125.0	45.0	21.2	2.4	2.78	2.12	2.332
7			2/24	338.2	163.2	113.2	20.6	2.07	1.44	5.48	1.0711
8			2/16	300.0	125.0	75.0	23.2	2.4	1.67	3.23	1.4843
9			0/15	299.9	125.0	45.0	13.6	2.4	2.78	3.31	3.887

Note: Refer to Table E-4, Appendix E for predicted deflections and values of constants.
Construction type 1 - HMAC layer over flexible base L-FA subbase.

^aActual percentage by weight.

^bElastic modulus values given in table are uncorrected values.

Table E-4. Predicted deflection basins and values of constants (37-month survey) - Site 2.

Section No	Predicted deflections at geophone locations (in mils)					Values of constants					Error
	W_1	W_2	W_3	W_4	W_5	m	n	C	B	H	$\epsilon^2 (10^{-8} \text{ in.}^2)$
2	0.452	0.427	0.357	0.253	0.131	0.659	0.366	1.192	1.143	68.67	1.495
3	0.472	0.448	0.379	0.276	0.155	0.58	0.367	1.234	1.303	68.57	1.239
4	0.374	0.353	0.291	0.200	0.096	0.693	0.352	1.178	1.105	70.15	0.7687
5	0.394	0.376	0.323	0.243	0.147	0.486	0.392	1.292	1.524	66.39	0.8653
6	0.598	0.569	0.487	0.364	0.216	0.425	0.314	1.347	1.895	73.66	2.332
7	0.575	0.550	0.478	0.369	0.236	0.407	0.384	1.354	1.829	66.67	1.0711
8	0.582	0.553	0.471	0.347	0.200	0.542	0.357	1.256	1.404	69.28	1.4843
9	0.857	0.820	0.715	0.554	0.358	0.346	0.318	1.421	2.314	72.89	3.887

Note: Refer to Table E-4 for predicted elastic moduli and to Table E-6, Appendix F, for field measured deflections.

Table E-5. Predicted elastic modulus of pavement layers - Sites 3, 4, 5 and 8.

Site No - Section No:	Lime-flyash Ratio ^a		Elastic modulus of layers (Ksi) ^b			Modular Ratios		Deflection basin fit.
	Flexible Base	L-FA Subbase	E ₁ Base	E ₂ Subbase	Esg Subgrade	K ₁ (E ₁ /E ₂)	K ₂ (E ₂ /Esg)	ε ² (10 ⁻⁸ in. ²)
3-1		3/6	125.0	75.0	28.7	1.67	2.61	7.5742
3-2		3/9	124.8	74.8	34.5	1.67	2.16	5.5159
3-3		1½/5	125.0	75.0	41.1	1.67	1.82	2.0385
3-5		2/8	125.0	75.0	38.3	1.67	1.96	3.0173
3-6		0/12	201.6	112.5	30.4	1.79	3.69	2.2311
4-2		3/6	124.9	74.9	23.8	1.67	3.15	2.417
4-3		3/9	125.0	75.0	26.9	1.67	2.78	2.6584
4-4		0/12	125.0	45.0	23.7	2.78	1.90	5.6059
4-5		1½/5	116.1	75.0	25.8	1.55	2.90	6.2628
4-6		2/6	163.7	93.1	22.0	1.76	4.23	2.6891
5-1		3/6	202.5	112.9	29.6	1.79	3.81	1.9954
5-2		3/9	124.9	75.0	34.1	1.67	2.19	3.1317
5-3		0/12	125.0	45.0	27.1	2.78	1.66	4.4355

Table E-5. Predicted elastic modulus continued.

Site No - Section No:	Lime-flyash Ratio ^a		Elastic moduli of layers (Ksi)			Modular Ratios		Deflection basin fit.
	Flexible Base	L-FA Subbase	E ₁ Base	E ₂ Subbase	E _{sg} Subgrade	K ₁ (E ₁ /E ₂)	K ₂ (E ₃ /E _{sg})	ε ² (10 ⁻⁸ in. ²)
5-4		2/8	189.3	130.1	23.8	1.45	5.47	2.8719
5-6		1½/5	125.0	75.0	29.5	1.67	2.54	3.6757
5-7		0/25	124.8	44.8	24.1	2.78	1.86	5.4578
5-8		0/23	125.0	45.0	28.3	2.78	1.59	5.026
8-2		2/4	189.3	124.1	30.1	1.52	4.12	0.973
8-3		2/6	125.0	75.0	26.6	1.67	2.82	1.836
8-4		2/8	142.8	82.3	27.2	1.73	3.02	1.853
8-5		3/6	125.0	75.0	31.5	1.67	2.38	1.1372
8-6		0/8	125.0	45.0	35.2	2.78	1.28	1.7278

Note: Site 3 - 10 in. base/6 in. subbase; Site 4 - 14 in. base 6/in. subbase; Site 5 and 8-12 in. base/6 in. subbase; Refer to Table E-6, Appendix E for predicted deflections and values of constants. All sites are construction type 3 - Flexible base over L-FA subbase. Survey periods: Site 3-33 months; Site 4-37 months; Site 5-33 months; Site 8-26 months.

^aActual percentage by weight.

^bElastic modulus value given in tables are uncorrected values.

Table E-6. Predicted deflection basins and values of constants - Sites 3, 4, 5 and 8.

Site No- Section No	Predicted deflections at geophone locations (in mils):					Values of constants					Error
	W ₁	W ₂	W ₃	W ₄	W ₅	m	n	C	B	H	$\epsilon^2(10^{-8} \text{ in.}^2)$
3-1	0.601	0.571	0.484	0.354	0.200	0.834	0.42	1.239	0.97	73.52	7.5742
3-2	0.533	0.495	0.416	0.298	0.159	0.907	0.407	1.197	0.897	73.72	5.5159
3-3	0.456	0.430	0.359	0.252	0.127	0.968	0.398	1.167	0.846	73.87	2.0385
3-5	0.482	0.456	0.381	0.269	0.139	0.944	0.401	1.179	0.865	73.81	3.0173
3-6	0.510	0.487	0.423	0.326	0.208	0.674	0.456	1.351	1.176	72.84	2.2311
4-2	0.599	0.573	0.498	0.384	0.246	0.644	0.368	1.277	1.265	76.7	2.417
4-3	0.545	0.521	0.450	0.342	0.213	0.691	0.359	1.242	1.186	76.87	2.6584
4-4	0.659	0.628	0.541	0.409	0.250	0.78	0.364	1.214	1.058	75.61	5.6069
4-5	0.565	0.540	0.467	0.355	0.221	0.679	0.359	1.247	1.206	77.0	6.2628
4-6	0.592	0.570	0.504	0.404	0.280	0.522	0.398	1.39	1.53	76.05	2.6891
5-1	0.483	0.464	0.406	0.318	0.210	0.611	0.422	1.36	1.307	74.47	1.9954
5-2	0.489	0.464	0.393	0.288	0.163	0.835	0.375	1.194	0.983	75.41	3.1317
5-3	0.639	0.607	0.515	0.377	0.213	0.882	0.39	1.198	0.931	74.0	4.4355

Table E-6. Predicted deflections continued.

Site No- Section No	Predicted deflections at geophone locations (in mils)					Values of constants					Error
	W_1	W_2	W_3	W_4	W_5	m	n	C	B	H	$\epsilon^2 (10^{-8} \text{ in.}^2)$
5-4	0.542	0.522	0.465	0.378	0.269	0.451	0.462	1.517	1.725	74.21	2.8719
5-6	0.547	0.520	0.445	0.330	0.194	0.782	0.384	1.226	0.044	75.25	3.6757
5-7	0.701	0.667	0.569	0.422	0.247	0.849	0.395	1.217	0.965	73.9	5.4578
5-8	0.617	0.586	0.496	0.361	0.202	0.894	0.388	1.192	0.92	74.04	5.026
8-2	0.471	0.451	0.395	0.309	0.204	0.582	0.423	1.374	1.367	74.73	0.973
8-3	0.591	0.564	0.484	0.364	0.219	0.741	0.391	1.252	1.096	75.12	1.836
8-4	0.566	0.540	0.466	0.354	0.219	0.71	0.398	1.275	1.138	74.92	1.853
8-5	0.520	0.495	0.421	0.310	0.179	0.806	0.38	1.211	1.015	75.32	1.1372
8-6	0.517	0.489	0.410	0.291	0.153	0.949	0.38	1.164	0.871	74.18	1.7278

Note: Refer to Table E-5 for predicted elastic moduli and Tables F-10, F-15, F-29, F-23, Appendix F, for field measured deflections.

Table E-7. Predicted elastic modulus of pavement layers (22 month survey) - Site 12.

Section No:	Lime-flyash Ratio ^a	Elastic modulus of layers (Ksi) ^b		Modular Ratios	Deflection basin fitting
	6 in. FA Stabilized Base	E ₁ Base	E _{sg} Subgrade	K ₁ (E ₁ /E _{sg})	ε ² (10 ⁻⁸ in. ²)
1	0/20	200.4	24.6	8.14	11.148*
2	0/30	1060.3	16.0	66.11	3.8644
3	0/40	467.3	18.3	25.42	8.1221
4	0/20	414.7	25.1	16.45	6.1299
5	0/40	1465.8	18.3	80.01	3.8439

Note: Refer to Table E-8, Appendix E, for predicted deflections and values of constants.
 High error ε² marked with asterisk. Construction type 4 - FA base over natural subgrade.

^aActual percentage by weight.

^bElastic modulus values given in tables on uncorrected values.

Table E-8. Predicted deflection basins and values of constants (22 month survey) - Site 12^a.

Section No	Predicted deflections at geophones locations (in mils)					Values of constants					Error
	W ₁	W ₂	W ₃	W ₄	W ₅	m	n	C	B	H	$\epsilon^2 (10^{-8} \text{ in.}^2)$
1	0.901	0.825	0.613	0.319	0.148	1.712	0.375	0.972	0.887	76.98	11.148*
2	1.078	1.014	0.832	0.563	0.257	1.004	0.289	1.055	0.99	66.98	3.8644
3	1.081	1.006	0.796	0.492	0.159	1.46	0.347	0.996	0.917	73.85	8.1221
4	0.829	0.766	0.592	0.344	0.077	1.586	0.361	0.984	0.901	75.46	6.1299
5	0.914	0.859	0.703	0.473	0.211	0.884	0.272	1.075	1.017	64.79	3.8439

^aRefer to Table E-7 for predicted elastic modulus and Table F-25, Appendix F, for field measured deflections. High error marked with asterisk.

Table E-9. Predicted elastic modulus^a of pavement layers (3 month, 12 month and 22 month survey) - Site 1.

Sect No	3 month survey				12 month survey				22 month survey			
	E ₁	E ₂	E _{sg}	ε ²	E ₁	E ₂	E _{sg}	ε ²	E ₁	E ₂	E _{sg}	ε ²
2	100.0	90.0	40.5	2.988	100.4	90.4	41.1	2.107	102.7	92.7	39.9	2.197
3	123.3	113.3	18.0	3.769	124.5	114.5	17.1	4.006	127.0	117.0	17.3	4.386
4	131.0	121.0	18.1	3.28	132.4	122.4	18.3	3.07	124.5	114.5	17.8	2.527
6	99.9	45.0	21.3	16.1*	109.0	54.0	21.3	7.7	99.9	45.0	21.7	9.463
7	99.9	45.0	29.8	17.2*	99.9	45.0	29.8	4.241	99.9	45.0	26.7	6.41
8	99.9	45.0	27.9	10.63*	123.4	68.4	27.6	2.553	121.0	66.0	27.3	3.556
9	99.9	45.0	24.3	9.66	129.7	74.7	23.1	3.1	127.0	72.0	21.8	5.08
10	99.9	45.0	17.6	31.02*	100.0	45.0	17.8	8.87	101.9	46.9	17.8	9.55

Note: Elastic moduli in Ksi; ε² in 10⁻⁸ in.²; high error ε² marked with asterisk;
Construction type 1 - L-FA base over L-FA subbase.

^aThe elastic modulus values given in tabel are uncorrected values.

Table E-10. Predicted elastic modulus^a of pavement layers (24 month survey) - Site 2.

Section No	24 month survey				
	E ₁	E ₂	E ₃	E _{sg}	ε ²
2	300.0	125.0	88.3	31.6	2.094
3	316.8	141.8	91.8	30.6	1.185
4	300.0	125.0	75.0	43.0	0.894
5	399.6	224.5	174.5	29.6	1.338
6	300.0	125.0	45.0	23.3	2.84
7	338.2	163.1	113.1	22.3	1.504
8	307.5	132.5	82.5	24.3	1.8
9	299.9	125.0	45.0	12.9	7.437

Note: Elastic moduli in Ksi; ε² in 10⁻⁸ in.²; Construction type 2 - HMAc layer over flexible base and L-FA subbase.

^a The elastic modulus values given in the table are uncorrected values.

Table E-11. Predicted elastic modulus^a of pavement layers (7 month and 12 month survey) - Site 3.

Section No	7 month survey				12 month survey			
	E ₁	E ₂	E _{sg}	ε ²	E ₁	E ₂	E _{sg}	ε ²
1	185.4	130.8	22.8	4.558	125.0	75.0	35.6	3.5081
2	185.4	130.8	22.8	4.558	124.9	75.0	42.7	3.581
3	191.3	120.2	29.6	2.365	125.0	75.0	43.3	1.99
5	191.5	105.2	29.2	2.735	125.0	75.0	39.4	2.646
6	208.2	126.1	23.4	3.457	217.4	127.1	31.8	1.995

Note: Elastic moduli in Ksi; ε² in 10⁻⁸ in²; Construction type 3 - Flexible base over L-FA subbase.

^aThe elastic modulus values given in the table are uncorrected values.

Table E-12. Predicted elastic modulus^a of pavement layers (19 month and 43 month survey) - Site 3.

Section No	19 month survey				43 month survey			
	E ₁	E ₂	E _{sg}	ε ²	E ₁	E ₂	E _{sg}	ε ²
1	125.0	75.0	32.0	2.925	125.0	75.0	29.1	5.326
2	110.8	75.0	37.5	2.305	124.9	75.0	38.3	6.311
3	125.0	75.0	39.1	1.691	124.8	75.1	36.3	4.0
5	125.0	75.0	36.1	2.428	125.0	75.0	35.9	3.881
6	215.0	131.8	27.9	1.505	185.4	96.3	26.3	2.996

Note: Elastic modulus in Ksi; ε² in 10⁻⁸ in.²; Construction type 3 - Flexible base over L-FA subbase.

^aThe elastic modulus values given in the table are uncorrected values.

Table E-13. Predicted elastic modulus^a of pavement layers (6 month, 12 month and 24 month survey) - Site 4.

Section No	6 month survey				12 month survey				24 month survey			
	E ₁	E ₂	E _{sg}	ε ²	E ₁	E ₂	E _{sg}	ε ²	E ₁	E ₂	E _{sg}	ε ²
2	124.9	75.0	21.2	18.76*	215.0	158.8	24.0	1.581	210.0	125.2	24.3	1.77
3	124.9	75.0	21.2	33.51*	125.0	75.0	22.9	4.012	125.0	75.0	25.0	3.524
4	124.9	45.0	18.6	54.38*	125.0	45.0	20.5	7.631	125.0	45.0	22.2	5.882
5	124.9	75.0	19.6	37.91*	125.0	75.0	21.3	6.1	125.0	75.0	23.3	5.113
6	124.9	75.0	18.3	31.25*	199.5	147.4	19.3	2.674	197.4	142.7	20.8	2.186

Note: Elastic moduli in Ksi; ε² in 10⁻⁸ in.²; high error ε² marked with asterisk;
Construction type 3 - Flexible base over L-FA subbase.

^aThe elastic modulus values given in the table are uncorrected values.

Table E-14. Predicted elastic modulus^b of pavement layers (8 month and 16 month survey) - Site 5.

Section No	8 month survey				16 month survey			
	E ₁	E ₂	E _{sg}	ε ²	E ₁	E ₂	E _{sg}	ε ²
1	229.5	161.5	30.4	2.253	239.8	188.1	26.4	1.154
2	125.0	75.0	34.8	2.39	228.5	128.9	33.1	1.124
3 ^a	125.0	45.0	27.5	5.197	-	-	-	-
4	219.8	158.4	27.6	2.795	234.6	183.0	23.6	1.89
6	123.6	73.6	34.8	4.386	125.0	75.0	29.2	3.047
7	124.9	45.0	24.4	9.215	124.9	44.9	24.3	3.933
8	125.0	45.0	26.9	5.142	125.0	45.0	27.2	5.363

Note: Elastic moduli in Ksi; ε² in 10⁻⁸ in.²; Construction type 3 - Flexible base over L-FA subbase.

^a 16 month survey data not available for Section 3.

^b The elastic modulus values given in the table are uncorrected values.

Table E-15. Predicted elastic modulus^a of pavement layers (21 month and 40 month survey) - Site 5.

Section No	21 month survey				40 month survey			
	E ₁	E ₂	E _{sg}	ε ²	E ₁	E ₂	E _{sg}	ε ²
1	239.8	186.5	27.9	1.637	125.0	75.0	30.8	3.11
2	125.0	75.0	35.4	3.019	124.9	75.0	33.9	4.364
3	239.5	108.6	28.4	2.481	125.0	45.0	28.6	4.41
4	232.1	179.9	25.0	2.242	125.0	75.0	25.3	4.234
6	125.0	75.0	30.3	3.599	123.3	75.0	32.4	3.51
7	125.0	45.0	23.5	5.5	124.9	45.0	26.2	5.946
8	215.0	107.2	26.2	2.933	125.0	45.0	31.1	4.279

Note: Elastic moduli in Ksi; ε² in 10⁻⁸ in²; Construction type 3 - Flexible base over L-FA subbase.

^aThe elastic modulus values given in the table are uncorrected values.

Table E-16. Predicted elastic modulus^a of pavement layers (6 month and 12 month survey) - Site 8.

Section No	6 month survey				12 month survey			
	E ₁	E ₂	E _{sg}	ε ²	E ₁	E ₂	E _{sg}	ε ²
2	111.5	75.0	29.9	3.935	125.0	75.0	29.2	4.959
3	127.3	49.3	24.9	4.296	125.0	75.0	25.8	5.997
4	124.9	75.0	26.3	4.96	120.4	75.0	23.8	2.261
5	124.9	75.0	30.3	7.537	124.8	74.8	30.6	4.55
6	214.9	45.0	34.3	8.267	124.4	45.0	35.6	5.106

Note: Elastic moduli in Ksi; ε² in 10⁻⁸ in.²; Construction type 3 - Flexible base over L-FA subbase.

^aThe elastic modulus values given in the table are uncorrected values.

Table E-17. Predicted elastic modulus^a of pavement layers (8 month and 44 month surveys) - Site 12.

Section No:	8 month survey			44 month survey		
	E ₁	E _{sg}	ε ²	E ₁	E _{sg}	ε ²
1	200.0	25.7	14.518*	200.0	25.2	14.32*
2	1322.0	15.8	6.731	1210.0	15.3	4.396
3	1600.3	16.3	13.677	342.5	17.8	9.744
4	389.8	23.3	8.919	328.3	24.3	8.45
5	440.0	17.4	9.874	1636.8	19.1	3.994

Note: Elastic moduli in Ksi; ε² in 10⁻⁸ in.²; Construction type 4 - FA base over natural subgrade; High error ε² marked with asterisk.

^aThe elastic modulus values given in the table are uncorrected values.

APPENDIX F.
Dynalect Deflection Measurements
of the Test Sites, Used in the Study.

Table F-1. Dynaflect deflection measurements
for Site No. 1 (3 month survey)^a

Average deflections (in mils) at geophone no:							
Test Section No	W ₁	W ₂	W ₃	W ₄	W ₅	SCI standard deviation	Points in average
1	0.523	0.383	0.265	0.205	0.151	0.054	21
2	0.574	0.415	0.266	0.192	0.139	0.043	21
3	0.874	0.660	0.492	0.391	0.312	0.080	21
4	0.763	0.616	0.468	0.386	0.311	0.071	21
5	1.067	0.819	0.599	0.475	0.369	0.054	21
6	1.149	0.753	0.448	0.343	0.264	0.078	21
7	1.056	0.708	0.402	0.269	0.189	0.064	21
8	0.964	0.631	0.378	0.275	0.202	0.037	21
9	1.010	0.696	0.436	0.321	0.232	0.035	21
10	1.499	0.994	0.592	0.434	0.319	0.088	21

^aMeasurements date 1-23-80, Dynaflect No. 39, mean air temperature 48.5°F (40°F-57°F). Pavement condition estimated to be 'wet' on the test date (27).

Table F-2. Dynaflect deflection measurements
for Site No. 1 (12 month survey)^a

Average deflections (in mils) at geophone no:							
Test Section No	W ₁	W ₂	W ₃	W ₄	W ₅	SCI standard deviation	Points in average
1	0.438	0.339	0.267	0.219	0.154	0.076	21
2	0.526	0.380	0.272	0.203	0.137	0.040	21
3	0.761	0.616	0.510	0.420	0.329	0.060	21
4	0.718	0.590	0.482	0.394	0.307	0.113	21
5	0.830	0.669	0.546	0.439	0.329	0.074	21
6	0.965	0.695	0.485	0.361	0.264	0.096	21
7	0.853	0.650	0.434	0.304	0.189	0.085	21
8	0.718	0.572	0.414	0.300	0.204	0.052	21
9	0.804	0.639	0.471	0.353	0.244	0.077	21
10	1.144	0.850	0.595	0.448	0.316	0.295	21

^aMeasurements date 10-1-80, Dynaflect No. 39, mean air temperature 79.5°F (74°-85°F). Pavement condition estimated to be 'wet' on the test date (27).

Table F-3. Dynaflect deflection measurements
for Site No. 1 (22 month survey)^a

Test Section No	Average deflections (in mils) at geophone no:					SCI standard deviation	Points in average
	W ₁	W ₂	W ₃	W ₄	W ₅		
1	0.434	0.348	0.266	0.211	0.151	0.057	21
2	0.527	0.396	0.272	0.200	0.141	0.052	21
3	0.721	0.613	0.489	0.414	0.326	0.047	21
4	0.790	0.672	0.492	0.402	0.316	0.066	21
5	0.895	0.740	0.564	0.461	0.345	0.086	21
6	1.047	0.735	0.479	0.364	0.259	0.106	21
7	0.959	0.732	0.476	0.335	0.211	0.100	21
8	0.746	0.567	0.399	0.302	0.206	0.089	21
9	0.860	0.667	0.457	0.360	0.258	0.086	21
10	1.120	0.853	0.564	0.440	0.316	0.120	21

^aMeasurements date 8-19-81, Dynaflect No. 39, mean air temperature 76°F (71°F-81°F). Pavement condition estimated to be 'wet' on the test date (27).

Table F-4. Dynaflect deflection measurements
for Site No. 1 (36 month survey)^a

Test Section No	Average deflections (in mils) at geophone no:					SCI standard deviation	Points in average
	W ₁	W ₂	W ₃	W ₄	W ₅		
1	0.478	0.369	0.271	0.203	0.140	0.079	21
2	0.559	0.414	0.272	0.182	0.121	0.042	21
3	0.828	0.712	0.534	0.400	0.307	0.071	21
4	0.877	0.726	0.532	0.395	0.299	0.157	21
5	1.051	0.824	0.593	0.503	0.465	0.149	21
6	1.163	0.810	0.487	0.355	0.238	0.092	21
7	1.030	0.807	0.484	0.316	0.190	0.116	21
8	0.836	0.610	0.400	0.279	0.187	0.156	21
9	1.036	0.817	0.493	0.332	0.228	0.121	21
10	1.236	0.925	0.568	0.405	0.278	0.101	21

^aMeasurements date 10-26-82, Dynaflect No. 39, mean air temperature 72.5°F (62°-83°F). Pavement condition estimated to be 'wet' on the test date (27).

Table F-5. Dynaflect deflection measurements
for Site No. 2 (24 month survey)^a

Average deflections (in mils) at geophone no:							
Test Section No	W ₁	W ₂	W ₃	W ₄	W ₅	SCI standard deviation	Points in average
1	0.808	0.599	0.472	0.368	0.281	0.045	17
2	0.593	0.426	0.319	0.244	0.178	0.039	17
3	0.534	0.403	0.316	0.233	0.184	0.021	17
4	0.422	0.311	0.231	0.176	0.131	0.011	17
5	0.477	0.354	0.262	0.225	0.190	0.026	17
6	0.690	0.501	0.373	0.299	0.242	-	-
7	0.630	0.492	0.382	0.315	0.253	0.038	17
8	0.646	0.487	0.374	0.304	0.232	0.085	17
9	1.132	0.868	0.649	0.523	0.435	0.370	15

^aMeasurements date 8-24-81, Dynaflect No. 39, temperature and time of day not recorded. Measurements were taken after the site was re-surfaced with 2" HMAC layer. Estimated mean air temperature 82°F on the test date and 'dry' condition of the pavement (27).

Table F-6. Dynaflect deflection measurements
for Site No. 2 (37 month survey)^a

Average deflections (in mils) at geophone no:							
Test Section No	W ₁	W ₂	W ₃	W ₄	W ₅	SCI standard deviation	Points in average
1	0.658	0.495	0.396	0.334	0.268	0.172	17
2	0.543	0.426	0.293	0.222	0.171	0.027	17
3	0.543	0.426	0.310	0.249	0.191	0.045	17
4	0.394	0.323	0.225	0.178	0.135	0.040	17
5	0.450	0.365	0.259	0.218	0.174	0.031	17
6	0.720	0.564	0.413	0.343	0.265	0.039	17
7	0.641	0.538	0.411	0.351	0.273	0.042	17
8	0.669	0.537	0.404	0.321	0.243	0.064	16
9	1.011	0.821	0.612	0.517	0.415	0.052	15

^aMeasurements date 10-27-82, Dynaflect No. 39, mean air temperature 77°F (72°-82°F). Measurements were taken after the site was re-surfaced with 2" HMAC layers. Pavement condition estimated to be 'slightly wet' on the test date (27).

Table F-7. Dynaflect deflection measurements
for Site No. 3 (7 month survey)^a

Test Section No	Average deflections (in mils) at geophone no:					SCI standard deviation	Points in average
	W ₁	W ₂	W ₃	W ₄	W ₅		
1	0.693	0.525	0.374	0.290	0.247	0.050	20
2	0.725	0.549	0.377	0.276	0.217	0.032	20
3	0.579	0.448	0.327	0.246	0.190	0.046	20
4	0.539	0.415	0.332	0.269	0.231	0.042	20
5	0.599	0.462	0.332	0.253	0.193	0.037	20
6	0.662	0.525	0.386	0.292	0.241	0.032	20

^aMeasurements date 7-15-80, Dynaflect No. 29, temperature and time of day not recorded. Estimated mean air temperature 90°F on the test date and 'dry' condition of the pavement (27).

Table F-8. Dynaflect deflection measurements
for Site No. 3 (12 month survey)^a

Test Section No	Average deflections (in mils) at geophone no:					SCI standard deviation	Points in average
	W ₁	W ₂	W ₃	W ₄	W ₅		
1	0.574	0.401	0.279	0.197	0.158	0.061	20
2	0.597	0.411	0.266	0.171	0.132	0.062	20
3	0.502	0.368	0.252	0.166	0.130	0.052	20
4	0.460	0.341	0.254	0.192	0.164	0.044	20
5	0.515	0.373	0.262	0.178	0.143	0.032	20
6	0.532	0.422	0.312	0.220	0.177	0.030	20

^aMeasurements date 12-2-80, Dynaflect No. 48, mean air temperature 58°F (57°-59°F). Pavement condition estimated to be 'dry' on the test date (27).

Table F-9. Dynaflect deflection measurements
for Site No. 3 (19 month survey)^a

Average deflections (in mils) at geophone no:							
Test Section No	W ₁	W ₂	W ₃	W ₄	W ₅	SCI standard deviation	Points in average
1	0.579	0.443	0.330	0.225	0.176	0.049	20
2	0.609	0.461	0.320	0.205	0.150	0.058	20
3	0.491	0.388	0.288	0.190	0.144	0.032	20
4	0.445	0.364	0.292	0.214	0.178	0.041	20
5	0.519	0.405	0.296	0.197	0.156	0.039	20
6	0.556	0.472	0.367	0.259	0.202	0.031	20

^aMeasurements date 7-20-81, Dynaflect No. 48, mean air temperature 110°F (109°-111°F). Pavement condition estimated to be 'dry' on the test date (27).

Table F-10. Dynaflect deflection measurements
for Site No. 3 (33 month survey)^a

Average deflections (in mils) at geophone no:							
Test Section No	W ₁	W ₂	W ₃	W ₄	W ₅	SCI standard deviation	Points in average
1	0.647	0.480	0.271	0.213	0.196	0.061	20
2	0.676	0.470	0.274	0.193	0.163	0.092	20
3	0.518	0.381	0.259	0.188	0.137	0.045	20
4	0.461	0.344	0.263	0.213	0.169	0.038	20
5	0.506	0.368	0.255	0.192	0.147	0.037	20
6	0.573	0.445	0.326	0.245	0.185	0.045	20

^aMeasurements date 9-9-82, Dynaflect No. 48, mean air temperature 89.5°F (85°-94°F). Pavement condition estimated to be 'dry' on the test date (27).

Table F-11. Dynaflect deflection measurements
for Site No. 3 (43 month survey)^a

Test Section No	Average deflections (in mils) at geophone no:					SCI standard deviation	Points in average
	W ₁	W ₂	W ₃	W ₄	W ₅		
1	0.702	0.471	0.328	0.247	0.193	0.068	20
2	0.714	0.463	0.302	0.215	0.147	0.080	20
3	0.619	0.402	0.277	0.204	0.155	0.052	19
4	0.516	0.360	0.276	0.223	0.178	0.032	20
5	0.552	0.372	0.265	0.209	0.157	0.045	20
6	0.666	0.510	0.377	0.291	0.214	0.069	20

^aMeasurement date 7-28-83, Dynaflect No. 48, mean air temperature 82.5°F (80°-85°F). Pavement condition estimated to be 'dry' on the test date (27).

Table F-12. Dynaflect deflection measurements
for Site No. 4 (6 month survey)^a

Average deflections (in mils) at geophone no:							
Test Section No	W ₁	W ₂	W ₃	W ₄	W ₅	SCI standard deviation	Points in average
1	0.988	0.602	0.442	0.352	0.288	0.066	19
2	1.054	0.607	0.420	0.330	0.266	0.086	21
3	1.200	0.688	0.457	0.282	0.265	0.079	20
4	1.498	0.786	0.595	0.314	0.303	0.122	20
5	1.273	0.676	0.473	0.299	0.287	0.079	20
6	1.255	0.733	0.589	0.323	0.308	0.042	20

^aMeasurements date 4-9-80, Dynaflect No. 29, temperature or time of day not recorded. Estimated mean air temperature on the test date 60°F and 'slightly wet' condition of the pavement (27).

Table F-13. Dynaflect deflection measurements
for Site No. 4 (12 month survey)^a

Average deflections (in mils) at geophone no:							
Test Section No	W ₁	W ₂	W ₃	W ₄	W ₅	SCI standard deviation	Points in average
1	0.493	0.435	0.354	0.291	0.264	0.024	20
2	0.537	0.457	0.349	0.270	0.235	0.035	21
3	0.634	0.504	0.374	0.284	0.246	0.034	20
4	0.792	0.586	0.417	0.317	0.274	0.054	20
5	0.686	0.505	0.373	0.294	0.264	0.032	20
6	0.643	0.535	0.413	0.325	0.292	0.015	20

^aMeasurements date 10-16-80, Dynaflect No. 48, mean air temperature 86°F (82°-90°F). Pavement condition estimated to be 'slightly wet' on the test date (27).

Table F-14. Dynaflect deflection measurements
for Site No. 4 (24 month survey)^a

Test Section No	Average deflections (in mils) at geophone no:					SCI standard deviation	Points in average
	W ₁	W ₂	W ₃	W ₄	W ₅		
1	0.530	0.450	0.382	0.298	0.260	0.028	20
2	0.570	0.462	0.363	0.275	0.232	0.044	21
3	0.594	0.460	0.360	0.269	0.225	0.035	20
4	0.769	0.556	0.413	0.306	0.254	0.048	20
5	0.703	0.488	0.366	0.276	0.242	0.076	20
6	0.624	0.500	0.403	0.315	0.271	0.018	20

^aMeasurements date 10-13-81, Dynaflect 48, temperature or time of day not recorded. Estimated mean air temperature 84°F on the test date and 'wet' pavement condition (27).

Table F-15. Dynaflect deflection measurements
for Site No. 4 (37 month survey)^a

Test Section No	Average deflections (in mils) at geophone no:					SCI standard deviation	Points in average
	W ₁	W ₂	W ₃	W ₄	W ₅		
1	0.583	0.489	0.377	0.314	0.251	0.075	20
2	0.695	0.558	0.399	0.315	0.237	0.052	21
3	0.649	0.497	0.347	0.274	0.209 ^b	0.051	20
4	0.794	0.572	0.385	0.308	0.238	0.072	20
5	0.767	0.525	0.340	0.279	0.218	0.070	20
6	0.647	0.519	0.385	0.323	0.256	0.024	20

^aMeasurements date 11-23-82, Dynaflect No. 48, mean air temperature 79°F (75°-83°F) Pavement condition estimated 'dry' on the test date (27).

^bMultiplier error in reading W₅ recorded as 2.090, corrected to 0.209 by graphical verification of basin shape.

Table F-16. Dynaflect deflection measurements
for Site No. 5 (8 month survey)^a

Test Section No	Average deflections (in mils) at geophone no:					SCI standard deviation	Points in average
	W ₁	W ₂	W ₃	W ₄	W ₅		
1	0.506	0.378	0.281	0.210	0.185	0.036	21
2	0.523	0.409	0.274	0.199	0.162	0.038	21
3	0.673	0.515	0.341	0.249	0.205	0.026	21
4	0.549	0.405	0.303	0.228	0.204	0.059	21
5	0.518	0.383	0.289	0.218	0.193	0.030	21
6	0.637	0.417	0.284	0.196	0.162	0.094	21
7	0.943	0.712	0.447	0.300	0.231	0.039	21
8	0.712	0.526	0.359	0.258	0.209	0.028	21

^aMeasurement date 12-4-80 for Sect. 1,4,5, & 6, mean air temperature 65°F (64°-66°F). Measurement date 3-9-81 for Sect. 2,3,7 & 8, temperature or time of day not recorded. Dynaflect 48 used for both measurements. Pavement condition estimated to be 'slightly wet' on the test date (27).

Table F-17. Dynaflect deflection measurements
for Site No. 5 (16 month survey)^a

Test Section No	Average deflections (in mils) at geophone no:					SCI standard deviation	Points in average
	W ₁	W ₂	W ₃	W ₄	W ₅		
1	0.499	0.407	0.348	0.257	0.213	0.036	21
2	0.476	0.378	0.307	0.216	0.170	0.033	21
4	0.557	0.440	0.365	0.281	0.239	0.054	21
5	0.488	0.390	0.330	0.258	0.220	0.025	21
6	0.634	0.460	0.343	0.242	0.193	0.077	21
7	0.815	0.641	0.451	0.311	0.232	0.028	21
8	0.617	0.476	0.358	0.262	0.207	0.028	21

^aMeasurements date 7-21-81, Dynaflect No. 48, temperature and time of day not recorded. Section 3 measurements in error therefore deleted. Pavement condition estimated to be 'dry' on the test date and mean air temperature 87°F (27).

Table F-18. Dynaflect deflection measurements
for Site No. 5 (21 month survey)^a

Test Section No	Average deflections (in mils) at geophone no:					SCI Standard deviation	Points in average
	W ₁	W ₂	W ₃	W ₄	W ₅		
1	0.496	0.406	0.302	0.239	0.202	0.036	21
2	0.463	0.362	0.260	0.191	0.159	0.033	21
3	0.565	0.439	0.322	0.243	0.198	0.026	21
4	0.549	0.428	0.329	0.262	0.225	0.047	21
5	0.504	0.404	0.314	0.250	0.213	0.024	21
6	0.595	0.434	0.301	0.228	0.186	0.074	21
7	0.830	0.628	0.428	0.309	0.240	0.031	21
8	0.609	0.470	0.342	0.263	0.215	0.031	21

^aMeasurements date 12-28-81, Dynaflect No. 48, mean air temperature 67.5°F (60°-75°F). Pavement condition estimated to be 'slightly wet' on the test date (27).

Table F-19. Dynaflect deflection measurements
for Site No. 5 (33 month survey)^a

Test Section No	Average deflections (in mils) at geophone no:					SCI standard deviation	Points in average
	W ₁	W ₂	W ₃	W ₄	W ₅		
1	0.541	0.416	0.314	0.244	0.190	0.049	21
2	0.633	0.467	0.316	0.221	0.165	0.068	21
3	0.675	0.517	0.360	0.272	0.208	0.061	21
4	0.632	0.483	0.363	0.291	0.237	0.065	21
5	0.619	0.487	0.372	0.300	0.240	0.034	21
6	0.671	0.477	0.331	0.249	0.191	0.085	21
7	0.854	0.649	0.430	0.316	0.234	0.048	21
8	0.622	0.459	0.340	0.216	0.199	0.040	21

^aMeasurements date 12-16-82, Dynaflect No. 48, mean air temperature 66.5°F (58°-75°F). Pavement condition estimated to be 'slightly wet' on the test date (27).

Table F-20. Dynaflect deflections measurements
for Site No. 5 (40 month survey)^a

Test Section No	Average deflections (in mils) at geophone no:					SCI standard deviation	Points in average
	W ₁	W ₂	W ₃	W ₄	W ₅		
1	0.587	0.398	0.320	0.248	0.183	0.091	21
2	0.682	0.449	0.330	0.239	0.166	0.083	21
3	0.678	0.460	0.359	0.270	0.197	0.066	21
4	0.690	0.473	0.375	0.297	0.223	0.076	21
5	0.630	0.445	0.363	0.292	0.219	0.047	21
6	0.659	0.433	0.328	0.246	0.174	0.078	21
7	0.862	0.581	0.437	0.308	0.215	0.037	21
8	0.599	0.398	0.330	0.256	0.181	0.047	21

^aMeasurements date 7-27-83, Dynaflect No. 48, mean air temperature 87.5°F (80°-95°F). Pavement condition estimated to be 'dry' on the test date (27).

Table F-21. Dynaflect deflection measurements
for Site No. 8 (6 month survey)^a

Test Section No	Average deflections (in mils) at geophone no:					SCI standard deviation	Points in average
	W ₁	W ₂	W ₃	W ₄	W ₅		
1	0.720	0.491	0.303	0.212	0.143	0.030	20
2	0.705	0.500	0.350	0.253	0.188	0.058	20
3	0.779	0.573	0.408	0.301	0.226	0.091	20
4	0.783	0.573	0.403	0.282	0.214	0.062	20
5	0.786	0.565	0.362	0.255	0.186	0.079	20
6	0.793	0.535	0.335	0.235	0.164	0.059	20

^aMeasurements date 9-11-79, Dynaflect 39, mean air temperature 80°F (72°-88°F). Pavement condition estimated to be 'wet' on the test date (27).

Table F-22. Dynaflect deflection measurements
for Site No. 8 (12 month survey)^a

Test Sections No	Average deflections (in mils) at geophone no:					SCI standard deviation	Points in average
	W ₁	W ₂	W ₃	W ₄	W ₅		
1	0.636	0.401	0.254	0.191	0.137	0.024	19
2	0.672	0.447	0.308	0.237	0.193	0.026	20
3	0.763	0.508	0.354	0.273	0.218	0.066	20
4	0.712	0.682	0.458	0.313	0.237	0.039	19
5	0.682	0.458	0.313	0.237	0.184	0.037	20
6	0.684	0.435	0.288	0.215	0.158	0.039	20

^aMeasurements date 3-11-80, Dynaflect No. 39, mean air temperature 53°F (46°-60°F). Pavement condition estimated to be 'slightly wet' on the test date (27).

Table F-23. Dynaflect deflection measurements
for Site No. 8 (26 month survey)^a

Test Section No	Average deflections (in mils) at geophone no:					SCI standard deviation	Points in average
	W ₁	W ₂	W ₃	W ₄	W ₅		
1	0.523	0.393	0.285	0.218	0.146	0.014	19
2	0.520	0.421	0.331	0.264 ^b	0.187	0.020	20
3	0.632	0.508	0.386	0.301	0.212	0.033	20
4	0.590	0.475	0.371	0.286	0.207	0.01	20
5	0.550	0.445	0.343	0.267	0.179	0.018	20
6	0.527	0.416	0.313	0.242	0.160	0.011	20

^aMeasurement date 5-5-81, Dynaflect No. 39, mean air temperature 62°F (59°-65°F). Pavement condition estimated to be 'slightly wet' on the test date (27).

^bTwo bad points in W₄ readings, 0.264 is average of 18 points.

Table F-24. Dynaflect deflection measurements
for Site No. 12 (8 month survey)^a

Test Section No	Average deflections (in mils) at geophone no:					SCI standard deviation	Points in average
	W ₁	W ₂	W ₃	W ₄	W ₅		
1	1.166	0.778	0.484	0.286	0.219	0.080	20
2	1.214	0.931	0.680	0.452	0.356	0.258	20
3	1.237	0.866	0.576	0.346	0.346	0.080	20
4	1.091	0.766	0.505	0.308	0.242	0.070	20
5	1.343	1.000	0.693	0.430	0.324	0.156	20

^aMeasurement date 7-8-80, Dynaflect No. 29, mean air temperature 97°F (87°-107°F). Pavement condition estimated to be 'dry' on the test date (27).

Table F-25. Dynaflect deflection measurements
for Site No. 12 (22 month survey)^a

Test Section No	Average deflections (in mils) geophone no:					SCI Standard deviation	Points in average
	W ₁	W ₂	W ₃	W ₄	W ₅		
1	1.136	0.850	0.514	0.323	0.229	0.103	20
2	1.183	1.015	0.712	0.498	0.352	0.074	20
3	1.250	0.979	0.643	0.411	0.307	0.099	20
4	0.981	0.750	0.472	0.299	0.224	0.092	20
5	1.024	0.836	0.592	0.408	0.308	0.070	20

^aMeasurements date 9-22-81, Dynaflect No. 48, mean air temperature 98°F (97°-100°F). Pavement condition estimated to be 'dry' on the test date (27).

Table F-26. Dynaflect deflection measurements
for Site No. 12 (44 month survey)^a

Test Section No	Average deflections (in mils) at geophone no:					SCI standard deviation	Points in average
	W ₁	W ₂	W ₃	W ₄	W ₅		
1	1.178	0.839	0.508	0.330	0.223	0.105	20
2	1.194	0.979	0.712	0.520	0.367	0.114	20
3	1.348	1.034	0.684	0.466	0.316	0.100	20
4	1.067	0.782	0.483	0.332	0.232	0.080	20
5	0.964	0.770	0.536	0.399	0.295	0.051	20

^a Measurements date 7-19-83, Dynaflect No. 48, mean air temperature 94°F (88°-100°F). Pavement condition estimated to be dry on the test date (27).

Table F-27. Dynaflect deflection measurements
for Site No. 13 (36 month survey)^a

Test Section No	Average deflections (in mils) at geophone no:					SCI standard deviation	Points in average
	W ₁	W ₂	W ₃	W ₄	W ₅		
1	1.098	0.804	0.554	0.414	0.343	0.137	23

^aMeasurements date 3-8-83, Dynaflect No. 48, air temperature 69°F.